ATOMIC WEAPONS RESEARCH ESTABLISHMENT

AWRE REPORT NO. O24/83

The Mk IIIC Vertical Component Force-Balance Seismometer System. Part 1: Design and Development

R F Burch

Recommended for issue by

A Douglas, Acting Superintendent

Approved by

F E Whiteway, Head of Division

ISBN 0 85518153 2

CONTENTS

CONTENTS (cont'd)

SUMMARY

AWRE, Blacknest have developed, in co-operation with the University of Reading, a broad band seismometer system for the measurement of the vertical component of ground motion. The system is now deployed at a network of recording sites throughout the UK. The seismometer is a Willmore Mk IIIA that has been modified in various ways, the most important of which is the attachment of a capacitative transducer to measure the relative displacement of mass and frame; the modified seismometer is thus referred to as the Mk IIIC (C for capacitor).

Although the Mk IIIC uses the inertial mass and suspension of a conventional short period seismometer, the inclusion of a displacement transducer and a feedback technique known as "force balance" enables the instrument to provide adequate signals over the frequency band of seismological interest from 0.01 to 10 Hz and eliminates the requirement for a separate long period seismometer.

This report is in two parts. Part 1 (this report) traces the history of the development of the system, discusses the shortcomings of conventional instruments and presents the theory and transfer functions of the feedback and subsequent signal circuits. The methods of routine calibration of conventional seismographs are discussed and are found to be inadequate for use with feedback instruments. Correct calibration requires monitoring of the instrument output with the feedback loop disconnected.

No currently available digital recorder can accommodate the large dynamic range of the basic feedback seismometer. A fifteen bit digital recording system is used here; this limits the dynamic range to a nominal 86 db. The seismometer output is amplified and filtered so as to make best use of the range of the recorder. A more realistic estimate of the dynamic range is obtained using model spectra for teleseismic earthquake and explosion signals and is expressed in terms of body wave magnitude m_b. The surface wave magnitudes M_s are calculated using single frequency amplitude values. Typical values of dynamic range are for m_b from 3.3 to 7.1 and for M_s from 2.1 to 6.4 (assuming a recording distance (Δ) of 72^o). These ranges are recalculated in the presence of different samples of seismic noise from which it is seen that the range decreases to zero when, under the noisiest condition, the spectrum of an event of magnitude m_b = 6.8 only just exceeds the noise spectrum at all frequencies but at the same time the sum of the two spectra causes the system to overload.

A brief analysis is made of teleseismic recordings from an underground explosion. A comparison is made of the signal amplitudes and waveshapes for both SP body waves and surface waves derived from broad band recordings from four feedback systems located at sites across England and Wales and from four sites (that use conventional long period seismometers) local to Blacknest. There is close agreement in wave shapes and magnitudes, the difference in magnitudes being only 0.1 to 0.2 units, which is remarkably small.

Part 2 (AWRE Report O25/83) is a technical description of the seismometer and its associated electronic circuits and includes detailed instructions for assembly and calibration.

1. INTRODUCTION

The first seismographs were insensitive mechanical devices that recorded ground displacement over a range of frequencies from about 0.1 to a few Hertz. These devices usually contained (like all the widely used seismographs that have been produced subsequently) a relatively large mass attached to the instrument frame by only a spring or a pivot. Ground motion produced a relative displacement between the mass and frame which was mechanically magnified and recorded as a visual seismogram. Now, in addition to the ground motion caused by seismic disturbances (earthquakes and explosions), the surface of the earth is in constant motion due to seismic noise which is generated mainly by the effects of the weather and the activities of man. The main component of the noise is from oceanic microseisms generated by wind action on the sea surface; these microseisms have frequencies in the range from about 0.12 to about 0.17 Hz and reach peak amplitudes of about 20 μm. The oceanic microseisms if recorded unattenuated tend to swamp all but the largest signals from earthquakes. As the first seismographs produced visual seismograms only and there was no possibility of applying any filtering to improve signal-to-noise ratios, the magnification was usually set so that the noise was just visible on the record. In practice, the mechanical seismographs did not have the potential to operate at much higher magnifications anyway.

With the introduction of the magnet/coil transducer to convert relative motion of mass and frame to electrical signals (a mass-frame system with a transducer that produces electrical signals usually being referred to as a seismometer) the way was open for the use of seismometer-galvanometer combinations to increase the sensitivity of seismographs and to allow frequency filtering to be applied to attenuate the main noise peaks. Most seismographs in current use are seismometer-galvanometer combinations and are of two main types: short period (SP) seismographs which record ground motion at frequencies of about 1 Hz (1 s period), that is frequencies greater than those of the oceanic microseisms, and long period (LP) seismographs which record ground motions with frequencies of about 0.05 Hz (20 s period), that is frequencies below those of the oceanic microseisms. In the SP band, compressional or P (Primary) waves from distances of > 3000 km are recorded with maximum signal-to-noise ratio; it is from the arrival times of these signals that the epicentres of most seismic disturbances are estimated. The main signals recorded by LP seismographs are surface waves which, as their name suggests, are waves that propagate along the surface of the earth and which diminish with depth below the earth's surface; P waves on the other hand are body waves that pass through the earth.

By the 1950's seismometers were available that were adequate for most seismological needs (1). However, in 1958 a conference held in Geneva (called the Conference of Experts) to look at ways of monitoring compliance with any treaty that might be signed to ban nuclear tests, concluded that the only way of detecting nuclear explosions fired underground was by the seismic signals they would generate; this led to intensive research on methods of detecting and identifying underground explosions by seismic means and included studies on ways of improving conventional seismographs. As a result of this work several new types of seismometer of high reliability and sensitivity were produced and by the middle of the 1960's well engineered LP and SP seismometers that were capable of recording down to the seismic-noise level over all the frequency range of interest, say, 0.01 to 10 Hz, were commercially available.

In 1959 responsibility for research in the UK on forensic seismology (that is on methods of detecting and identifying underground explosions) was given to AWRE*. Some work was done at AWRE on seismometer design in the early years of the research programme (2,3) but when seismometers of suitable design became available commercially this first phase of seismometer research at AWRE ceased.

The past 20 years have seen not only improvements in seismometers but also improvements in the methods of recording seismic data particularly with the introduction of magnetic tape recording. Initially magnetic tape recorders were used simply to record more or less the same data that was written on to conventional SP and LP visual seismograms. However, a better way to record data when a magnetic tape recorder is used is to record as wide a band of frequencies as possible and filter these data on playback as required, to obtain seismograms with optimum signal-to-noise ratio. Over the past 10 years a number of research groups, including that at Blacknest, have demonstrated that there are advantages in recording wide band (say, 0.01 to 5 Hz) seismic data with the whole bandwidth covered by one type of seismometer.

The simplest way to achieve wide band recording using electronic amplification is to use an LP seismometer. Such instruments are bulky and heavy (~ 80 kg) and sensitive to changes in temperature and pressure but environmental effects can be minimised by careful design, precision engineering and the provision of a large but rigid pressure-jacket with good thermal insulation. The research group at Blacknest has been operating such a broad band (BB) recording system since 1970 using high quality LP seismometers of conventional design (Geotech S-11's) and electronic amplification. Such has been the improvement in the design of LP seismometers since 1958 that, whereas early designs needed daily attention, two Geotech S-11's operated by Blacknest at two different sites have required no attention whatsoever for the past 8 years. (Some recordings from these instruments are shown in section 5.) Although the inertial mass in these instruments has drifted within the working range during operation, they have continued to operate satisfactorily because the magnet/coil transducers give an output that depends on the relative velocity of mass and frame (they are

---

*In 1959 AWRE was part of the United Kingdom Atomic Energy Authority. In 1973 AWRE was transferred to the Ministry of Defence. Over the whole of the time AWRE has been responsible for UK research in forensic seismology and since 1961 the bulk of the research has been carried out at Blacknest, an outstation of AWRE.

velocity transducers as opposed to displacement transducers which give an output proportional to the relative displacement of mass and frame) and so are not sensitive to long-term drift.

It has been demonstrated that the BB recording system described above can be used to simulate both SP and LP seismograms and use of this type of system has been advocated by the Blacknest group (4) as a way of getting SP, LP and BB seismograms without the need for separate SP and LP seismometers. Since November 1975 an array of four Geotech S-11 seismometers has been in operation at Blacknest producing broad band recordings. The response of these recording systems differs somewhat from that of the original BB system for, whereas the original system had a frequency response that was constant for constant amplitude of ground displacement in the pass band, the latest system has a response that is constant for constant amplitude of ground velocity in the pass band. As the response of a seismometer equipped with a velocity transducer is flat to ground velocity at all frequencies above the natural frequency, by simply applying a low noise amplifier to the output of a Geotech S-11 (natural frequency 0.05 Hz) gives a response that is flat to ground velocity over the major portion of the pass band of interest; this response that is flat to velocity is termed the Velocity Broad Band (VBB) response. The principle disadvantage of VBB systems built around conventional LP seismometers is that the seismometers are expensive and, being large, difficult to handle.

In the late 1960's it was suggested that LP seismometers could be made much smaller than those in current use by designing them to operate with electronic feedback and this stimulated new research programmes to design compact instruments that would allow both SP and LP recordings to be made from the same seismometer. Such miniature seismometers that would record all frequencies of interest would be much easier to isolate from environmental changes than large instruments; they could also be easily installed in boreholes. Installing seismometers in boreholes has two advantages:-

(a) The borehole reduces the effect on the seismometer of surface variations in temperature and pressure, and

(b) Seismic noise tends to decay with depth so that signals recorded from borehole seismometers should have larger signal-to-noise ratios than those recorded from surface instruments.

Various seismometers that would operate in boreholes and produce LP recordings were designed using conventional principles but none of these seem to have been entirely satisfactory.

More recently the Blacknest research group began a co-operative project with the Department of Cybernetics at the University of Reading to develop feedback seismometers and investigate the possible advantages of their use in wide band recording. The specific objective of this project was to develop a feedback seismometer that could be installed in a shallow 8 in. diameter borehole.

Two types of feedback seismometer were developed during the co-operative project. One system is based on a small commercially available SP seismometer (a Willmore Mk IIIA) which has been modified to operate as a feedback instrument; this instrument is known as the Mk IIIC. The second type of instrument is a borehole system built around mechanical systems developed by the University of Reading.

This report describes the design and development of the Mk IIIC system. The system has been thoroughly tested and is currently being installed at a network of sites in the UK (UKNET; see section 1.2). Examples of signals recorded by the Mk IIIC systems of UKNET are presented and the signals are compared with signals recorded by Geotech S-11 seismometers of the Blacknest array (BNA).

The report also discusses:-

(a) Some general problems of seismometer design and the advantages and disadvantages of seismometers that use feedback compared to those that do not.

(b) The optimum system for recording seismic data to make best use of the dynamic range of magnetic tape (particularly digital) recording systems.

The report also contains a detailed technical description of the Mk IIIC system (see Part 2, AWRE Report O25/83).

The borehole system which was built as part of the Blacknest-University of Reading project is currently undergoing further development and testing, and will be described elsewhere when development is complete. A brief history of the co-operative project is given below.

1.1 History of the development of the Mk IIIC seismometer

In 1966 Professor P B Fellgett of the University of Reading showed (5) that theoretically a seismometer could be designed with a performance equal to that of a conventional LP instrument but which used only a small suspended mass with a displacement transducer and feedback over the whole seismic band. (A number of seismometers and closely related instruments using feedback have been described in the literature (6-10) before 1966 but none of the instruments described was specifically for a seismometer using feedback over the whole of the frequency band of interest.) The practical realization of such an instrument was delayed mainly because the electronic amplifiers then available had electronic noise levels and drift rates which were too high. Stimulated by the publication in 1970 of the results obtained by Block and Moore (11), using a small quartz seismometer, Fellgett obtained a grant from the Natural Environmental Research Council in 1971 to develop a practical instrument. The project was assigned to I W Buckner under the guidance of M J Usher.

The financing of this project was taken over by AWRE in June 1974 by means of an Extra Mural Research Contract with the Department of Cybernetics, University of Reading and the contract continued until 1980. By June 1974 a small horizontal component feedback instrument had been constructed and tested. Further testing was then carried out during 1975 by installing the seismometer in the AWRE vault at Wolverton (see figure 1) and directly comparing the outputs with those of the Geotech S-11 seismometer system. The comparison showed that the performance of the feedback instrument was satisfactory (12,13).

However, the main requirement for AWRE was for a seismometer measuring the vertical component of the ground motion. Between 1971 and 1974 the University of Reading had designed and made several types of miniature vertical component mass/spring systems but none proved to be satisfactory. As the feedback principle had been proved with the horizontal instrument, the author suggested that our requirement for a vertical seismometer could most quickly and simply be met by modifying a Willmore Mk IIIA - a conventional SP seismometer - even though it has a large inertial mass of 1.3 kg (compared with the 40 g mass of the proved horizontal instrument).

Theoretical studies showed that the feedback system developed by the University of Reading should be capable of operating with a Willmore Mk IIIA and work began in 1975 on developing such a feedback seismometer; this work led to the development of the Mk IIIC. The prototype of the Mk IIIC was produced by Usher and Guralp of the University of Reading and ancillary circuits were designed at Blacknest to enable the instrument to operate with the standard Blacknest recording system. Usher, Burch and Guralp (14) described a laboratory version of the Mk IIIC that operates on mains power.

Further development and redesign has been undertaken to enable the complete system to operate unattended as a component of a network or an element of an array. Such a network is UKNET.

1.2 UKNET

The Mk IIIC system is designed to be powered from either mains or batteries and to transmit the output signals in FM form over either cables or British Telecom telephone lines to a recorder. The system has been tested in various modes of operation and several instruments are now in continuous operation. The most extensive use of the system has been in UKNET.

UKNET is a network of 9 stations (figure 1 and table 1) in the UK, eight of which are equipped with a Mk IIIC system and with the output signals transmitted over British Telecom lines to recorders at Blacknest. Five of the Mk IIIC systems are installed in Royal Observer Corps (ROC) posts and the equipment is powered by batteries; three stations of UKNET are at existing seismological stations and have mains power. The first three stations of UKNET were installed in the summer of 1981 and installation of the full network was completed by early 1983. The one non-standard station is that at an ROC post in Cornwall (SBD). The instrument is a conventional SP seismometer and is due for conversion to the Mk IIIC system in July 1983.

Two multiplexed frequency-modulated (FM) signals can be transmitted from each station. In routine operation these are a broad-band output which has a response as a function of frequency that is constant in the passband (0.02 to 4 Hz) to an input which has a flat amplitude spectrum for ground velocity (the response is very similar to the VBB response of the BNA) and an LP narrow band (LPNB) output which has a response that is sharply peaked at about 0.04 Hz. The

LPNB signal could be derived from the VBB signal after transmission but, as two channels are available from each station to Blacknest and the LPNB is easily formed at the station, it is convenient to transmit both VBB and LPNB signals.

At Blacknest the VBB signals are fed into a special purpose device to convert the FM signal direct to digital form without the need for demodulation (15). The LPNB signals however are first demodulated and the resulting analogue signals are then converted to digital form using a conventional ADC device. The VBB signals are written on to tape at 10 samples/s (giving a Nyquist frequency of 5 Hz) and the LPNB at 1 sample/s (giving a Nyquist frequency of 0.5 Hz).

1.3 BNA

The Mk IIIC system is now being used to increase the number of elements in this local array to 10. Additional sites are already in existence, and connected with mains power and telephone lines. Four sites in this array (figure 1 and table 1) have been in continuous operation since 1974 using Geotech S-11 long period seismometers to generate the VBB response. Two emplacements (BKN and WOL) are seismic vaults whereas the instruments at HD and BW are installed in large fibreglass containers with the seismometer 6 ft below ground surface. For the additional future installations the Mk IIIC instruments will be installed in 1 m length of 8 in. diameter steel pipe the top of which will be just below the ground surface.

TABLE 1

Co-ordinates of Broad Band Recording Sites

(a) UKNET

EKA	Eskdalemuir, Scotland	55.333N	3.159W
MMY	Middlesmoor, Yorkshire	54.176N	1.869W
CWF	Charnwood Forest, Leicester	52.738N	1.307W
LLW	Llanuwychllyn, Wales	52.849N	3.665W
LAM	Lampeter, Wales	52.114N	4.068W
SCK	South Creek, Norfolk	52.880N	0.751E
BHM	Barham, Kent	51.213N	1.174E
WOL	Wolverton, Hampshire	51.313N	1.223W

(b) BNA (Blacknest Local Array)

HD	Headley	51.358N	1.264W
BW	Bucklebury West	51.409N	1.225W
WOL	Wolverton	51.313N	1.223W
BKN	Blacknest	51.364N	1.187W

2. CONVENTIONAL AND FEEDBACK SEISMOMETERS

The design of a conventional seismometer depends on the component of ground motion to be measured. To measure vertical motion the mechanical system is usually a mass suspended by a spring; to measure horizontal motion some form of pendulum is usually used. For simplicity conventional seismometers are discussed below in terms of vertical-component instruments but most of the discussion also applies to horizontal-component seismometers.

A mass-spring system has a natural frequency of oscillation (ω_0) and once disturbed will, in the absence of any damping, oscillate for ever; such an instrument is of little use. Damping has therefore to be applied to turn the mass-spring system into a practical instrument for measuring ground motion; in a seismometer such damping is usually electrical. For ground disturbances with frequencies ω well above ω_0 the mass effectively does not move so that the relative motion of mass and frame is a direct measure of ground displacement. At frequencies well below ω_0 the relative motion of mass and frame decreases as $(\omega/\omega_0)^2$ decreases and at very-low frequencies the mass effectively follows the frame.

If the relative displacement of mass and frame at frequency ω is written $a \sin \omega t$, then their relative velocity is $\omega a \cos \omega t$ and so the output for a velocity transducer falls off with decreasing frequency for constant amplitude of relative displacement. Thus, at frequencies well below ω_0 the response to constant amplitude of ground displacement for a seismometer with a velocity transducer is proportional to $(\omega/\omega_0)^3$. This rate of fall-off can be used to advantage in an SP seismometer designed to detect signals of about 1 Hz and attenuate oceanic microseisms because by setting $\omega_0/2\pi \approx 1$ Hz, then microseism signals with frequencies of, say, 0.15 Hz will be reduced in amplitude relative to signals at 1 Hz by a factor of about $(0.15)^{-3} \approx 300$.

Seismometers with velocity transducers were originally designed to drive galvanometers for use with a photographic recording system (and many such instruments are still in operation) without any means of electronic amplification. The natural frequency of the galvanometer is also chosen to reject frequencies of ground motion where the signal-to-noise ratio is low. Thus, a 4 Hz galvanometer is often used with SP systems to reject high frequency man-made (sometimes called cultural) noise due to railways, traffic on roads, factories and so on. With LP seismometers, galvanometers are used with natural frequencies of about 0.011 Hz (90 s period) to give a "bass boost" effect and again attenuate ground motion at the frequencies of the seismic microseisms. Conventional LP and SP seismographs of the above type allow signals to be recorded in pass bands on either side of the oceanic microseism peak, that is in bands where the signal-to-noise ratio will usually be greatest. Examples of typical SP and LP responses are shown in figure 2. Note that in practice such LP systems do not attenuate oceanic microseisms very effectively.

The introduction of electronic amplification enables electronic filters to be used to attenuate oceanic microseisms and it might appear that it would be possible to take any seismometer and simply apply filters to shape any required system response. However, it is difficult to obtain satisfactory recording of LP ground motion using a conventional seismometer other than one with ω_o near or below the frequencies of the ground motion of interest. As noted above the output of a seismometer with a velocity transducer falls off as ω^3 below ω_o so if ω_o lies well above the frequencies of interest, the output of the seismometer will be low. Now in the LP pass-band, that is at frequencies of 0.05 Hz (20 s period) and smaller, electronic noise is proportional to ω^{-1} (this is the so-called 1/f noise) so that in trying to use a seismometer with ω_o well above the frequencies covered by the LP pass-band, not only is the output signal weak but electronic noise of conventional amplifiers tends to be large; to design an amplifier with electronic noise low enough to allow weak signals to be seen above the noise is difficult.

The effects of electronic noise can be reduced if a capacitance displacement transducer is used. For although at signal frequencies of a few Hertz both displacement and velocity transducers have the same signal-to-noise ratios, the ratio decreases for velocity transducers as the frequency of the signal decreases whereas for displacement transducers it remains constant. Capacitance transducers also have the advantage that they can be made small and light, whereas to obtain a high signal-to-system-noise ratio from a velocity transducer it must be physically large (a strong magnet and a coil of many turns).

It can be shown that a small SP seismometer (with $\omega_0/2\pi = 1$ Hz) with a displacement transducer can be made to have a performance at long periods equivalent to that of a large and more expensive conventional LP seismometer (with $\omega_0/2\pi = 0.05$ Hz) that has a velocity transducer. Thus, it would appear that by fitting a displacement transducer to an SP seismometer the required broad band seismometer could be produced. However, there are two disadvantages with such a system: (a) there is a corner in the response at $\omega_0/2\pi = 1$ Hz due to the natural frequency of the mechanical system and as this corner lies in the seismic band of interest it may be undesirable, and (b) a displacement transducer gives an output proportional to the slow drift of the mass from its initial position due to environmental changes and this results in large offsets on the signal-output voltage and in non-linearity.

It might be argued that at least the difficulty with the corner in the response could be overcome by making the natural frequency of the seismometer much greater than 1 Hz. Such a mass-spring system would be easy to construct but as the output is inversely proportional to ω_0^2 below the natural frequency, this would again result in poor signal-to-electronic-noise ratios.

Both the problem of the corner in the response in the pass band of interest and the problem of drift can be overcome by the use of electronic feedback. The feedback takes the form of a force that is applied to the inertial mass by a simple magnet/coil transducer which can be of low efficiency as the only requirement is that it produces a force proportional to the current through the coil. The force is arranged to be proportional to the relative displacement of mass and frame produced by the ground motion. The effect of the feedback is to attempt to oppose relative motion of the mass and frame which effectively stiffens the suspension and so increases the natural frequency of the seismometer. Provided that no extra noise is introduced into a system, the use of feedback does not change the signal-to-electronic-noise ratio so that in this way the acceptable signal-to-noise ratio of a 1 Hz seismometer is retained but with the added advantage that the corner in the response is now out of the signal band. In addition, drift of the mass is reduced as the sensitivity of the seismometer to environmental changes is proportional to $(1/\omega_0)^2$.

The use of feedback has other advantages as well as those given above; for example, the linearity of a seismometer using feedback is much better than the equivalent seismometer without feedback. Also because both the natural frequency and sensitivity of a feedback instrument depend principally on the feedback parameters, then the spring of the suspension system and the capacitance plates of the transducer do not have to be made with small tolerances and this simplifies manufacture.

The reduction in size that is possible with feedback seismometers is only limited in theory to the dimensions at which the Brownian noise of the suspended mass approaches that of the electronic noise of the transducer. This suggests that masses of the order of a few grams could be used (instead of kilograms for conventional instruments), although in practice it is necessary to increase the dimensions to the order of ~ 100 g in order to manufacture simple and reliable suspension systems.

2.1 Theory of force-balance feedback seismometers

2.1.1 Response to give a constant output to ground acceleration

To develop the theory of feedback seismometers we consider first the (open loop) response of a mass-spring system. The relationship between x_r the displacement of the mass relative to the frame and $\ddot{x}$ is given by

$$x_r/\ddot{x} = (s^2 + 2n_0\omega_0 s + \omega_0^2)^{-1},$$

where ω_0 is the natural frequency of the system, n_0 is the damping factor and s is the Laplace operator $\sigma + j\omega$. If a displacement transducer-amplifier combination with a sensitivity of A V/m is used to measure the relative motion of mass and frame, the output sensitivity is

$$v_0/\ddot{x} = A/(s^2 + 2n_0\omega_0 s + \omega_0^2), \qquad \ldots. \ (1)$$

where v_o is the output voltage. The frequency response of such a system is shown in figure 3.

Ignoring the effect of damping it can be seen that the response is flat to ground acceleration from 0 to f_o Hz (where $f_o = \omega_o/2\pi$) and has a sensitivity below f_o of A/ω_o^2 volts/m/s^2 (equation (1)). The response at frequencies above f_o falls off as ω^2, that is the response is flat for constant ground displacement.

For signal frequencies about f_o the response is dependent on the damping of the mass-spring system. For small seismometers this natural frequency is usually in the SP band at about 1 to 2 Hz. We now look at how f_o for a seismometer can be increased by using feedback; in this way the natural frequency of an SP seismometer can be moved to higher frequencies out of the pass band to give an output flat to ground acceleration through the entire range of seismic frequencies of interest.

A diagram of the force feedback seismometer is shown in figure 4(a). The amplified output of the displacement transducer is connected via a parallel RC combination to a force transducer (magnet/coil assembly with a sensitivity of G Newtons/Ampere) which is also mounted between the mass and frame. Such feedback seismometers are usually referred to as "closed loop" systems because part of the output is fed back around a loop; this distinguishes this type of seismometer from those without feedback which can thus be considered as "open loop" systems.

A block diagram of the system is shown in figure 4(b) showing a summing junction of the forces on the inertial mass. A simplified form is shown in figure 4(c) from which these forces can be equated as $M\ddot{x} - \beta V_o = V_o/KA$ which re-arranged gives the basic feedback equation of

$$\frac{V_o}{\ddot{x}} = M\left(\frac{KA}{1 + KA\beta}\right) = M\,\frac{(\text{forward path})}{(1 + \text{complete loop path})}.$$

This gives the seismometer voltage output sensitivity for ground motion acceleration. It is immediately seen that if $KA\beta \gg 1$, then it reduces to $V_o/\ddot{x} = M/\beta$, ie, only dependent on the feedback fraction

The parameters of figure 4(a) can be used to derive β as follows:-

The impedance Z of the RC combination is $R(1 + sCR)^{-1}$ and this allows a current i (= V_o/Z) to pass through the feedback coil and generate an opposing force of Gi Newtons. But β = force/V_o = Gi/V_o = G(1 + sCR)/R. Replacing K with $(M(s^2 + 2n_o\omega_o s + \omega_o^2))^{-1}$ and β with G(1+sCR)/R in the equation for the acceleration sensitivity shown above gives

$$V_o/\ddot{x} = A/(s^2 + (2n_o\omega_o + CAG/M)s + (\omega_o^2 + AG/MR)). \quad .... \quad (2)$$

If A, R and C are the only variables, then

(a) If $R \to \infty$ and $C \to 0$, the expression reverts to the open loop case.

(b) If $AG/MR \gg \omega_o^2$, the acceleration sensitivity of the seismometer at low frequencies (~ 0 Hz) is given by $v_o/\ddot{x} = MR/G$, that is the sensitivity depends on R only.

(c) The new natural frequency W_o is $(\omega_o^2 + AG/R)^{\frac{1}{2}}$ which is greater than ω_o; if $AG/MR \gg \omega_o^2$, then W_o depends mainly on A and R and not ω_o.

(d) The new damping factor N_o is $(2n_o\omega_o + CAG/M)/W_o$ and for $AG/MR \gg \omega_o^2$ then N_o depends on A, C and R.

From this it is seen that the order of selection is: calculate R to give the required sensitivity, A to give W_o and finally C to give N_o.

Suppose now we wish to choose the parameters of the Mk IIIC to have a sensitivity $v_o/\ddot{x}$ at 0 Hz of 10^4 V/m/s^2; a value of F_o(= $W_o/2\pi$) of 16 Hz and a damping factor N_o of 0.7. Assuming $AG/MR \gg \omega_o^2$, this requires R = 1.23 × 10^6 Ω, A = 1.01 × 10^8 V/m and C = 11.32 nF, the other parameters being typical values for a Mk IIIC seismometer of f_o = 1.67 Hz (ω_o = 10.49), n_o = 0.01, G = 160 N/A with M = 1.3 kg. The true values of the sensitivity, F_o and N_o, obtained using the above values of R, A and C are 9.80 × 10^3 V/m/s^2, 16.09 Hz and 0.697 respectively, that is the actual values differ from the chosen values by less than 1%.

The effects of varying the parameters A and R can also be seen using the Bode plot, as shown in figure 5. We set the displacement transducer and amplifier gain at 1.01×10^{8} V/m with a mechanical frequency f_0 of 1.67 Hz. If the circuit was operating "open loop", then the dc acceleration sensitivity would be $A/\omega_0^2 = 9.2 \times 10^5$ V/m/s ^{2} falling off as ω^2 above the natural frequency. This open loop response is shown by the line abe. The response that we have obtained using feedback is shown as the line cde intersecting the open loop response at frequency $F_0 = 16$ Hz and sensitivity = 10^4 V/m/s ^{2}.

If we keep the transducer gain (A) constant and alter the feedback resistor R to change the sensitivity, then the corner frequency will be determined by the geometry of the open loop response, eg, for a sensitivity of 10^5 V/m/s ^{2} we will obtain a corner at 5 Hz (line fge). In order to recover our original corner at 16 Hz at this new higher sensitivity we must increase the transducer gain A by a factor of 10 to give a new open loop response hij and a resulting closed loop feedback response fkj. However, we are not able to increase this gain A without limit; above a certain value the circuit is unstable and oscillates with the feedback applied. Fortunately this problem of stability is predictable and is discussed in section 2.2.

2.1.2 Response to give a constant output to ground velocity

It has been shown by several research groups that the optimum response for recording ground motion in the seismic band of interest is one that is flat to ground velocity. Such a response makes better use of the available dynamic range of both seismometer and recording systems and produces a roughly white spectrum of seismic noise in the frequency band of interest (see section 4.4). So far we have used feedback to shift the unwanted response corner out of the band but this leads to a response that is constant for constant ground acceleration.

A further disadvantage of this response is its high sensitivity to local cultural noise that generates signals that intrude into the high frequency end of the band. This sets the limit to the feedback circuit sensitivity which must not be allowed to overload. Conversion from the response flat to acceleration to that of velocity can be achieved by using a filter (integrator) external to the loop but this will not prevent the loop from overloading. For the Mk IIIC seismometers used in UKNET the conversion to a velocity response is made within the loop. The method makes use of the properties of the response of the basic seismometer when the damping term is large. Whereas figure 3 is shown as the response to acceleration it is now shown as the response to velocity in figure 6 but with $n_o \gg 1$.

For any value of the damping factor n_o the output at the natural frequency f_o is $(2n_o)^{-1}$ times the value predicted by the intersection on a log-log plot of the asymptote to the response at frequencies below f_o with the asymptote to the response at frequencies above f_o. If $n_o \gg 1$, then the response will be very nearly flat for ground velocity around f_o; the response is 3 db down at $2n_of_o$ and $0.5n_of_o$. Similarly for a closed loop system the velocity response will be flat around F_o with 3 db points at $2N_oF_o$ and $0.5N_oF_o$.

As shown earlier the damping of the feedback seismometer is determined by the value of the feedback capacitor C. Unfortunately increasing C to the value required to give the flat velocity response causes the loop circuit of this simple design to become unstable and extra circuit components must be included to prevent this instability.

2.2 Stability of the feedback loop

The basic block diagram is shown in figure 4(c) from which the relationship of the output to the input (transfer function) was determined as $V_o/\ddot{x} = MKA/(1 + KA\beta)$.

Although the feedback signal is assumed to be real and positive, it enters the negative summing junction of the forces to give negative feedback. For the seismometer circuit K, A and β are all functions of ω (the signal frequency) and have phase responses that vary with it. From the simple equation above it can be seen that if the phase of $KA\beta$ totals 180^o with its amplitude equal to unity, then V_o will become infinite and the system will be unstable. To estimate the stability of a system it is useful to plot the loop transfer locus. This is a polar graph plot of the transfer function of the complete loop ($KA\beta$) but with the feedback disconnected from the summing junction. Amplitude is plotted as radius against phase for signal frequencies from zero to infinity (see figure 7 which is also known as a Nyquist plot). The Nyquist criterion of stability determines absolutely whether the system will be stable or not but this is difficult to apply. The practical use of this plot is to determine the margin of stability. The system must become unstable if the locus passes through the point -1,j0. The two margins (phase and grain) are shown in figure 7 and empirical values that should be allowed to give satisfactory performance in its response to transients are that the phase margin should exceed 40^{o} and the gain margin should exceed 50%. The problems with stability mentioned in section 2.1.1 can now be visualised. For the acceleration response (section 2.1.1 and figure 5) the corner frequency was increased to W_o by increasing the loop gain A. The limit is approached as the gain margin goes to zero. For the velocity response (section 2.1.2 and figure 6) the damping n_o was increased to N_o by increasing the capacitor C. The effect of this is to increase the phase lag of the loop while the amplitude is still greater than unity and so reduce the phase margin. Thus, unless stability can be maintained by merely reducing the gain, components that generate a phase lead must be added to the circuit to decrease the phase lag. As will be seen later (section 3) this does affect the overall response ($V_o/\dot{x}$) and results in small perturbations in the flatness of the response in the passband.

2.3 Calibration of seismometer systems

The requirements and methods of calibrating seismographs depends on the response under investigation. For conventional SP systems it is often considered sufficient to determine the seismometer output sensitivity and damping characteristics in the laboratory, assume its response by checking the natural frequency of the instrument in the field, and to thereafter calibrate only the electronic amplifiers, usually at only one specified signal frequency. This is the method used at the AWRE sponsored SP array stations and is only acceptable because the recordings are used mainly for event detection purposes and for approximate amplitude measurements which are taken from an impulsive waveform. This is not so for LP system recordings where not only is the amplitude of the dispersed surface waves required over a wide band, but their analysis requires their detailed phase relationship as modified by the recording system. The problem is made worse by the use of the electronic filters with sharp attenuation characteristics within the band that are used in the LPNB systems. The system (complete with inertial mass) can be calibrated for both amplitude and phase if a seismometer is equipped with a "calibration coil".

The calibration coil consists of relatively few turns which are normally wound on the same former as the main data coil output. Thus, the coil is a force transducer generating a force directly on to the inertial mass proportional to any current passing through the coil. This constant is known as the motor constant G_c for the magnet and coil combination and is only dependent on the strength of the magnetic flux and the number of turns of the coil that is in the flux. If a current i Amperes is passed through the coil, the force developed on the inertial mass M is $G_c i$ Newtons and is thus equivalent to a ground motion acceleration of $G_c i/M$ m/s^2.

One method of calibration is to apply a current step to the coil and then, after say 2 min, remove it. The resulting waveform is shown in figure 8. Daily calibrations of this kind are easy to automate and allow a simple visual check to be made on the operation of the system. The waveform can in principle be analysed using Fourier techniques to obtain the amplitude and phase response of the seismograph. In practice, this method gives poor results due not only to the presence of seismic noise on the recording but also to the fact that the input signal (the step of acceleration) is predominantly that of a very low frequency fundamental with decreasing amplitudes for the higher frequency signals.

A second method uses sinusoidal input currents as the driving force. A sine wave of constant amplitude and frequency is applied to the coil and after allowing several cycles of oscillation for the transients to decay to zero the steady state amplitude of the system output can be measured with its phase relative to the input current. The response can thus be determined for any signal frequency in the band. In practice, the theoretical response of the system is known and this sinusoidal current method is used only to check the amplitude response at a few spot frequencies.

The calibration methods described above are routinely used for both conventional and feedback seismometer systems. Unfortunately this simple procedure will not detect any change in sensitivity for the feedback system that would be recognised with a conventional seismometer system. Consider the simplified signal and calibration circuits for the conventional and feedback instruments shown in figures 9(a) and (b). As stated above the value of the calibration coil constant G_c is a function only of the number of turns in the winding and the strength of the magnet. Suppose the magnet strength is halved, then the sensitivity of the conventional system will be halved as will the motor constant G_{ca} of the calibration coil. This will result in output calibration signals with an amplitude of one-quarter of those previously obtained. The sensitivity of the feedback system will have doubled because, as shown in section 2.1, the sensitivity is MR/G. But the motor constant of the calibration coil G_{cb} is again halved and so the resulting output calibration signals will have an identical amplitude even though the sensitivity has doubled.

In some small feedback seismometer systems a common coil is used for both the feedback and for calibration; this does not alter the above reasoning but leads to the single equivalent diagram of figure 9(c). For very low frequencies, if the input calibration current is derived from a generator of V_{in} volts and passed through a resistor of equal value to the feedback resistor R_F, then the output signal voltage will be numerically the same value but reversed in sign. This again demonstrates the failure of this calibration system to detect changes in sensitivity.

Therefore if the calibration coil system is to be used with confidence with feedback systems, the force transducer must be completely independent of the feedback coil with its own separate magnet. If this is not possible, then the calibration coil only needs to be routinely relatively calibrated with the feedback connection disconnected (open loop). For an instrument with separate coils (such as the Mk IIIC), this open loop method becomes the same configuration as the conventional seismometer system (figure 9(a)) where the feedback coil is now used as a signal (data) coil (G_D), the output from which is amplified and the waveform that results from a current step is observed as in figure 8 but of an oscillating nature due to the lack of damping.

For an instrument with only one coil the output from the displacement transducer can be taken and displayed. This signal will consist of an oscillating waveform superimposed on a step displacement of the recording due to the displacement of the mass. For both types of instrument a direct check on the natural frequency of the seismometer suspension and its damping is an additional feature of this method.

3. THE SIGNAL CIRCUITS OF THE MK IIIC FEEDBACK SEISMOMETER SYSTEM

The principal components of the seismometer signal circuits are shown in figure 10. Full circuit diagrams and component values are given in Part 2 (AWRE Report O25/83).

The displacement transducer is a differential capacitor; the outer two capacitor plates (upper and lower) are attached to the frame of the seismometer and the inner plate is attached to the mass. In the absence of ground motion the spring supporting the mass is adjusted so that the inner plate is in a central position between the two outer plates. When an acceleration is applied to the frame, it moves and the mass tends to remain in a fixed position with the result that the inner plate is displaced from its central position.

The method used to measure the displacement is to apply a constant amplitude carrier signal of 50 kHz to each of the outer plates but with opposite phase. This results in zero voltage output when the inner plate is central. Displacement of the inner plate gives a 50 kHz output signal with its amplitude proportional to the displacement and with a phase shift relative to the drive oscillator of 0 or π depending on whether the central plate moves up or down respectively.

The output of the differential capacitor is now fed via a preamplifier and two high-frequency amplifiers (together called the channel amplifier) to a circuit known as a phase sensitive detector that converts the 50 kHz output signal into an analogue voltage that is directly proportional to the displacement.

The analogue signal is then passed through a "controller" stage whose purpose is to ensure stability of the feedback loop and optimise its performance. In the absence of this stage the feedback current and hence the force would be proportional to the analogue voltage signal of the mass displacement. The addition of a capacitance in the feedback of the controller amplifier integrates the signal at low frequencies and in this form is known as a Proportional plus Integral (or P + I) controller. The advantages of the addition of integral control are two-fold: the infinite gain as $\omega \rightarrow 0$ allows a large amount of feedback to be employed with safety as the phase margin is 90° (as will be seen later), and the response of the system to a disturbance is enhanced, allowing the system to recover in a minimum time. A further addition to this controller is a phase lead circuit consisting of a resistor and capacitor in parallel. The purpose of this arrangement is to maintain stability of the loop.

The output of the P + I stage, which is referred to as the acceleration (ACC) output of the system, is now fed back via a resistor and capacitor in parallel to one of the main velocity transducer coils of the original Mk IIIA seismometer.

Provided that the gain in the feedback loop is high, the ACC output is flat to ground acceleration from zero frequency to 0.05 Hz (20 s period); from 0.05 to 10 Hz the ACC output is proportional to ground velocity.

The output of the main feedback loop is now fed to a high pass filter to remove any dc offset in the ACC signal before further amplification. (This dc offset is due to drift in the stiffness of the suspension spring supporting the mass and is caused mainly by temperature variations in the seismic vault.) This filter is a simple high pass stage with a corner at 0.05 Hz; combined with the corner at 0.05 Hz of the main feedback loop the resulting output at this stage is equivalent to the output from a LP (open loop seismometer) with a natural frequency of 0.05 Hz (20 s period), a damping factor of 1 and a velocity (magnet/coil) transducer. The output at this stage is referred to as the VEL output.

The VEL output is the principal output of the Mk IIIC system. To allow the signals to be recorded on digital recorders at 10 samples/s (giving a Nyquist of 5 Hz) the VEL signal is passed through anti-aliasing filters to give the VBB output; these are low pass filters cutting off at about 4 Hz and are described in detail later.

To obtain the LPNB output the VEL output is passed through a further series of filters and amplifiers; these filters and amplifiers are described in section 3.3.

The response of the circuit of the system is now considered in detail in three parts: the force feedback loop circuit, the overall signal response when the loop is closed, and the filters following the loop. The method that is used is to derive the "transfer functions" of the various stages from which the poles and zeros can be obtained and then to operate with these together with the corresponding multipliers.

The transfer function of a system or part of a system relates the output signal to its input. It is usually a function of the complex signal frequency s but the input and output need not be the same physical quantities although it is assumed that the input has the form Ke^{-st}. In general, any transfer function of a linear system can be written in the form $A(a_o + a_1 s + a_2 s^2 + \ldots a_m s^m)/(b_o + b_1 s + b_2 s^2 + \ldots b_n s^n)$. The roots of the numerator (called zeros), together with the roots of the denominator (called poles) and the constant multipliers, can completely specify the transfer function.

A zero is defined as the value of the complex frequency s which makes the transfer function numerically equal to zero, while a pole is defined as the value of s which makes it infinite.

3.1 Transfer function of the force feedback loop

A block diagram of the feedback circuit is shown in figure 11(a). Simplified circuits with component values and transfer functions of two of the units in the loop are shown as figures 11(b) and 11(c). The transfer functions of the displacement transducer and preamplifier are derived in appendices A and B. As the bandwidth of these components is very wide they can be coupled with the gain of the wide-band channel amplifiers and phase sensitive detector and then represented by a transducer with a transfer function of K volts/m independent of frequency. The transfer function of the elements in the forward path are referred to as T_F and those in the return path as T_R.

The relative amplitude and phase of the returning force into the force balance determines the stability of the circuit when the feedback loop is closed (section 2.2). We first consider the transfer function of the whole loop $T_L = T_F T_R$ assuming that the returning force is not connected to the balance point. Note that for these calculations the position around the loop of the final circuit output V_{OUT} is immaterial and only for convenience has the total loop been split into T_F and T_R; that is the voltage output signal when the loop is closed will not affect the stability. From figure 11(a) it can be seen that T_F is given by $M^{-1}(s^2 + 2n\,\omega_o s + \omega_o^2)^{-1} KC(s)$ and T_R by D(s). C(s) and D(s) are given in figures 11(b) and (c) respectively. The poles, zeros and frequency independent multipliers of T_F, T_R and hence T_L are given in table 2. For this reason a method of estimating the response is now given using the geometry of the s plane to enable the effects of adjusting circuit components to be predicted in order to maintain stability. (A text book covering pole, zero constellations and s plane geometry is given as reference (16).) The left-hand side of the s plane is given in figure 12 showing the relative positions of the constellation of poles and zeros. Inspection of this figure allows a straight line Bode plot to be constructed for the amplitude response and an estimate of the phase response to be plotted. These approximate responses are shown in figure 13. It is seen that the Bode response is flat from $0.28 < \omega < 10$. An estimate of the amplitude of T_L over this region can be found by choosing a value of s in the centre of this band as, say, $|s| = 2$. It is seen from the transfer function T_L that, with the exception of the two factors $(s + 0.28)$ and s, the roots are much larger than s, thus allowing the factors to be replaced by these roots. The amplitude response is thus given by the real part of this simplified transfer function $14.2\ s^{-1}(s + 0.28)$ which for $|s| = 2$ gives 14.1. Figure 13(a) also shows the amplitude response calculated from the exact transfer function; it can be seen that in the band from about $\omega = 0.4$ to $\omega = 7$, the response is close to 14.1, the rough estimate.

TABLE 2

Poles and Zeros of the Transfer Functions of the Forward and Return Paths of the Feedback Loop

		Poles	Zeros
1.	Forward Path (T_F)		
		(-0.09556, + 10.618)	(- 14.71, 0.0)
		(-0.09556, - 10.618)	(-119.0, 0.0)
		(0.0, 0.0)	
		(-666.7, 0.0)	
		(-12,024, 0.0)	
		Multiplying factor = 2.117×10^{10}	
2.	Return Path (T_R)		
		(-7108, 0.0)	(-0.2806, 0)
		(-80.2, 0.0)	
		Multiplying factor = 197.5	
3.	Loop Path $T_L (= T_F T_R)$		
		Sum of 7 poles plus 3 zeros given above	
		Multiplying factor = 4.182×10^{12}	

Figure 13(b) shows the estimated phase response compared with the response calculated from the exact transfer function. The agreement between them is good over the seismic band of interest. The major disagreement occurs at $\omega > 100$ and can be accounted for by the omission from the estimate of poles at 7000 and 12000.

The exact amplitude and phase responses are combined to give a Nyquist plot which, due to the large range in amplitudes involved, is shown in three sectional graphs as figures 14(a), (b) and (c). Figure 14 (c) shows that the system will be very stable as the gain margin is 98% and the phase margin is 60^o. (Also plotted on this graph as a dashed line is the corresponding response for the gain increased by a factor of 20.) Now the gain margin is seen to be 65% but the phase margin is reduced to only 20^o and the system will be unstable. Further discussion on the open loop transfer function is postponed until the response that results from closing the loop has been derived.

3.2 Transfer function of the closed loop system (ACC output)

With the loop closed the voltage signal output V_{OUT} is related to the force at the balance point by the expression $V_{OUT}/\text{Force} = T_F/(1 + T_F T_R)$ from which the transfer function of V_{OUT} relative to ground acceleration $\ddot{x}$ can be derived as $V_{OUT}/\ddot{x} = M\ T_F/(1 + T_F T_R) = M\ T_F/(1 + T_L)$.

To evaluate the poles and zeros the closed loop transfer function requires the solution of a 7th order polynomial to find the poles of the transfer function and a 4th order polynomial to find the zeros. In addition, evaluation of the coefficients of the powers of s in these polynomials is tedious; a sensible way to find the coefficients and the roots is to use a computer program. A series of three programs have been used here to set up the coefficients, find the roots and evaluate the transfer function.

The main purpose of the first program of the sequence (FBD written in BASIC) is to form, from the values of the circuit components, the coefficients of the polynomials in s that make up the closed-loop transfer function. The program FBD also allows the poles and zeros of T_L to be evaluated (table 2); these are required to determine if the feedback system will be stable when the loop is closed.

Given a stable system FBD gives the coefficients of the polynomial in s and POLRT (written in FORTRAN) finds their roots (table 3). Programs ROF and ROT (written in BASIC) can then be used to evaluate the transfer function as a function of frequency and period respectively. As well as the usual amplitude and phase (ϕ) response, phase correction ($\phi(\omega)/\omega$ in seconds) and group delay ($d\phi(\omega)/d\omega$ in seconds) as a function of frequency are also given. The amplitude response is plotted in figure 15(a).

TABLE 3

Poles and Zeros of the Closed Loop Acceleration Response (ACC Output)

Poles	Zeros
(-0.2618, 0.0)	(-14.70, 0.0)
(-18.39, 0.0)	(-80.34, 0.0)
(-68.18, 62.91)	(-119.0, 0.0)
(-68.18, -62.91)	(-7.107×10^3, 0.0)
(-542.5, 0.0)	
(-5.996×10^3, 7.443×10^3)	
(-5.996×10^3, -7.443×10^3)	

Total 7 poles 4 zeros

Multiplying constant to give output in $V/m/s^2$ is 2.752×10^{10}

The amplitude response expresses voltage output for given ground acceleration. By adding a further zero the response in terms of ground velocity can be computed and by adding two zeros at zero the response in terms of ground displacement is obtained. This response to ground velocity is shown in figure 15(b).

At $\omega = 0$, $T_F \rightarrow \infty$ due to the capacitor in the feedback path around the amplifier in the (P + I) stage. Thus, the acceleration sensitivity, $V_{out}/\ddot{x} \rightarrow MT_R$. Also at $\omega = 0$ the effect of the inductance of the coil (L) becomes zero so that T_F reduces to $G/(R_6 + R_7)$ and substituting for the component values $V_{out}/\ddot{x} \rightarrow 1.34 \times 10^4$ V/m/s^2. From figure 15(a) the value at 100 s is seen to be 1.30×10^4 V/m/s^2.

It is seen from figure 15(b) that the response has a peak at $T < 0.1$. The origin of this peak can be understood from the Bode amplitude plot for the closed loop system (figure 16). The peak is seen to originate from the zero at (- 80.3,0); ideally this zero should be at position (σ, 0) where $\sigma << -93$ and so would be cancelled out by the effect of the poles at (-68,± 63). Similarly the zero at (-14.7,0) and the pole at (-18.4,0) should ideally coincide and cancel out. The changes that would be required to the circuit components to minimise the effects of the zeros at (-80.3,0) and (-14.7,0) can be determined as follows. Rewriting factors of the form $(s + p_i)$ as P_i and $(s + z_i)$ as Z_i in the transfer functions of T_F and T_R, where P_i and Z_i are respectively the pole and zero positions, then T_F can be written as $K_1 Z_1 Z_2/(P_1 P_2 P_3 P_4 P_5)$ and T_R as $K_2 Z_3/(P_6 P_7)$; K_1 and K_2 are simple multipliers. Then the closed loop transfer function becomes

$$MK_1 Z_1 Z_2 P_6 P_7 / (P_1 P_2 P_3 P_4 P_5 P_6 P_7 + K_1 K_2 Z_1 Z_2 Z_3).$$

Thus, the four zeros in the closed loop transfer function are the two zeros of T_F and the two poles of T_R. The zero at (-80.3,0) was originally the pole at (-80.3,0) and is equal to $(R_7 C_4)^{-1}$. The pole position could be made more negative by decreasing C_4 but this would require a corresponding increase in R_6 to maintain the corner at 0.262 $(R_6^{-1} C_4^{-1})$. Such a change in R would increase the closed loop sensitivity by the same ratio and the position of the poles at (-68, ± 63) would also change. In practice, the small peak in the response due to the zero at (- 80.3,0) is not of practical importance as the peak is outside the seismic passband of interest and would only be a problem if the system was operated at very high gain in an environment subject to cultural noise. Similarly, the difference in position of the pole and zero at $\omega \approx 15$ is also difficult to minimise but fortunately is not significant in operation although it is in the passband of interest.

Figure 17 shows the responses of six instruments. It can be seen that, although the open loop gains vary from 0.34×10^6 to 1.05×10^6 V/m, the output sensitivities differ by only 3% in the signal passband (0 to 10 Hz).

The variation at $T < 0.1$ ($f > 10$ Hz) is almost entirely due to the variation of this open loop gain. If this gain was reduced to 10^5 V/m, then the attenuation will increase at higher frequencies but will cut into the band of interest; if it is increased, then the response will progressively peak towards the higher frequencies and with a value of 10^7 V/m will become unstable with a gain margin of 37% (decreasing to 0 at 1.6×10^7 V/m) and a phase margin of only 10°.

3.3 Transfer function of the signal circuits following the main feedback loop

(The references to circuit stages are for diagrams in Part 2, AWRE Report O25/83.)

To obtain the VEL output, the output of the feedback loop is fed through a combined highpass filter and amplifier stage (IC9 in figure 8 of Part 2). The resulting VEL signal is fed as the common input to both the VBB and LPNB filters which are shown in figure 10 of Part 2. The VBB filter consists of two lowpass stages (IC1 and IC3) followed by an amplifier stage IC5. The LPNB filter consists of three lowpass stages (IC2, 4, 6), one highpass stage (IC8) and an amplifier stage (IC9). The transfer functions of the common ACC to VEL filter, VBB and LPNB filters are given in table 4 (a), (b) and (c) respectively together with the poles, zeros and multiplier factors.

The transfer function for the final outputs (VBB and LPNB) must include those for the closed loop seismometer (given in table 3) plus those in table 4(a) plus 4(b) or 4(c). The sum of these poles and zeros will give the outputs in terms of V/m/s^2. It is more conventional to use the output of the VBB trace in terms of ground velocity (V/m/s) and this is achieved by adding a single zero at the origin (0,0).

The LPNB output is more usually used as a magnification, ie, response to ground displacement. Addition of a second zero at the origin (0,0) will give an output in terms of V/m and to convert to the dimensionless magnification requires the constant multiplier to be divided by 100. This magnification is the value when the analogue electrical signal is replayed on to a pen recorder at a sensitivity of 1 cm deflection per volt.

To summarise the total number of poles and zeros required for:-

ACC output to ground acceleration	is 7 poles + 4 zeros	to give	V/m/s^2,
VEL output to ground velocity	is 9 poles + 7 zeros	to give	V/m/s,
VBB output to ground velocity	is 13 poles + 7 zeros	to give	V/m/s,
LPNB output to ground displacement	is 17 poles + 10 zeros	to give	V/m.

TABLE 4

Transfer Functions of the Circuits Following the Feedback Loop

Stage/IC Number	Transfer Function	Equivalent Damping	Equivalent Natural Frequency $\omega_o(T_o s)$	Pole Locations	Zero Locations	Multipliers
(a) ACC to VEL						
High Pass Filter	$\dfrac{s\{s + (R_2 + R_3)/R_2R_3C_2\}}{\{s + (R_1C_1)^{-1}\}\{s + (R_3C_2)^{-1}\}}$	-	0.314 (20 s)	(-0.3135,0)	(0,0)	1
(IC9; figure 8 of Part 2)				(-1000,0)	(-26640,0)	
			Total =	2 Poles	2 Zeros	Multiplier = 1
(b) VBB Filter						
4 Hz Low Pass Filter (IC1, figure 10 of Part 2)	$\omega_o^2/(s^2 + 2\eta\omega_o s + \omega_o^2)$	1.0	24.42 (0.26 s)	(-24.42,0) (-24.42,0)	- -	596.3
4 Hz Low Pass Filter IC3, figure 10 of Part 2)	$\omega_o^2/(s^2 + 2\eta\omega_o s + \omega_o^2)$	0.377	24.33 (0.26 s)	(-9.181,22.5) (-9.181,-22.5)	- -	592.1
Amplifier (IC5, figure 10 of Part 2)	$(R_6 + R_5)/R_5$	-	-	-	-	10.1 old (2.471) new
			Total =	4 Poles	No Zeros	Product of Multiplier for VBB $= 3.566 \times 10^6$ old $= (8.724 \times 10^5)$ ne

TABLE 4 (Continued)

Stage/IC Number	Transfer Function	Equivalent Damping η	Equivalent Frequency $\omega_o(T_o s)$	Pole Location	Zero Location	Multiplier
(c) LPNB Filter						
1/IC2 (figure 10 of Part 2)	$\omega_o^2/(s^2 + 2\eta\omega_o s + \omega_o^2)$	0.7071	0.2074(30.30)	(-0.14663, + 0.14663) (-0.14663, - 0.14663)	- -	0.042999
2/IC4 (figure 10 of Part 2)	$\omega_o^2/(s^2 + 2\eta\omega_o s + \omega_o^2)$	0.5767	0.2953(21.28)	(-0.1703, + 0.2413) (-0.1703, - 0.2413)	- -	0.08721
3/IC6 (figure 10 of Part 2)*	$\omega_o^2/(s^2 + 2\eta\omega_o s + \omega_o^2)$	0.5767	0.2953(21.28)	(-0.1703, + 0.2413) (-0.1703, - 0.2413)	- -	0.08721
4/IC8 (figure 10 of Part 2)	$s/\{s + (C26(R24 + R25))^{-1}\}$	-	0.03157(199)	(-0.03157, 0.0)	(0.0, 0.0)	1.0
5/IC9 figure 10 of Part 2)	$\dfrac{\{s + ((R33 + R34 + R35)/(R33 + R34)R35C35)\}}{\{s + (R35C35)^{-1}\}}$	-	-	(-25.64,0.0)	$(-1.003 \times 10^4$,0.0)	1.0
			Total =	8 Poles	2 Zeros	Multiplier 3.2703×10^{-4}

*Stage 3 is identical to Stage 2.

The response curve for the VBB output for ground velocity is shown as figure 18(a) and that for the LPNB output for ground displacement is shown as figure 19(a). The curves for the phase, phase correction and group delay for each response is shown as figures 18(b), (c) and (d), and 19(b), (c) and (d).

4. DYNAMIC RANGE OF THE SEISMOMETER AND RECORDING SYSTEM

The range of amplitudes of seismic signals and noise is very large; for example, the rms amplitude of the noise in the pass band 0.025 to 5 Hz at a quiet site (Queens Creek, Arizona) is about 20 nm (17), whereas the peak signal amplitude recorded in this band at 30^{o} from a magnitude 8 earthquake is 3×10^{4} nm. So that to record both signals with amplitude close to the noise level and those from magnitude 8 earthquakes requires a recording system with a dynamic range of over 80 db. Only digital recording systems have such large dynamic ranges, the dynamic range of analogue recorders being only about 50 db.

If the purpose of a recording system is simply to produce a seismogram of all signals without clippping, then it is enough to record the seismometer output at several magnifications (gains); the small amplitude signals will then be available on the high-gain channel and the large amplitude signals on the low gain channel. However, if small signals are to be detected in the presence of large signals, as is required by the system described here, then such a gain ranging system is useless and the data have to be recorded on a single channel of high dynamic range.

Even when a recorder with a true dynamic range of 80 db is used to record the output of a seismometer the full dynamic range of the system - in seismological terms - is not necessarily 80 db. The principal reason for this is that the spectra of the system noise, seismic noise and seismic signals usually have different shapes and dynamic range can be defined in different ways depending on the assumptions made about the spectrum of the smallest and largest signal the system has to record.

In this section various definitions of dynamic range are considered and it is shown that there are several ways that dynamic range can be specified. Those quantities that seem to be the most useful for the seismograph system described in this report are then derived.

There are several dictionary definitions of dynamic range, for example:-

(a) For radio: "The range of intensities in a sample of radio programme ... as measured on a meter ... expressed in decibels" (18).

(b) For television: "The ratio of maximum to minimum brightness in the original or reproduced image" (18).

(c) "Of a transmission system, the difference in decibels between the noise level of the system and its overload level" (19).

Definitions (a) and (b) use measurements of the signal, whereas (c) specifically admits and includes the system noise. None of the definitions specifically includes the frequency band to be used or the sensitivity level, although both are implied. Based on (c) a further more specific definition could be: the further gain required in order to make the noise level of the system just overload its output. However, this also does not take into account the spectral content of the required signal. It is suggested therefore that elements of (a) and (c) should be combined to give a definition of dynamic range for a seismometer system as: <u>the ratio of the largest seismic signal that can be recorded without overloading to the smallest seismic signal which has its power spectral density not less than that of the system noise at any frequency in a specified frequency band using a specified response and sensitivity</u>.

Ideally the dynamic range would be expressed in terms of seismic magnitude - the scale used by seismologists to measure the size of seismic sources. The definition of magnitude varies somewhat depending on epicentral distance and wave type but all magnitude formulae have the general form

$$M = \log_{10} (A/T) + B(\Delta,h),$$

where A is the amplitude of ground motion in microns, T the period and $B(\Delta, h)$ a term that corrects for the decay of amplitude with distance (Δ) and for depth of focus (h). The dynamic range of a seismometer system in terms of some particular magnitude scale could thus be specified as covering the range M_{min} to M_{max} for sources at epicentral distance Δ^{o}, where M_{max} is computed from the largest seismic signal that can be recorded by the system and M_{min} the smallest seismic signal where largest and smallest are as defined in the previous paragraph.

To apply the definition of dynamic range described above requires that not only must the spectrum of the largest (just not overloading) seismic signal be known but also that of the smallest. The spectrum for the system noise must also be known. Whereas for an open loop seismometer this spectrum can be obtained by recording the output of the system at high gain with the seismometer mass "blocked" (to eliminate the earth motion signal), for a feedback system this is not possible as the system would then revert to an open loop system with very high gain. If the noise due to environmental effects and the mechanical stability of the mass/spring system is ignored, the system noise can be estimated by calculating and summing the noise spectra of the major components of the electronic circuits and of the Brownian motion of the suspended mass, the latter noise source being the fundamental limit to the detection of ground motion.

With a properly designed system the maximum output will only be limited by the maximum excursions at the output stage and this will be directly related to the voltage V of the power rails. If A(f) is a power spectrum for ground acceleration in $(m/s^2)^2/Hz$ and R(f) is the responsivity of the system that is the factor in $V/(m/s^2)$ that converts from ground acceleration to volts at frequency f, then $R^2(f)A(f)\delta f$ gives the voltage power output over a small frequency band δf. The total voltage power output in the pass band V_o^2 between f_1 and f_2, the band of interest, is given by

$$V_o^2 = \int_{f_1}^{f_2} R^2(f)A(f)df.$$

The rms amplitude is then V_o. For a signal that has a random phase - that is the signal can be treated as noise - then the maximum peak to peak signal assuming a Gaussian distribution of amplitude will only exceed the rms amplitude 1% of the time. Thus, if the output-stage power rails are $\pm$ V volts, then if clipping is not to occur, $3V_o$ must be slightly less than V.

Similarly if B(f) is the power density of the smallest seismic signal that can be recorded (where smallest is as defined earlier), then the signal voltage power at the output is

$$V_L^2 = \int_{f_1}^{f_2} R^2(f)B(f)df,$$

so that the ratio of the powers of the largest to smallest signal is $V_o^2/9V_L^2$ and the ratio of these amplitudes is $V_o/3V_L = V/V_L$. From the above discussion it can be seen that the dynamic range is proportional to the output stage power rail voltages and inversely proportional to the responsivity (or "gain") of the system.

The dynamic range of a seismometer system can be increased by reducing the bandwidth. At the upper end of the range the smaller $(f_2 - f_1)$, the larger A(f) can be before the signal clips. At the lower end of the range the smallest signal that can be recorded in a given bandwidth is that for which at some frequency the signal-to-system-noise ratio is unity (but is nowhere less than unity). If now the bandwidth is reduced, this may cut out the frequency where the signal-to-system-noise is unity, thus enabling the bottom of the dynamic range to be lowered to the level set by the size of signal that has a signal-to-system-noise ratio of unity at some frequency in the new band.

4.1 System noise

4.1.1 Brownian noise

The fundamental limit to the detection of ground motion is set by the Brownian motion of the mass. It is shown in appendix B that for a frequency band δf the noise equivalent acceleration for a mass M, natural frequency f_o, and damping factor n is $(8\pi kTf_o n\ \delta f)/M$ where k is Boltzman's constant (1.38×10^{-23} J/°K) and T is the absolute temperature. (Using the values of M, f_o and n for the Mk IIIC gives a noise equivalent acceleration in power of 2.66×10^{-21} $(m/s^2)^2/Hz$.)

4.1.2 Transducer noise

The capacitance transducer within the seismometer is a source of noise. To determine the contribution from the transducer consider figure 20 which shows the circuit both in its actual form and as a simplified equivalent circuit. The series noise equivalent resistance R_n of the circuit is given by

$$R_n = R_{nv}[\{(C_e + C_s)/C_s\}^2 + (\omega^2 C_s{}^2 R_e{}^2)^{-1}] + (\omega^2 C_s{}^2)^{-1}(R_{ni}^{-1} + R_e^{-1}),$$

where the symbols are as defined in the caption to figure 20. Using the numerical value for the circuit elements (see figure 20) then at its operating frequency (~50 kHz) R_n is about 4 k Ω. The noise equivalent acceleration (in power) is shown in appendix C to be $4R_n kT\delta f \{(s^2 + 2n\omega_o s + \omega_o^2)/r\}^2$ where r is the sensitivity of the displacement transducer in V/m. At long periods this becomes $(\omega_o^2/r)^2\, 4R_n kT\delta f$. With $r = 5 \times 10^3$ V/m, $\omega_o = 10.68$ rad/s then at long periods the noise (power) equivalent acceleration is $3.37 \times 10^{-20}\ (m/s^2)^2/Hz$. Above the natural frequency the noise increases as ω^4 (40 db/decade).

4.1.3 Filter noise

Consider now the instrument noise in the LPNB system. The system has a bandwidth of only 0.04 Hz (40 to 15 s period) so that using the value for the transducer noise given above (and neglecting the Brownian noise which is an order of magnitude smaller) the total noise power out of the seismometer is $1.4 \times 10^{-21}\ (m/s^2)^2$. At a sensitivity of 1.3×10^4 V/m/s^2 this gives 5×10^{-7} V rms at the ACC output. Assuming that the maximum signal (with a spectrum the same shape as that of the transducer noise in the band 40 to 15 s period) could be 8.5 V rms, the amplitude range is 1.7×10^7. To digitise the signal at this point and take full advantage of the dynamic range requires the number of bits to be > m where m is given by $2^m = 1.7 \times 10^7$, that is 24. A digitiser with 24 bit resolution is not readily available. It will be shown that the system noise approaches that of the seismic noise in the LP band. For the purpose of detecting signals in the seismic noise it is necessary to amplify the signals in order to record them at this level (and to include the system noise) with the 16 bits of resolution that are available.

At the output of the feedback loop (ACC output) there will usually be a dc offset due to drift of the mass from its zero position which prevents simple amplification. To remove this offset the signal is passed through a simple RC low-pass filter. The corner of the filter is chosen to be at 0.05 Hz (20 s period) so that combined with the corner due to the response of the loop the output simulates that of a conventional open loop seismometer with a natural frequency of 0.05 Hz (20 s period) and damping factor of unity.

Unfortunately the low pass filter contributes some electronic noise. There are three major contributors to the noise: two of these, amplifier current noise and amplifier voltage noise, are specified (as a function of frequency) by the manufacturer as current noise-density/Hz and voltage noise-density/Hz respectively. The third source of noise is the Johnson noise of the source resistance R and is given in V^2/Hz by 4kTR where R is in ohms.

The most important source of noise in the low-pass filter arises from the amplifier current-noise; this gives rise to a voltage noise which is the product of the impedance connected across the input and the amplifier current noise. As the impedance at the input of the long period filters (due to the large values of capacitance and resistance that are required in order to obtain a long time constant) is large so the voltage noise is large. The total noise of the low-pass filters is obtained by summing the noise powers from the three noise sources and this can be equated to equivalent ground acceleration given the sensitivity (in $V/m/s^2$) as a function of frequency at the acceleration output.

The power densities of the seismometer noise (Brownian noise and transducer noise) and that of the low pass filters are shown in figure 21. From this figure it can be seen that the filter noise exceeds the seismometer noise only at frequencies of less than 0.025 Hz (periods greater than 40 s). For comparison typical spectra of instrument noise from high quality open-loop SP and LP seismometers are plotted. Also shown are the ground acceleration power densities for Queen Creek, Arizona recognised to be a very quiet site (17) and the smoothed spectra for the UKNET site LLW when the noise level is high (December) and when it is low (May).

From figure 21 it can be seen that:-

(a) The total instrument noise of the feedback instrument is marginally better than the long period open loop seismometer at all signal frequencies less than 5 Hz (at which frequency the open loop SP seismometer has a higher detectivity).

(b) The power density curve for the open loop SP seismometer shows that, for signal periods greater than 9 s, the seismic noise at the UKNET sites will be exceeded by the seismometer-electronic noise during the summer months.

(c) The feedback system can just detect the Queen Creek noise over the whole bandwidth 0.01 to 10 Hz (period 0.1 to 100 s).

(d) The spectra of the seismic noise at UKNET sites during the summer are close to those of Queen Creek for signal frequencies between 0.05 and 0.16 Hz (6 to 20 s period) and between 2 and 4 Hz (0.25 to 0.5 s period).

(e) The spectra of the UKNET sites are high compared to Queen Creek at the conventional short period centre frequency of 1 Hz.

Note that the system noise level could be reduced by increasing the capacitance of the transducer. If the plate spacing were halved, the value of R_n would decrease from 4 to 2.25 kΩ and the value of the sensitivity r would increase by 2. This would result in a seven-fold reduction in the transducer noise to 4.8×10^{-2} $(m/s^2)^2$ which is of the same order as the Brownian noise. For LPNB the noise from the low-pass filter would be dominant but its effect could be reduced by increasing the sensitivity of the closed-loop seismometer before the input to the filter.

4.2 Dynamic range of the VBB system

The combined seismometer and system noise will appear as an analogue signal voltage at the output of the VBB channel. The spectrum of this noise, which is the product of the sum of the system noise equivalent accelerations shown in figure 21 and the square of the VBB responsivity to ground acceleration, is shown in figure 22. The total signal voltage power over the band 0.01 to 4 Hz is 3.4×10^{-8} V^2 giving a maximum zero to peak amplitude (3 rms) of 5.5×10^{-4} V. If the minimum signal that can be detected is defined as being equal to this noise level and the maximum signal cannot exceed 10.5 V (determined by the dc power rails), then the dynamic range in db is 20 log $(10.5/(5.5 \times 10^{-4}))$, that is 86 db. This dynamic range is only possible if the detected signals have spectra that have the same shape as the system noise.

The spectra of seismic signals will usually differ markedly from that of the system noise so that an estimate of dynamic range based on system noise is perhaps not very useful. An attempt is made to specify the dynamic range of the VBB system in a more practical way using model spectra for signals from earthquakes and explosions.

4.2.1 Using earthquake model spectra

To determine the magnitude m_b of the largest earthquake that can be recorded by the system it is assumed that the earthquake will have a spectrum with the form of the observed M = 7 earthquake of Berkhemer (20).

This spectrum has been converted using the response of the VBB channel to give voltage power density and is shown in figure 22. The total power output from this spectrum gives 25 V^2, ie, 5 V rms. Treating this signal as noise would give 15 V zero to peak which when convolved with the velocity sensitivity of the system of 8.5×10^5 V/m/s (figure 18(a)) results in a ground velocity of 1.76×10^{-5} m/s. Dividing by 2π converts this ground velocity to the parameter A/T required for the calculation of the unified magnitude m_b (m_b is the sum of log A/T and a distance correction term). Assuming a distance correction term of 3.9 this magnitude is calculated as $m_b = 7.3$. However, this event would have overloaded our system because we are limited to a maximum zero to peak voltage signal of 10.5 V. Therefore we can scale the above example (M = 7, $m_b = 7.3$) by the ratio log 10.5/15 to give $m_b = 7.1$ as the magnitude of the earthquake signal which would just not overload our system. Berkhemer also gives theoretical spectra for earthquakes for a range of magnitudes M. That for M = 4 has been converted to voltage power density and is shown in figure 22. Using the numerical procedure outlined above results in a unified magnitude m_b of 5.1. The curves for M = 7 and M = 4 ($m_b = 7.3$ and $m_b = 5.1$) can be extrapolated to the point where the spectrum first touches that of the system noise. This is shown in figure 22 and calculations on this spectrum give $m_b = 4.4$. Thus, the magnitude range for earthquakes is $m_b = 4.4$ to 7.1 or 54 db.

The above discussion neglects the effects of seismic noise. If the minimum signal has to have a spectrum that is everywhere greater than or equal to some specified seismic noise spectrum, then the minimum magnitudes must be greater than that obtained using the system noise. The VBB output voltage density spectra for the three conditions of seismic noise (Queen Creek, UKNET in May, UKNET in December) are shown in figure 23. The minimum magnitudes were found by fitting signal spectra to the seismic noise spectra in such a way that the signal spectrum is always greater than or equal to the noise spectrum, the signal spectra being obtained by interpolation from the graphs of Berkhemer (20) and figure 22. Calculations for these spectra would give magnitudes of $m_b = 5.7$ for Queen Creek, $m_b = 6.1$ for UKNET (May) and $m_b = 6.8$ for UKNET (December). Note that for the case of the seismic noise spectrum with the largest amplitude - UKNET (December) - the noise is so large that it increases significantly the amplitude of signals with m_b as large as 7.1 and so the clipping level is set by the signal + noise amplitude. This means that the largest signal that can be recorded without clipping in the presence of UKNET (December) noise is less than 7.1 and is in fact about $m_b = 6.9$. For the other two samples of seismic noise the effect of noise on the clipping level is negligible. Thus, the range of earthquake signal magnitudes in the presence of seismic noise is:-

Queen Creek noise	m_b = 5.7 to 7.1	28 db
UKNET (May)	m_b = 6.1 to 7.1	20 db
UKNET (December)	m_b = 6.8 to 6.9	2 db

4.2.2 Using explosion model spectra

To estimate the dynamic range of the VBB system for explosion signals it has been assumed that the power density spectrum of the explosion is flat for ground displacement over the range 0.33 to 2 Hz (0.5 to 3.0 s period). The voltage power density spectra are shown in figure 22 for the limiting (clipping) case and for the case where the signal at 3 s period reaches the system noise level. Using similar methods to those used for the earthquake spectra the magnitudes of the limiting explosion and the threshold explosion are calculated as $m_b = 7.2$ and $m_b = 3.3$, a range of 78 db. In the presence of the three different noise spectra the ranges become:-

Queens Creek:	6.0 to 7.2	24 db
UKNET (May):	6.6 to 7.2	12 db
UKNET (December):	7.1 to 7.0	Zero

Note that because the maximum power (60%) of the assumed explosion spectrum lies in the 1 to 2 Hz band the magnitude of the signals recorded on the VBB should only be about 0.1 magnitude units above conventional SP systems.

4.2.3 Surface waves from both earthquakes and explosions

To compute the clipping level for surface waves on the VBB system it is assumed that the waves are well dispersed and that the maximum amplitude will be at a single period (T = 15 s) and that this will give a 0-peak output of 10.5 V. Dividing 10.5 V by the sensitivity of the system at T = 15 s (ie, 2.7×10^5 V/m) gives the zero to ground displacement of 3.9×10^{-5} m (3.9×10^4 nm). Assuming a distance factor B(Δ) of 2.0 (when the amplitude is expressed in nm) and a path correction of -0.2 gives a maximum surface wave magnitude M_s of 6.4 that can be recorded without clipping. The magnitudes of the minimum signals and the dynamic ranges for various noise conditions are calculated and given in table 5.

The event magnitude ranges are displayed as a bar chart in figure 24.

4.3 Dynamic range of the LPNB system

For surface waves recorded on the LPNB system the largest amplitude will have periods of about 20 s. If the maximum signal gives a 0-peak output of 10.5 V, then as the sensitivity (V/m) of the system is 1.6×10^6 at 20 s period (figure 19(a)) the maximum zero to peak ground displacement is 6.6×10^3 nm which gives an M_s of 5.8. The minimum detectable signals and dynamic ranges assuming a maximum signal of M_s = 5.8 for the system noise and for three different seismic noise conditions are given in table 6 and shown as figure 26.

4.4 The optimum broad band response

It is obvious from the foregoing discussion that the range of size of seismic signals that can be recorded depends on the response of the system. As the system is designed to record broad band it is natural to ask if there is any alternative response that would make better use of the available dynamic range of the digital recorders.

TABLE 5

Surface Wave Magnitudes Using the VBB Response

Noise Type	Voltage Power Density 0.25 - 100 s	3 × RMS Volts	$20 \log \frac{10.5}{3 \times RMS}$	$M_{s_{MIN}} = 6.4 \frac{db}{20}$	$M_{s_{MAX}}$	Dynamic Range, db
System	3.4×10^{-8}	5.5×10^{-4}	86	2.1	6.4	86
Queen Creek	2.3×10^{-3}	1.5×10^{-1}	37	4.6	6.4	36
UKNET (May)	1×10^{-2}	3×10^{-1}	31	4.9	6.4	30
UKNET (December)	2.1	4.3	8	6.0	6.2*	4

*For UKNET (December) the large amplitude of the noise reduces the magnitude of the clipping signal by 0.2 magnitude units. For all other noise conditions the clipping level remains at that calculated in the text as $M_s = 6.4$.

TABLE 6

Dynamic Range of LPNB Channel for Surface Waves for Various Noise Conditions

Noise Type	Noise Power, V^2	RMS × 3, V	Dynamic Range* $(20 \log(\frac{10.5}{\text{RMS volts} \times 3}))$ db	Equivalent Magnitude when $B(\Delta) = 2.0$ ($\Delta = 73^\circ$)
System Noise	3.8×10^{-6}	5.8×10^{-3}	65	2.5
Queen Creek Noise	3.0×10^{-5}	1.6×10^{-2}	56	3.0
UKNET (May)	1.1×10^{-4}	3.1×10^{-2}	51	3.2
UKNET (December)	1.2×10^{-3}	1.0×10^{-1}	40	3.8

Sensitivity in V/m $= 1.6 \times 10^6$ at T = 20 s

Distance factor $B(\Delta)$ = 2.0

Maximum magnitude M_s = 5.8

*See figure 26

Because the spectrum of seismic signals is so variable and the general features only poorly known, it is probably best to discuss the optimum response solely in terms of how best to accommodate the seismic noise spectrum to make best use of the dynamic range. Assuming that the choice of optimum amplitude response is limited to simple shapes - high, low or band pass filtering without any band stop filtering - then the choice is restricted to responses that are flat to either constant ground displacement, velocity or acceleration. What is required is a response that will present to the digitiser a signal with all frequencies of seismic noise in the pass band at about the same amplitude. For the samples of noise considered here it can be seen (figures 21 and 23) that a response that is flat for constant ground velocity does indeed best flatten the seismic noise spectrum, by equalising the power densities at the ends of the band.

5. COMPARISON BETWEEN RECORDINGS FROM UKNET USING THE MK IIIC SYSTEM AND THOSE FROM BNA USING CONVENTIONAL SEISMOMETERS

The mechanical and electronic systems used on the Mk IIIC are more complex than those of conventional seismographs but despite this the system has proved to be remarkably reliable. During the whole of the development and operational period only one electronic component has failed (on a single instrument) even though only commercial quality components were used.

Since the Mk IIIC seismometer system was first installed for continuous operation as part of UKNET, a large number of signals have been detected. On the primary VBB recordings the signal-to-noise ratio for many of the signals is poor but the conventional SP and LP seismograms which show larger signal-to-noise ratios than those of the VBB can easily be obtained. The SP seismograms for example can be obtained by multiplying the spectrum of a section of VBB record by $b(\omega)/a(\omega)$ and transforming back into the time domain; $a(\omega)$ is the response of the VBB instrument as a function of frequency ω and $b(\omega)$ is the response of the SP instrument. To obtain the seismogram as it would have been recorded by other instruments $b(\omega)$ is simply replaced by the desired response.

5.1 Signals from an underground explosion

Figures 27 and 28 show the VBB P signals from an underground explosion in E Kazakh USSR as recorded at four of the UKNET sites and at the four BNA sites. Figures 29, 30, and 31, 32 show respectively the SP P signals and LP surface wave signals derived from the VBB. The VBB seismogram for one station of UKNET, CWF, is shown for comparison. Note that on the VBB seismogram the surface waves are completely masked by microseismic noise. At the time of this recording the only station with an LPNB output available for direct recording was WOL. It is shown in figure 32 for comparison with that derived from the VBB.

A comparison of the magnitudes of the P signals as recorded on the VBB and SP seismograms at each station of UKNET with those obtained from the four elements BNA array (equipped with open loop Geotech S-11 seismometers) is given in table 7. Table 8 shows the surface wave magnitude recorded at the four UKNET sites compared to those for the BNA.

TABLE 7

Measurements of Body Wave Amplitudes from a Teleseismic Underground Explosion

	Station	log A/T from VBB	log A/T from SP
UKNET	SCK	Not Measured*	2.41
	CWF	2.54	2.42
	LLW	2.76	2.70
	LAM	2.77	2.72
BLACKNEST ARRAY (BNA)	HD	2.64	2.58
	BW	2.86	2.81
	WOL	2.69	2.67
	BKN	2.90	2.79
Average m_b for UKNET		6.59 ± 0.08	6.46 ± 0.09
Average m_b for BNA		6.67 ± 0.07	6.61 ± 0.06
Average m_b for all sites		6.64 ± 0.05	6.54 ± 0.05

*Signal-to-noise too low to give reliable readings.
All magnitudes computed on the assumption that the distances term is 3.9.

TABLE 8

Measurements of Surface Wave Amplitudes from a Teleseismic Underground Explosion

	Station	$\log_{10}A$	Period Ts	M_s
UKNET	CWF	2.73	18	4.35
	SCK	2.67	18	4.29
	LAM	2.88	18	4.47
	LLW	2.51	18	4.13
BLACKNEST ARRAY (BNA)	WOL	2.98	15	4.51
	HD	2.92	15	4.45
	BW	2.91	15	4.53
	BKN	3.06	15	4.59
Average M_s for UKNET				4.31 ± 0.07
Average M_s for BNA				4.52 ± 0.03
Average M_s over all sites				4.42 ± 0.05

Direct recording LP at WOL gives $M_s = 4.51$

Uncertainties are standard errors of mean

$M_s = \log A + B(\Delta) + P(T)$

where $B(\Delta) = 1.68$ (for $\Delta = 47^{o}$) $P(T) = -0.15$ for $T = 15$ s

$= -0.18$ for $T = 18$ s

From an inspection of the seismograms it is clear that with the exception of station SCK signal-to-noise ratio of both the SP recordings of the P wave and the LPNB recordings of the surface waves are superior at the UKNET sites. At SCK the predominent noise appears to be at a signal period of ~ 1.5 s which degrades the SP trace although the LPNB recording (figure 31) appears to be similar to those from the other UKNET sites. The amplitudes (magnitudes) of the recorded signals are seen to be consistent, varying by only 0.2 magnitude units between the mean and individual stations.

5.2 Spectra of seismic noise

The spectrum of the seismic noise using VBB recordings has been investigated in the past (21,22), but these studies related only to local sites around Blacknest, and did not extend beyond 20 s period into the LP band. In order to give some support for the reasoning and calculations concerning dynamic range (section 4) a section of the recording from all eight sites was selected covering a common 27 min (16384 data points) period that ended a few minutes prior to the arrival of the P wave of the explosion signal. The computed spectra are shown in terms of ground acceleration power density in figures 33 (UKNET) and 34 (BNA). To obtain a more continuous spectrum at the higher frequencies a form of logarithmic smoothing has been applied -- this retains the narrow bandwidth of 0.00244 s at signal periods between 100 and 26 s yet progressively widens the bandwidth to 0.085 s for frequencies between 4.3 and 5 Hz. The level of the background 6 s microseismic noise was found to be high. In order to obtain an estimate of the seismic noise during the quieter summer months a section of VBB recording was selected for a period during May when the 6 s noise was observed to be low. The corresponding spectra for ground acceleration for the four UKNET sites and four BNA sites are shown in figures 35 and 36 respectively. From figures 33 and 35 the spectra for the UKNET site LLW was chosen for section 4 for the calculation on dynamic range.

From these spectra the following points of interest can be noted:-

(1) At short periods the site of SCK (North Norfolk) is excessively noisy with a large peak at ~ 1.5 s period and exceeding the other UKNET sites at periods between 0.4 and 3 s, although its LP noise is average. This explains the reason for the poor signal-to-noise ratio of the body wave signals for SCK in figures 27 and 29. Work is now in progress to replace this site and a preliminary noise survey has been undertaken (23) which indicates that the predominant 1.5 s noise is common to North Norfolk and that a relatively quiet site in East Anglia can only be found if located some tens of miles further south of the present site.

(2) At all sites the peak of the noise is at 6 s period during the December sample but at 4 s during the May sample.

(3) The local sites (BNA) exhibit a second peak of noise at ~ 2 s period which is absent from the UKNET sites (with the exception of SCK).

(4) The high frequency noise (0.2 to 0.3 Hz) which is mainly due to vehicular traffic on nearby roads, etc, is, as expected, generally higher at the BNA sites. Probably because the December sample (28 December) occurred during the Christmas/New Year holidays the cultural noise is exceptionally low whereas this noise level at the BNA sites during May is remarkably high. (The May sample of noise was selected to be at ~ 4 am to correspond with the December sample.)

(5) For both samples of noise the UKNET sites (except SCK) are quieter than the BNA sites at 1 s period which is the nominal signal period used for the detection of body waves. The difference is about an order of magnitude in power density and equivalent to a factor of three in amplitude.

(6) The small peak at a period of 13 to 15 s is seen on all spectra. This peak is also significant on the Queen Creek noise shown in figure 21.

6. CONCLUSIONS

From experience of operating Mk IIIC seismometers in UKNET for over a year the following conclusions can be drawn:-

(a) The system is reliable and can be used to obtain both SP and LP seismograms from primary VBB recordings.

(b) Analysis of recordings from teleseismic earthquakes and underground explosions and of the background seismic noise has shown that the dynamic range of the system is consistent with the design specifications.

(c) The system is easier to instal, is physically smaller and costs less to manufacture than the equivalent open loop LP seismometer system. (Conventional LP seismometers are not commercially manufactured in the UK.)

(d) The calibration of the system should occasionally be checked with the feedback circuit disconnected.

(e) Although the LPNB signal can be successfully recovered from VBB broadband signal offline, a second separate LPNB channel that is transmitted with the VBB allows continuous real time chart and tape recordings to be made.

REFERENCES

1. P L Willmore: "The Detection of Earth Movements". Methods and Techniques in Geophysics, Runcorn. Interscience Publishers Ltd (1960)

2. AWRE: "The Detection and Recognition of Underground Explosions". A Special Report of UKAEA (1965)

3. A D Beech: "A New Long Period Vertical Component Seismometer". AWRE Report O70/65 (1965)

4. P D Marshall, R F Burch and A Douglas: "How and Why to Record Broad Band Seismic Signals". Nature (15 September 1972)

5. P B Felgett: "Improvements in Seismometers and Other Accelerometers". Private Communication (1966)

6. M J Tucker: "An Electronic Feedback Seismograph. J Sci Instr, 35, 167-171 (1958)

7. W R MacDonald: "Acceleration Transducers of the Force Balance Type". In Flight Test Instrumentation, Ed M A Perry, Oxford-Pergamon, pp15-23 (1961)

8. B S Melton and D P Johnson: "Inertial Seismograph Design - Limitations in Principle and Practice". Proc IRE, 50 (1962)

9. B Block and R D Moore: "Measurements in the Earth Mode Frequency Range by an Electrostatic Sensing and Feedback Gravimeter". J Geophys Res, 71, 4361-4375 (1966)

10. R V Jones: "The Measurement and Control of Small Displacements". Phys Bull, 18, 325-336 (1967)

11. B Block and R D Moore: "Tidal to Seismic Frequency Investigations with a Quartz Accelerometer of New Geometry". J Geophys Res, 75, 1493-1505 (1970)

12. I W Buckner: "The Design of a Horizontal Component Feedback Seismometer". PhD Thesis (Unpublished), University of Reading (1975)

13. M J Usher, I W Buckner and R F Burch: "A Miniature Wideband Horizontal Component Feedback Seismometer". J Phys (E) Sci Instr, 10, 1253-1260 (1977)

14. M J Usher, R F Burch and C Guralp: "Wideband Feedback Seismometers". Phys Earth and Planet Int, 18, 38-50 (1979)

15. B D Hopkins: "Direct High-Resolution Digitisation of a Frequency-Modulated Carrier". J Phys E Sci Instr, 12, 1027-1028 (1979)

16. W A Lynch and J G Truxal: "Signals and Systems in Electrical Engineering". McGraw-Hill (1962)

17. J E Fix: "Ambient Earth Motion in the Period Range from 0.1 to 2560 s". Bull Seis Soc Am, 62 (1972)

18. T C Collocott (Ed): "Dictionary of Science and Technology". W & R Chambers Ltd, Edinburgh

19. S Handel: "A Dictionary of Electronics"

20. H Berkhemer: "The Concept of Wide Band Seismometry". Proceedings of the XII Assemblee Generale de la Commission Seismologique Europeanne, Luxembourg (21-29 September 1970)

21. A Douglas and J B Young "The Estimation of of Seismic Body Wave Signals in the Presence of Oceanic Microseisms". AWRE Report O14/81 (1981)

22. R W Hurley: Private Communication

23. R F Burch: Private Communication

APPENDIX A

THE TRANSFER FUNCTION OF THE CAPACITANCE TRANSDUCER AND PREAMPLIFIER

A1. THE CAPACITANCE DISPLACEMENT TRANSDUCER

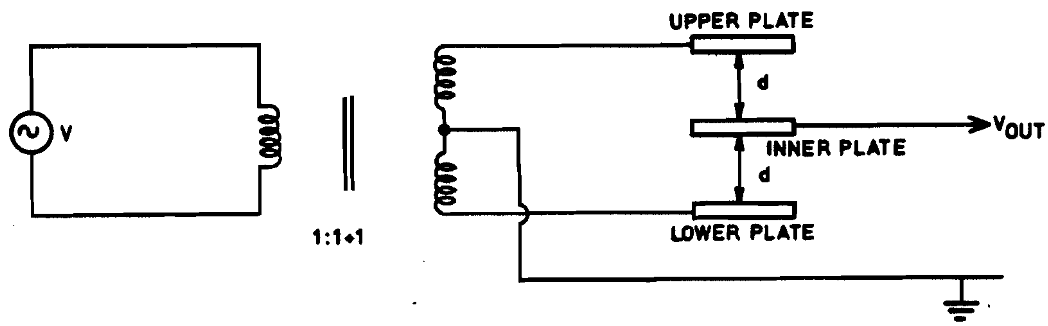

This arrangement can be looked on as the bridge circuit shown below.

When the inner plate is exactly central at a distance d from the two identical outer plates then, provided that the two halves of the transformer secondary windings are identical, the output of the bridge will be zero. Now the capacitance between two plates separated by a distance d is proportional to d^{-1}. Let C_0 be the capacitance between each outer plate and the inner plate when it is central. If the inner plate is moved a distance a towards the upper plate, then its capacitance to the upper plate C_U is $C_0 d/(d - x)$ and to the lower plate C_L is $C_0 d/(D + x)$. If the impedance of C_U is $Z_U = 1/sC_U$ and of C_L is $Z_L = 1/sC_L$, then the output of the bridge V_{OUT} is $2V\times Z_L(Z_L + Z_U) - V$. Replacing the impedances by the capacitances gives $V_{OUT} = V(C_U - C_L)/(C_U + C_L)$. Using the expressions for C_U and C_L in terms of x and d then $V_{OUT} = Vx/d$ giving the transfer function as V/d volts/metre. For the Mk IIIC V~ 15 V (~ 5 Volts rms) peak to peak, d ~ 1 mm giving 1.5×10^4 V/m (5×10^3 V rms/m).

A2. PREAMPLIFIER

The circuit diagram of figure 4 of Part 2 can be represented by

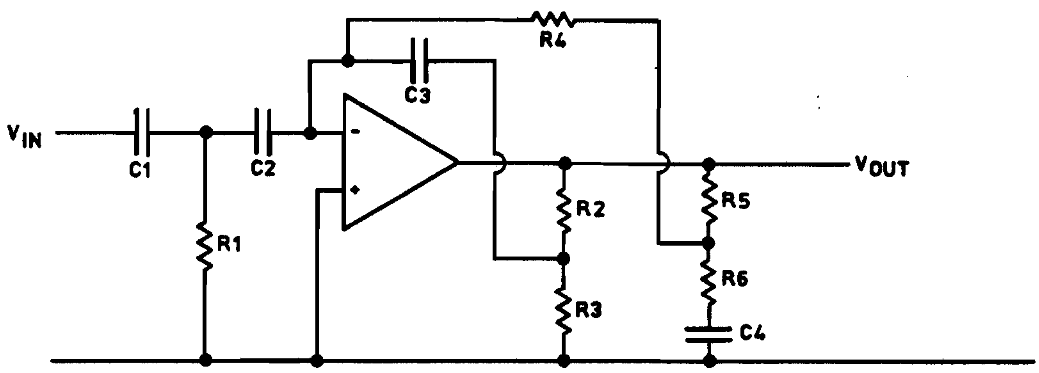

where Cl is the capacitance of the displacement transducer and is ~ 10 pF. The transfer function can be shown to be

$$\left(\frac{ADEH}{BJ}\right)\left(\frac{s^2(s + E^{-1})(s + H^{-1})}{(s + B^{-1})(s^2 + Ks/J + J^{-1})}\right),$$

where
A = R1C1C2,
B = R1(C1 + C2),
C = R6C4,
D = R4 + R5,
E = (R4R6C4 + R5R6C4 + R4R5C4)/(R4 + R5),
F = R3C3,
G = R2 + R3,
H = (R2R3C3)/(R2 + R3),
J = (CGH + FDE)/G,
K = (HG + CG + FD)/G.

Inserting component values results in:-

four zeros	three poles
-0,0	-0.5,0
-0,0	-545, + 181
-3.14,0	-545, - 181
-2.2×10^{8},0	

with a multiplier constant of 1×10^{-7}. A Bode plot can be sketched as:-

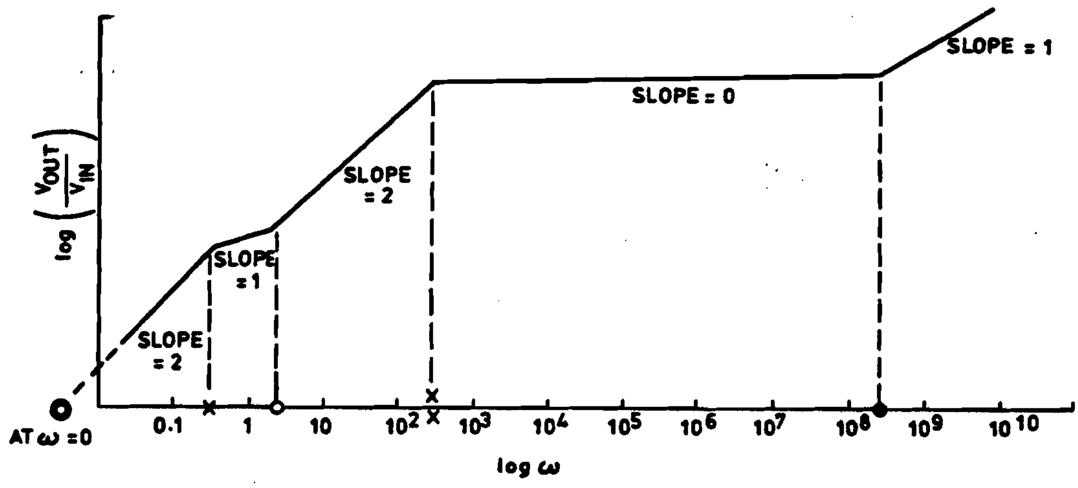

From the above sketch the response is seen to be flat from $\omega = 574$ ($\sim$ 100 Hz) to $\omega = 2.2 \times 10^8$ (35 MHz) and the operating frequency of the Mk IIIC carrier of 50 kHz ($\omega \sim 3 \times 10^5$) is in the middle of the passband. To find the expression for the gain at 50 kHz we replace s by $j\omega$ in the transfer function and extract the real part. This gives a precise value of 22.02. However, it will be found that the real part can be simplified to be equal to

$$AG/BF = (R1C1C2)(R2 + R3)/(R1)(C1 + C2)(R3C3)$$

as C1 << C2

$$V_{OUT}/V_{IN} = \frac{C1}{C2} \times \frac{(R2 + R3)}{R3} = \frac{10\ pF}{5\ pF} \times \frac{11K}{1K} = 22$$

Thus, the gain of the preamplifier is determined by the ratio of the transducer capacitance to the preamplifier feedback capacitor and is multiplied by a gain factor determined by R2 and R3.

APPENDIX B

BROWNIAN MOTION AND SEISMOMETERS

Consider a mass on a spring

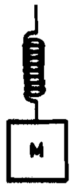

spring stiffness = C N/m deflection.

The equipartition theorem gives the energy of the system as $\frac{1}{2}C(\bar{x})^2 = \frac{1}{2}kT$ where k = Boltzmann's constant = 1.38×10^{-23} J/°K and T is absolute temperature.

The mean square displacement of the mass $(\bar{x})^2 = kT/C$.

This result implies that the Brownian noise motion of the mass could be reduced if a very strong spring was used. This is true - unfortunately it would not be useful as a seismometer as the inertial mass would always follow the frame and there would be no signal output.

Let us take the case of a real seismometer with some damping and consider its response to a force applied to the mass.

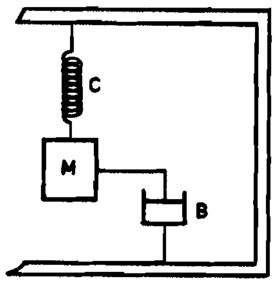

Let relative motion between mass and frame be x.

Equating forces $M\ddot{x} + B\dot{x} + Cx = F$, ... (B2)

$$\ddot{x} + \frac{B\dot{x}}{M} + \frac{Cx}{M} = \frac{F}{M}.$$

However, the natural frequency of the suspension $\omega_o = \sqrt{C/M}$ and if we let

$$\frac{B}{M} = 2n\omega_o = \frac{\omega_o}{Q},$$

then $$\ddot{x} + \frac{\omega_o}{Q}\dot{x} + \omega_o^2 x = \frac{F}{M}.$$

The steady state solution for

$$x = \frac{F}{M((\omega_o^2 - \omega^2) + j\omega_o\omega/Q)} \qquad .... \text{(B3)}$$

If we assume that the Brownian Force F is essentially white, then $(\bar{F})^2 = A\Delta f$, where A is a constant and Δf is the bandwidth

$$\text{Put } \frac{1}{((\omega_o^2 - \omega^2) + j\omega_o\omega/Q)} = (\text{response } (f)),$$

Thus, the mean square displacement $= \bar{F}^2(\text{response } (f))^2/M^2$
$= A(\text{response } (f))^2 \Delta f/M^2$ where A is the power density of the Brownian force.
The mean square value integrated over all frequencies
$= \int_0^\infty A(\text{response } (f))^2 df/M^2$.

This expression when integrated and evaluated gives

$$(\bar{x})^2 = \frac{AQ}{4\omega_o MC}. \qquad \text{.... (B4)}$$

Equation (B1) showed that $(\bar{x})^2 = \frac{kT}{C}$,

$$\text{so } \frac{AQ}{4\omega_o MC} = \frac{kT}{C} \text{ and therefore } A = \frac{4\omega_o Mkt}{Q}. \qquad \text{.... (B5)}$$

$$\text{Thus, } (\bar{x})^2 = \frac{4\omega_o MkT}{M^2 Q} \int_{f_1}^{f_2} (\text{response } (f))^2 df. \qquad \text{.... (B6)}$$

$$\text{Displacement density} = (\bar{x})^2/\text{Hz} = \frac{4\omega_o kT}{MQ} \times (\text{response } (f))^2. \qquad \text{.... (B7)}$$

Equation (B4) shows that the integral from 0 to ∞ of the (response (f))^2 is proportional to Q. The multiplying constant of equation (B6) contains Q^{-1} therefore the total noise is independent of Q when accounted for over the whole band of frequencies. The constant (response^2) and product are shown in figure 37 plotted with linear co-ordinates and logarithmic co-ordinates.

We have only considered motion of the mass due to the Brownian forces acting upon it. The response of the system to motion of the case of acceleration $\ddot{y}$ is given by

$$\ddot{x} + \frac{B\dot{x}}{M} + \frac{Cx}{M} = \ddot{y}.$$

The steady state solution putting $\frac{C}{M} = \omega_o^2$ and $\frac{B}{M} = \frac{\omega_o}{Q}$ is

$$x = \frac{\ddot{y}}{((\omega_o^2 - \omega^2) + j\omega_o\omega/Q)}. \qquad \text{.... (B8)}$$

This has the same form as (B3).

$$(x)^2 = \frac{(\ddot{y})^2}{((\omega_o^2 - \omega^2) + j\omega_o\omega/Q)^2} = (\ddot{y})^2 \times (\text{response } (f))^2. \quad \text{.... (B9)}$$

But $(\bar{x})^2 = \frac{A}{M^2}$ (response $(f))^2\Delta f$,

therefore $(\ddot{y})^2/\Delta f = \frac{A}{M^2} = \frac{4\omega_o kT}{MQ}$ $(m/s^2)^2/Hz$.

Thus, in figure 37 the noise equivalent acceleration is given by sketches (1) and (2) and sketches (5) and (6) give the output of the suspension system to this white input.

Now it is seen that, although we can obtain a low value of noise equivalent acceleration by making Q large, if we include the natural frequency of the seismometer in our bandwidth of recording, the total sum of the noise will appear as a signal of the same amplitude as if we had made Q small.

The seismic signal will also be very large and concentrated about ω_o. This is undesirable and a way must be found of removing it. If conventional damping methods are used (using air damping or by connecting a resistor across a magnet/coil transducer), then the system reverts to $(\ddot{y})^2 = (4\omega_o kT\delta f)/MQ$ and becomes high. This is because the system is supplying its own power to damp itself and is doing work. If the same effect can be achieved using an external source, then $(\ddot{y})^2$ does not increase. Provided that the external source is noiseless, then the response can be modified at will without affecting the signal ratio. A feedback signal can be applied as the source of the signal is now an external amplifier and power supply and can be used not only to damp the instrument but also to change the response by causing the closed loop natural frequency to be outside the band of interest.

Because the signal-to-noise ratio is unaltered it is permissable to use the open loop response characteristics when considering the noise equivalent acceleration for components in the electronic amplifier section of the circuit following the displacement transducer.

It can be seen from figure 21 that the Brownian noise at 3×10^{-21} $(m/s^2)^2/Hz$ is one order of magnitude below the transducer noise. This is the result of using a large mass (1.3 kg). We can now continue the discussion to include the effects of decreasing this mass and to predict other measures that would have to be taken in order to retain the low Brownian level noise.

As shown above the Brownian noise equivalent acceleration

$$\frac{(\ddot{y})^2}{\delta f} = \frac{4\omega_o}{QM}kT.$$

The Johnson/Nyquist noise for a resistor = $(\bar{e})^2$ = 4RkTB where B is the frequency bandwidth, ie, $\frac{(\bar{e})^2}{\delta f} = 4RkT$.

Thus, the suspension system behaves like a resistor with the equivalent ground acceleration power density $(\ddot{y})^2$/Hz = $4R_s kT$ where $R_s = \frac{\omega_o}{MQ} = \frac{2\pi}{MQT_o}$.

Thus, the product MQT_o must be maximised to minimise the noise. Let us now consider these parameters for the case where the only damping on the system is due to air damping. This damping force is $B\dot{x}$ (equation (B2)).

$\frac{B}{M} = \frac{\omega_o}{Q}$, therefore $R_s = \frac{B}{M^2}$, ie, for the particular mass $\frac{\omega_o}{Q}$ is a constant.

For air damping using the same geometry of the mass and capacitor plates the force ∝ area of the mass. The weight of the mass = density × volume, therefore $R_s \propto \frac{\text{area}}{\text{volume}^2} \propto \frac{1}{(\text{dimension})^4} \propto \frac{1}{M^{4/3}}$.

Therefore the Brownian noise power density is proportional to $M^{-4/3}$.

If we were to miniaturise the seismometer to result in a mass weight of 150 g, then the Brownian noise would increase by a factor of $(1.3/0.15)^{4/3} = 18$. The only method of decreasing the noise is to operate the transducer and suspension in an evacuated vessel. This will have the effect of reducing ω_o/Q by increasing Q while keeping ω_o constant. (Merely changing ω_o is of no use as Q is proportional to ω_o.) The Mk IIIC, although enclosed in a pressure jacket, is operated at atmospheric pressure with $n_o \approx 0.01$, ie, $Q \approx 50$. For a miniature version to operate with the same Brownian noise level using a mass of 150 g the suspension must have a Q of 50 × 18 ≈ 900.

APPENDIX C

THE NOISE EQUIVALENT ACCELERATION OF THE TRANSDUCER NOISE AND BROWNIAN NOISE

A block diagram is shown in figure 38. In section 4.1.2 it was stated that the transducer noise can be equated to that of a series resistor R_n and thus has a white noise power density spectrum. Whereas in appendix B we derived the Brownian noise acting on the seismometer mass as an equivalent acceleration power density ($= 4R_s kT$ where $R_s = \omega_o/MQ$) and then used the suspension response to determine the displacement output, for the transducer noise we need to work back through the suspension response to find the equivalent acceleration power density.

Thus, the output noise of the transducer of $4R_n kT$ volts^2/Hz becomes

$$(\ddot{Z})^2/\mathrm{Hz} = \frac{4R_n kT}{r^2(\mathrm{response}(f))^2},$$

where r is the transducer sensitivity in V/m.

However, the Brownian noise acceleration power density $(\ddot{y})^2/\mathrm{Hz} = 4R_s kT$.
So the total noise acceleration power density is $(\ddot{Z})^2/\mathrm{Hz} + (\ddot{y})^2/\mathrm{Hz}$. This sum represents the detection level of the seismometer in terms of ground acceleration and assumes no other source of electrical or mechanical noise. This total noise can then be used with the transfer function of the closed loop seismometer to derive the power density of the noise at the output of the system as

$$((\ddot{y})^2/\mathrm{Hz} + (\ddot{Z})^2/\mathrm{Hz})(\mathrm{T.F.}(f))^2 = 4\ kT\left(R_s + \frac{R_n}{r^2(\mathrm{response}(f))^2}\right)(\mathrm{T.F.}(f))^2.$$

It is useful to note how $(\ddot{Z})^2/\mathrm{Hz}$ varies with r and with ω_o. From the equation shown above $(\ddot{Z})^2/\mathrm{Hz} \propto (r^2(\mathrm{response}\ (f))^2)^{-1}$. Thus, immediately we see the improvement by increasing the sensitivity r of the transducer. Figure 39 shows a sketch of $(\ddot{Z})^2/\mathrm{Hz}$ for constant r but with varying values of the seismometer natural frequency ω_o. From this it can be seen that for frequencies $\gg \omega_o$ the noise equivalent is independent of ω_o, but for frequencies $< \omega_o$ the need to make ω_o as low as possible is apparent.

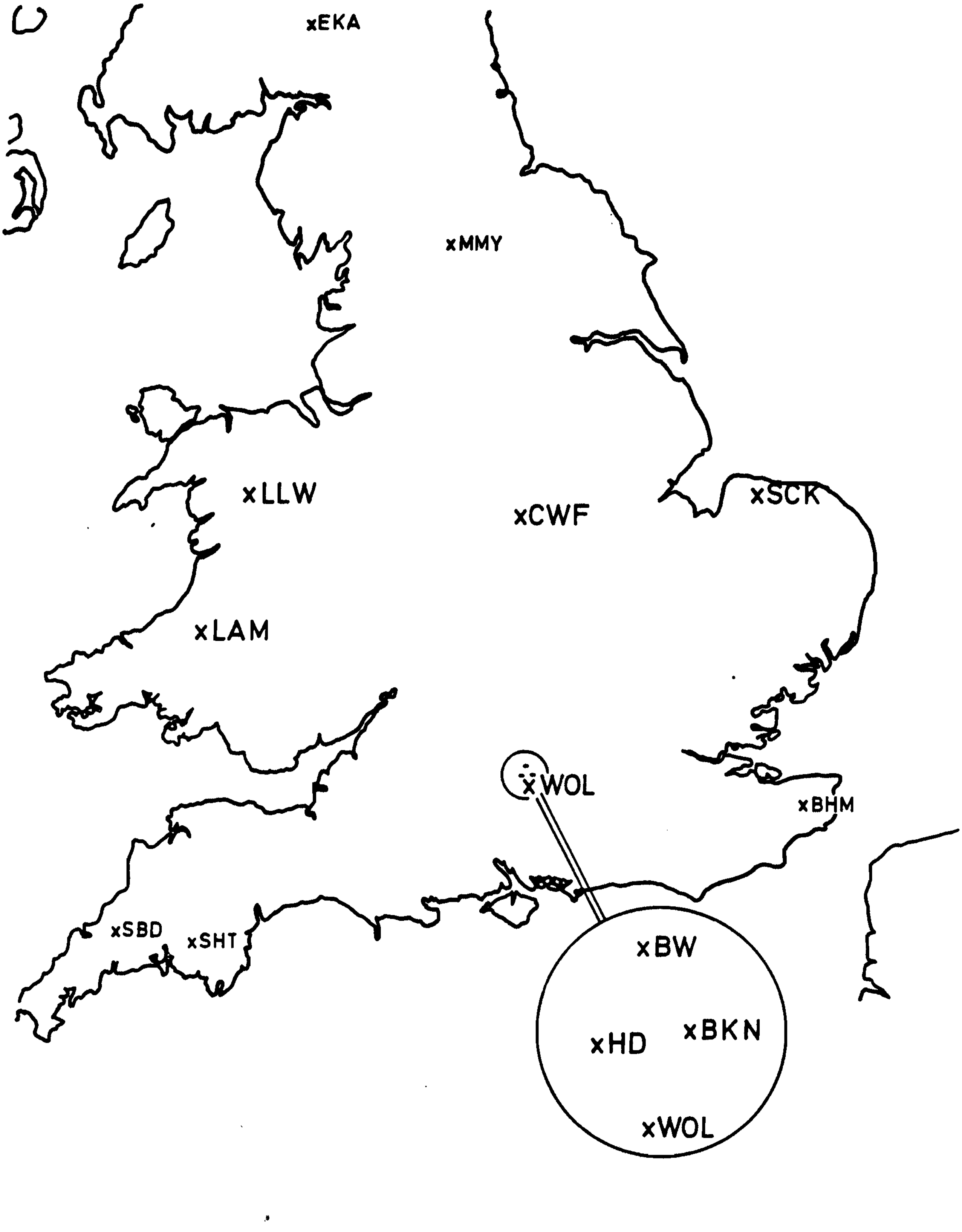

Figure 1 Locations of Broad Band Recording Sites

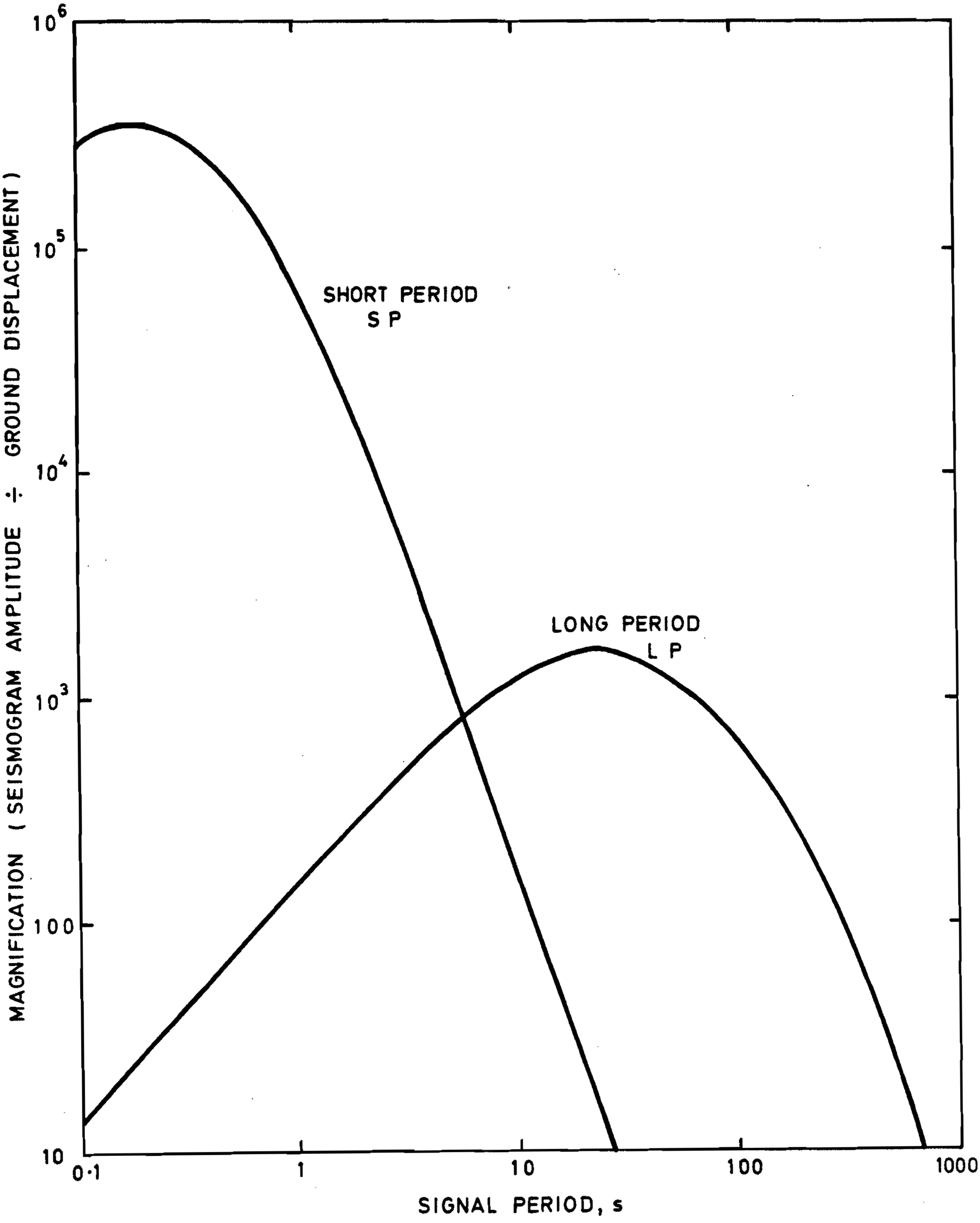

Figure 2. Typical Response Curves for Conventional Seismographs.

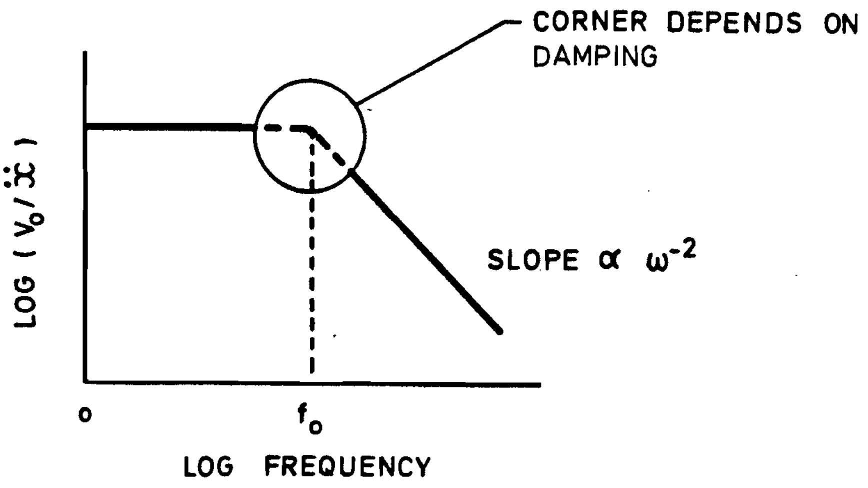

Figure 3 Sketch of Response to Acceleration of Sprung Mass with Displacement Transducer

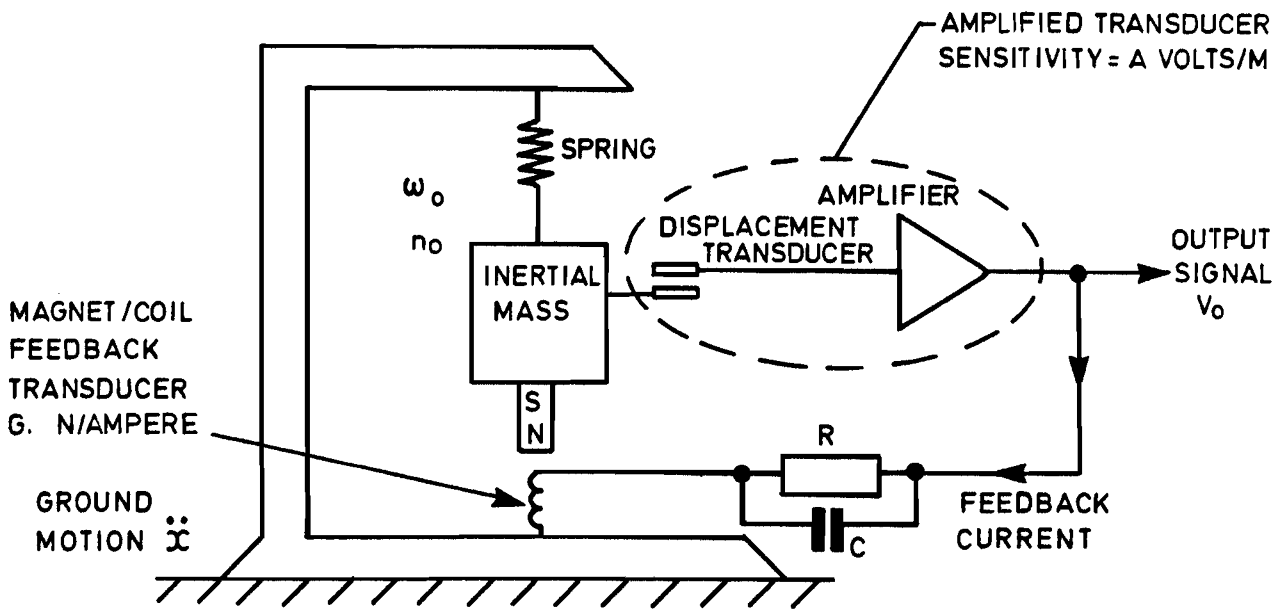

Figure 4(a) Schematic Diagram of Feedback Seismometer

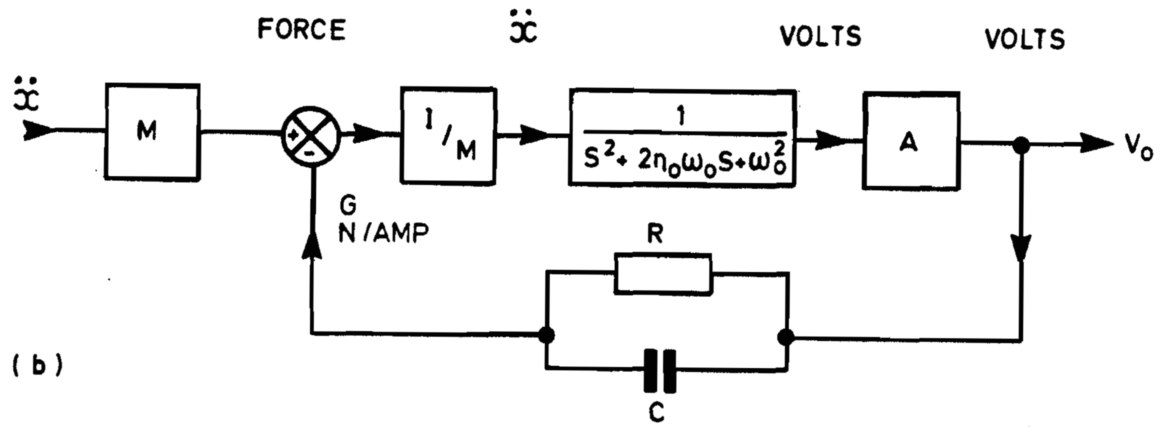

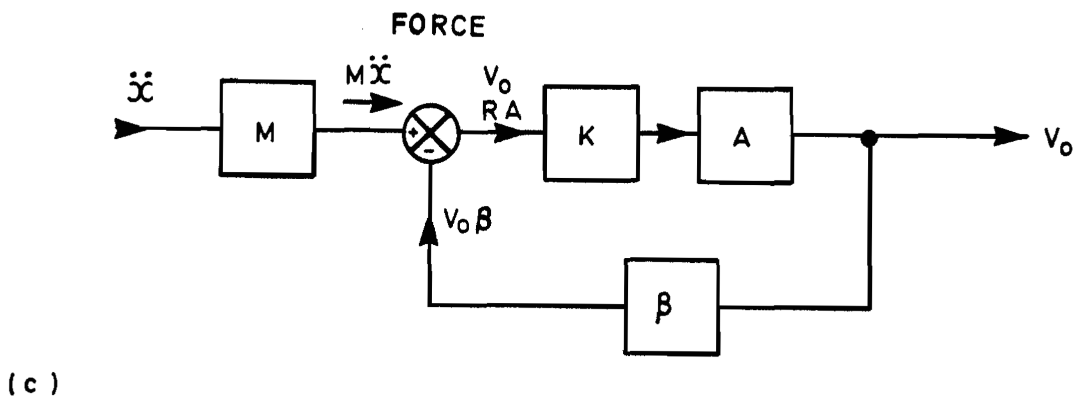

Figure 4(b): 4(c) Block Diagrams for Feedback Seismometer

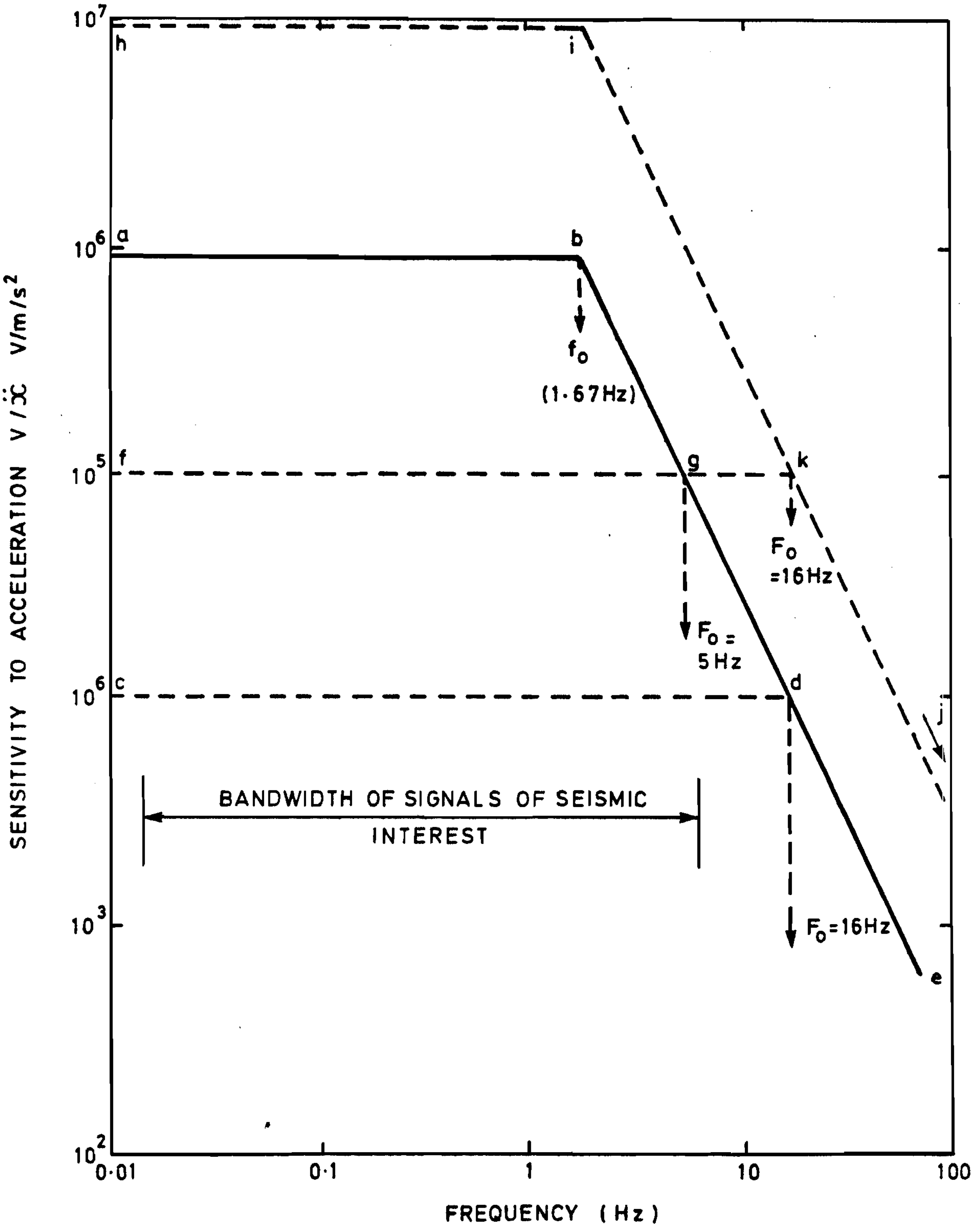

Figure 5 Bode Plots for Worked Example

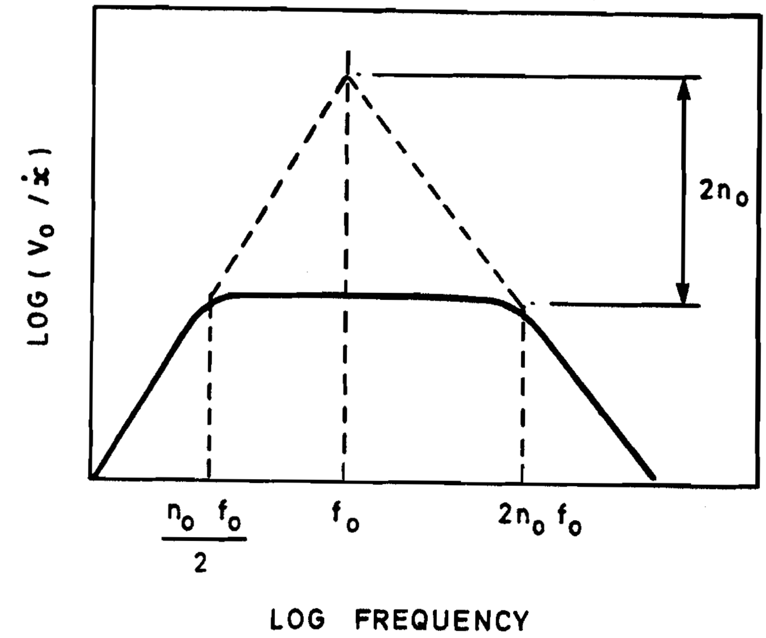

Figure 6 Response to Ground Velocity of an Over-damped Accelerometer

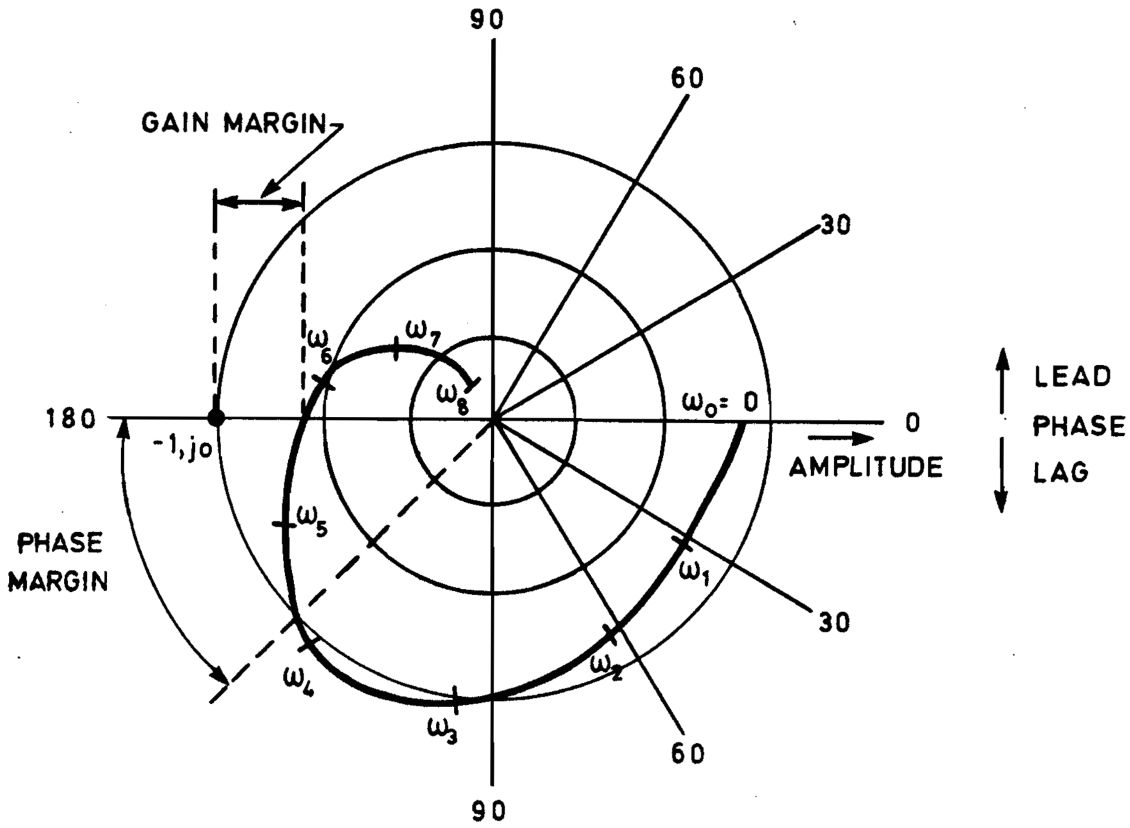

Figure 7 Example of Root Locus Plot (Nyquist Plot)

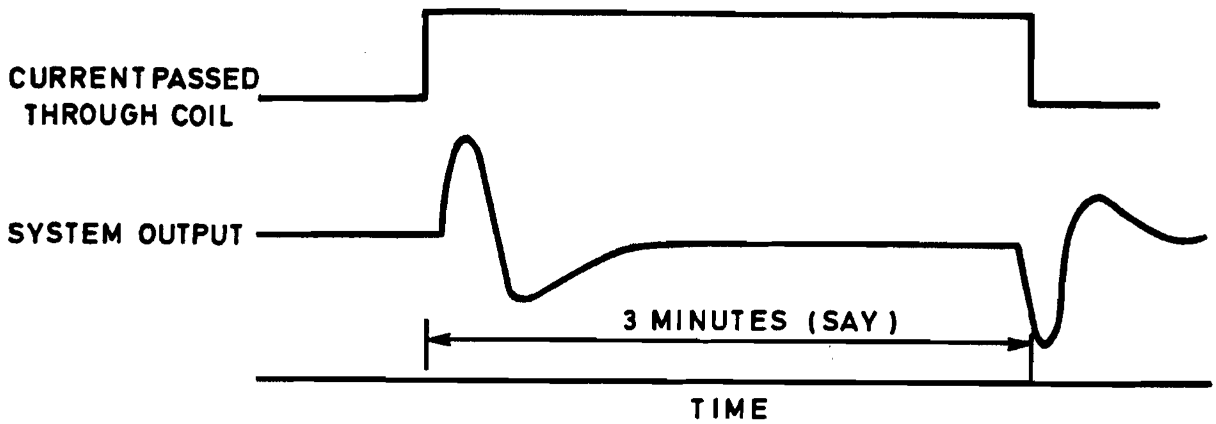

Figure 8 Response of Conventional Long Period Seismometer to a Current Step Passed through its Calibration Coil

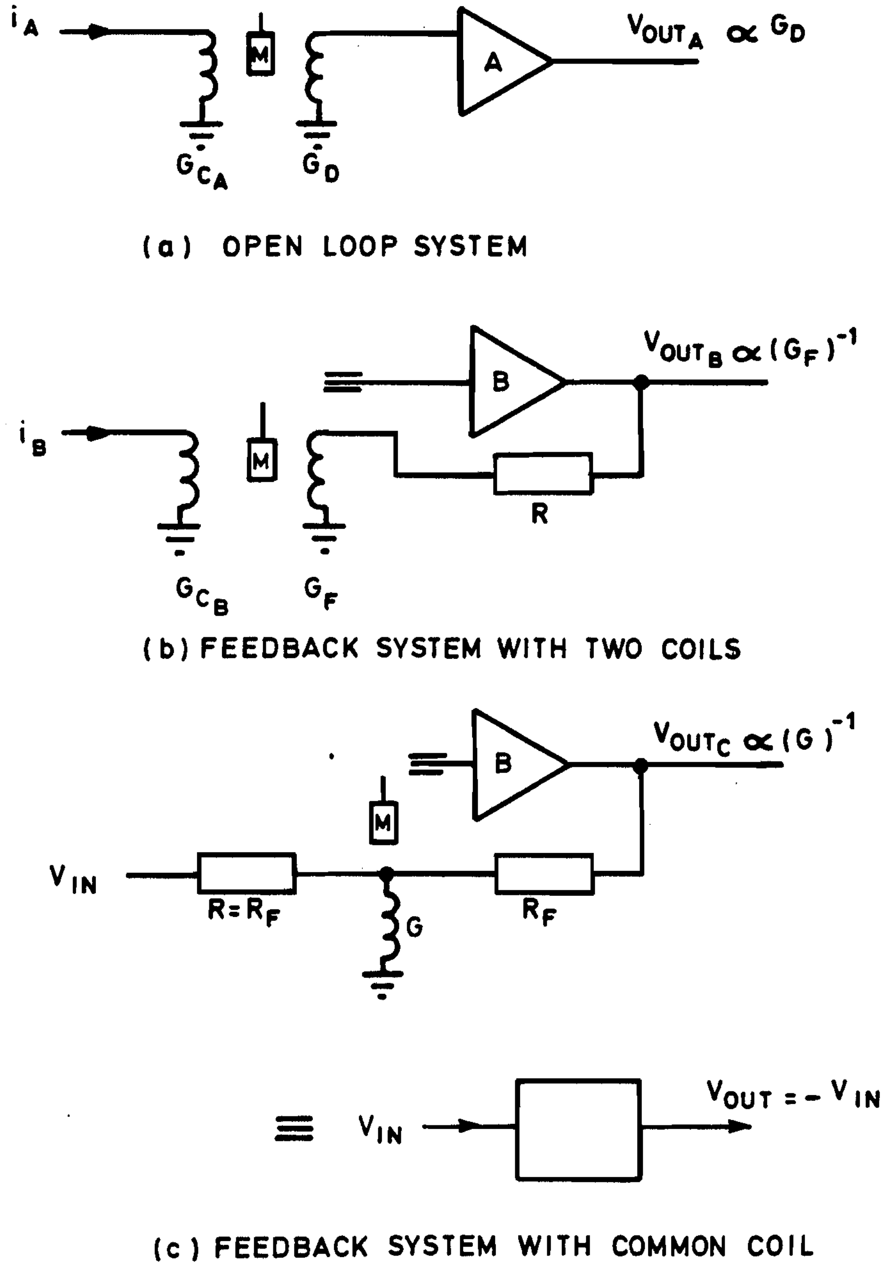

Figure 9 Calibration Coil Seismometer Combinations

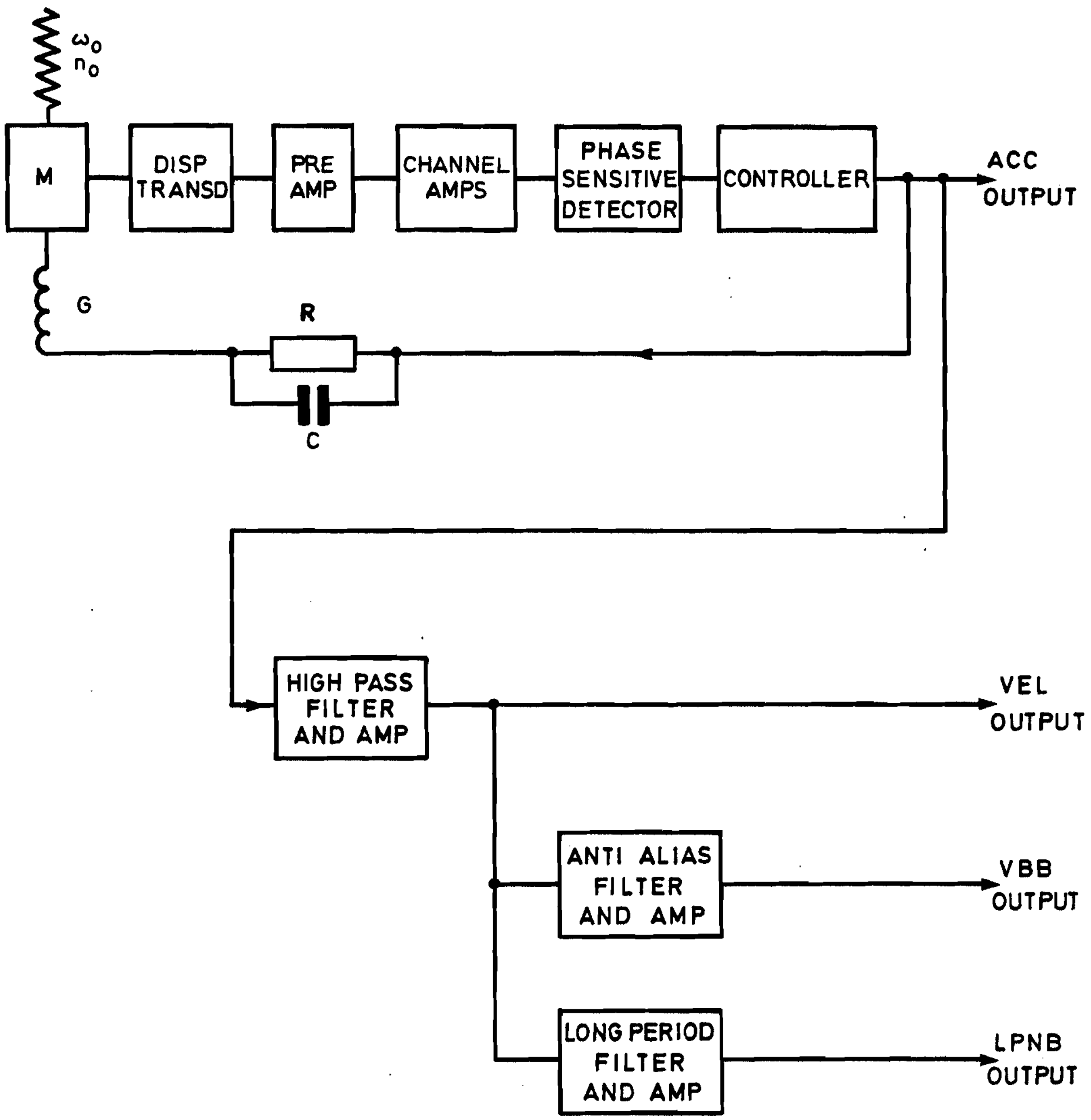

Figure 10. Block Diagram of Signal Paths

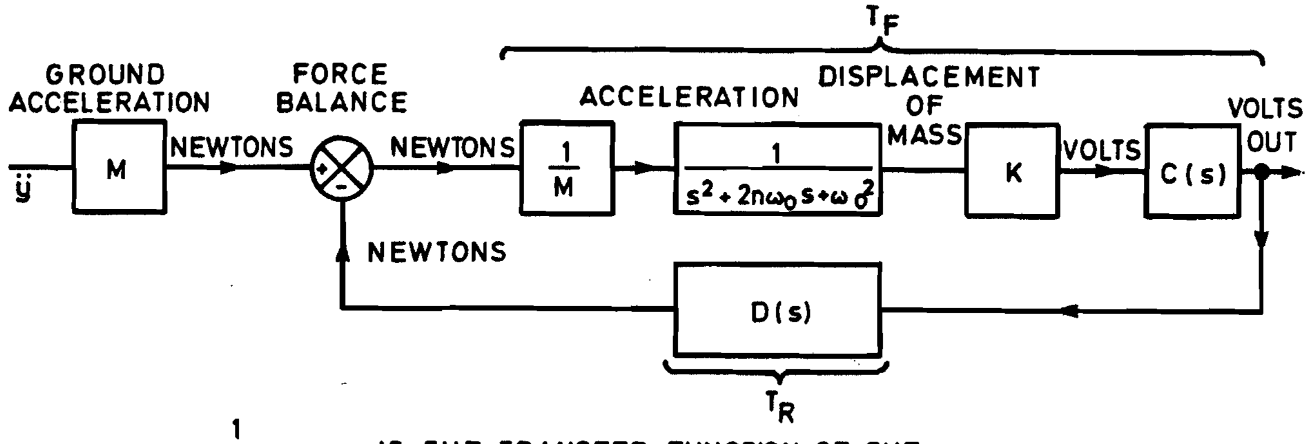

$\frac{1}{(s^2+2n\omega_0 s+\omega_0^2)}$ IS THE TRANSFER FUNCTION OF THE MECHANICAL SPRING/MASS SYSTEM ($m/m/s^2$)

n = 0.009 $f_0 = 1.69\ Hz$ $\omega_0 = 2\pi\ 1.69$

M = MASS OF SEISMOMETER INERTIAL MASS = 1.3 Kg

K = DISPLACEMENT TRANSDUCER SENSITIVITY AFTER GAIN FROM PREAMPLIFIER AND CHANNEL AMPLIFIER AND PHASE SENSITIVE DETECTOR = 0.34×10^6 v/m

Figure 11 (a) Block Diagram of Force Balance Feedback Seismometer

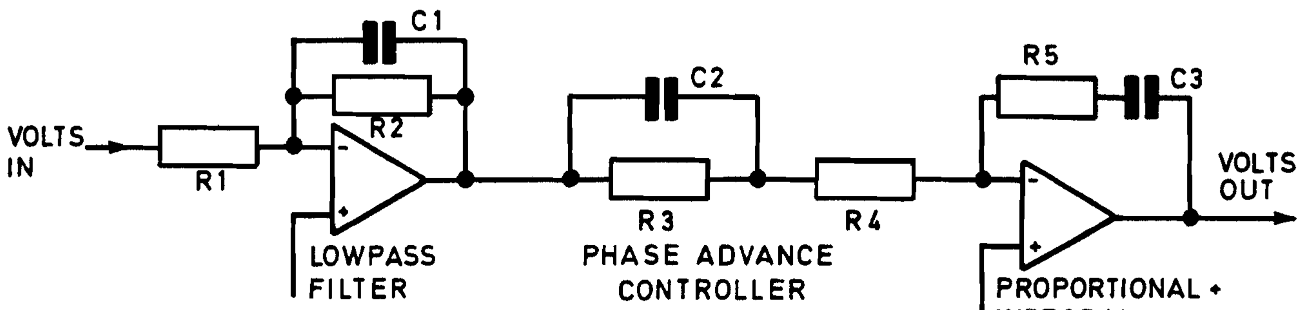

R1 = 10KΩ
R2 = 10KΩ
R3 = 56KΩ
R4 = 560Ω
R5 = 68KΩ

C1 = 0.15μF
C2 = 0.15μF
C3 = 1μF

$$C(s) = \left(\frac{R5}{R1R4C1}\right) \frac{(s+(R5C3)^{-1})\,(s+(R3C2)^{-1})}{(s)(s+(R2C1)^{-1})(s+(R3+R4)/R3R4C2)}$$

Figure 11 (b) Circuit and Transfer Function of Block C(s) of Figure 11 (a)

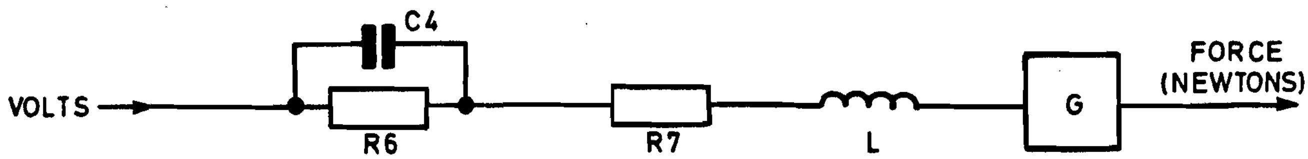

R6 = 1.62MΩ (CONTROLS CLOSED LOOP GAIN (VOLTS/m/s^2))
R7 = 5.75KΩ (RESISTANCE OF FEEDBACK TRANSDUCER COIL)
L = 0.8H (INDUCTANCE OF FEEDBACK TRANSDUCER COIL)
G = 158N/AMP (MOTOR CONSTANT OF FEEDBACK TRANSDUCER)
C4 = 2.2μ F (CONTROLS DAMPING OF CLOSED LOOP SEISMOMETER)

$$D(s) = \frac{G}{L}\ \frac{(s+(R6C4)^{-1})}{(s^2+((R6R7C4+L)/R6C4L)s+(R6+R7)/R6C4L)}$$

Figure 11 (c) Circuit and Transfer Function of Block D(s) of Figure 11 (a)

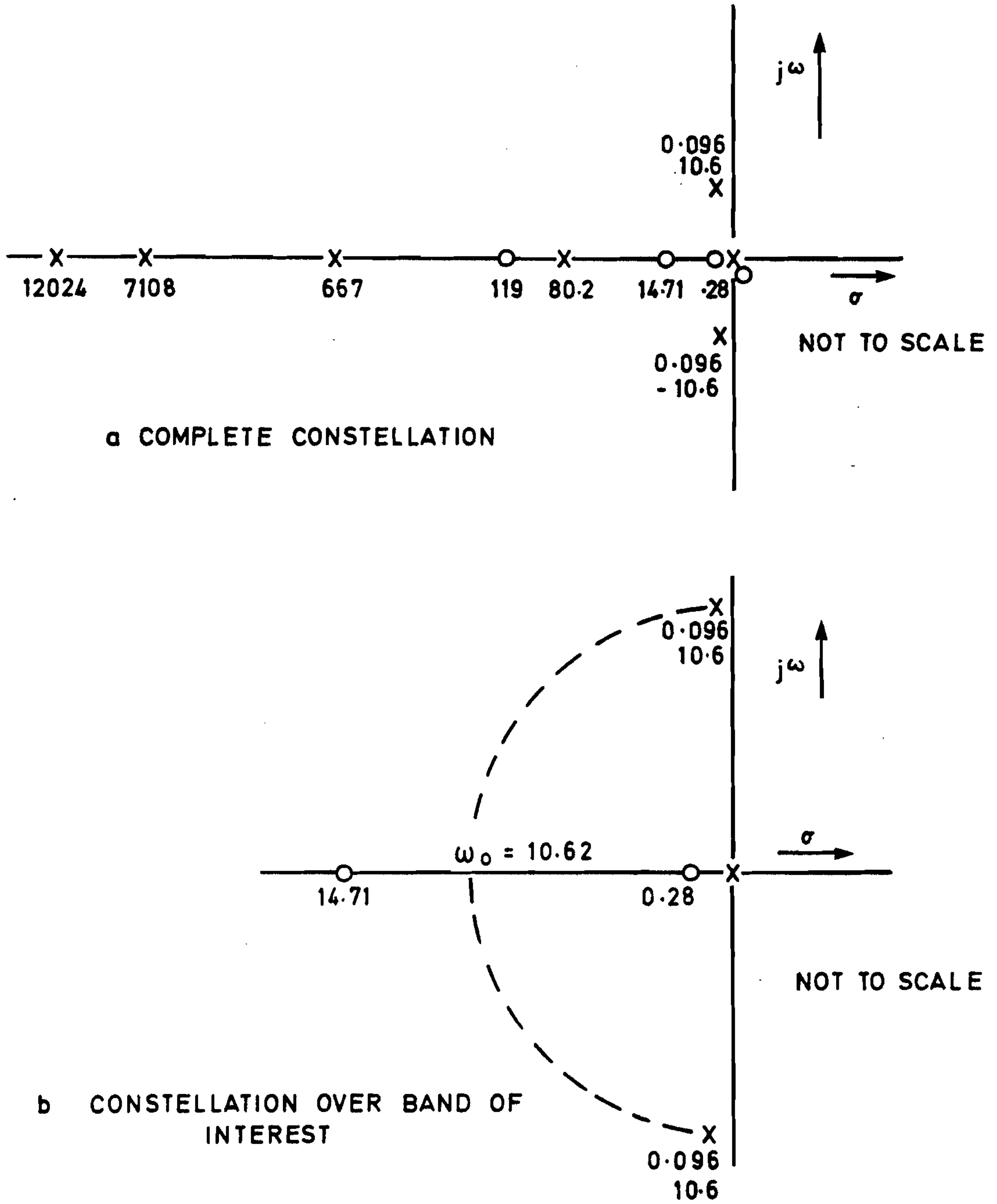

Figure 12 Constellation of Poles and Zeros for Open Circuit Total Loop ($T_L = T_F \times T_R$)

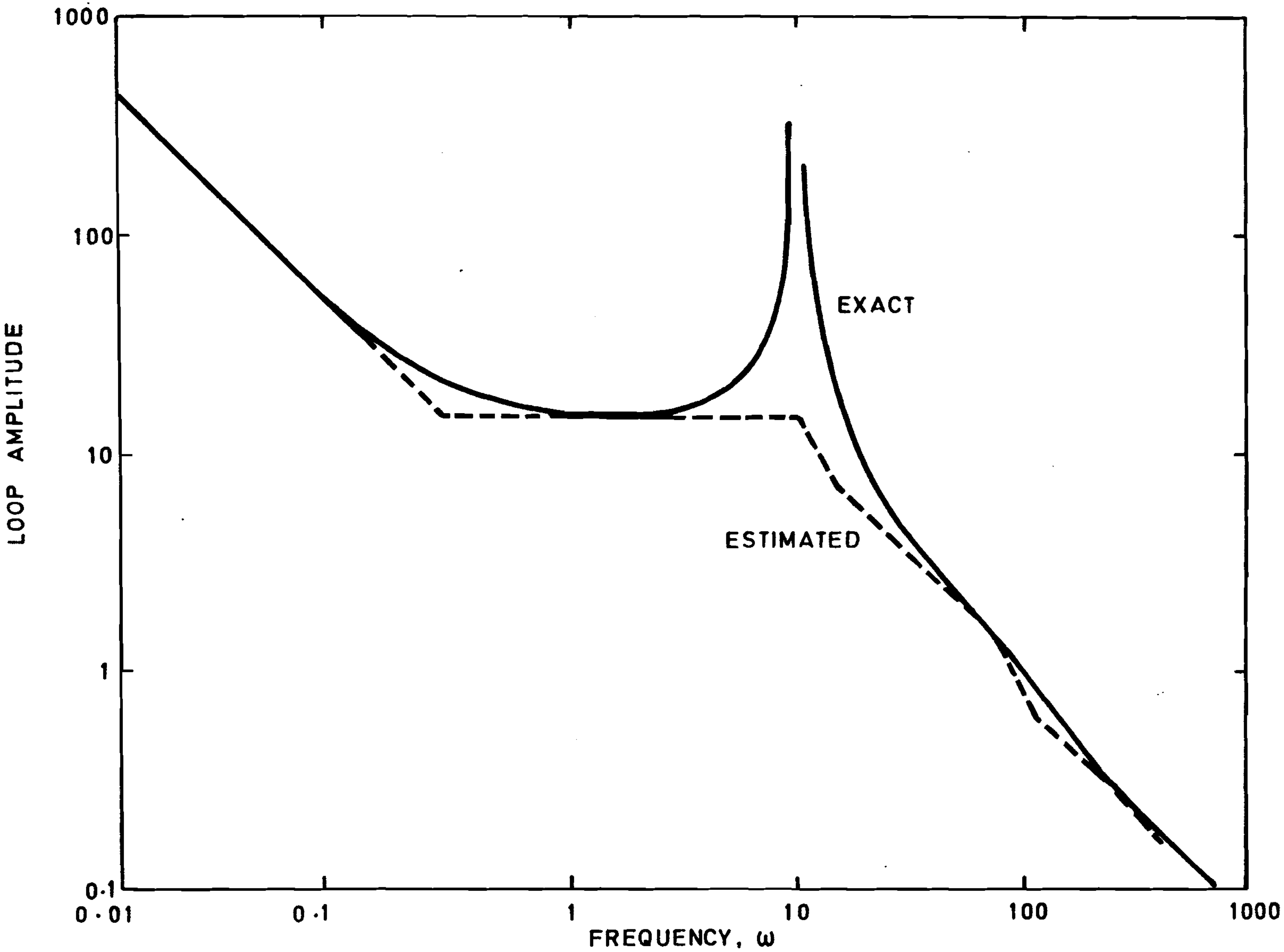

Figure 13(a) Estimated and Exact Amplitudes of the Loop Transfer Function

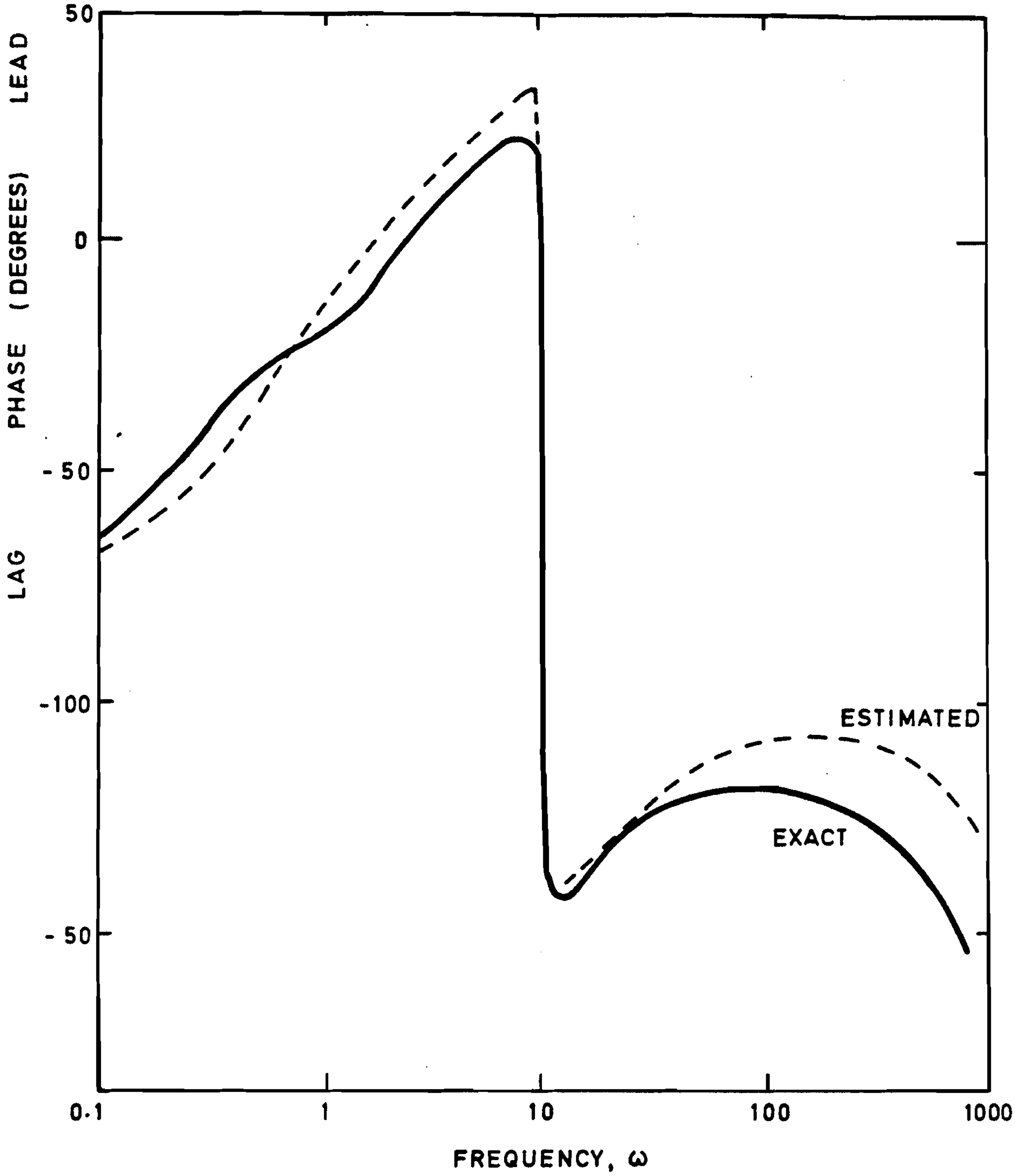

Figure 13(b) Estimated and Exact Phase of the Loop Transfer Function

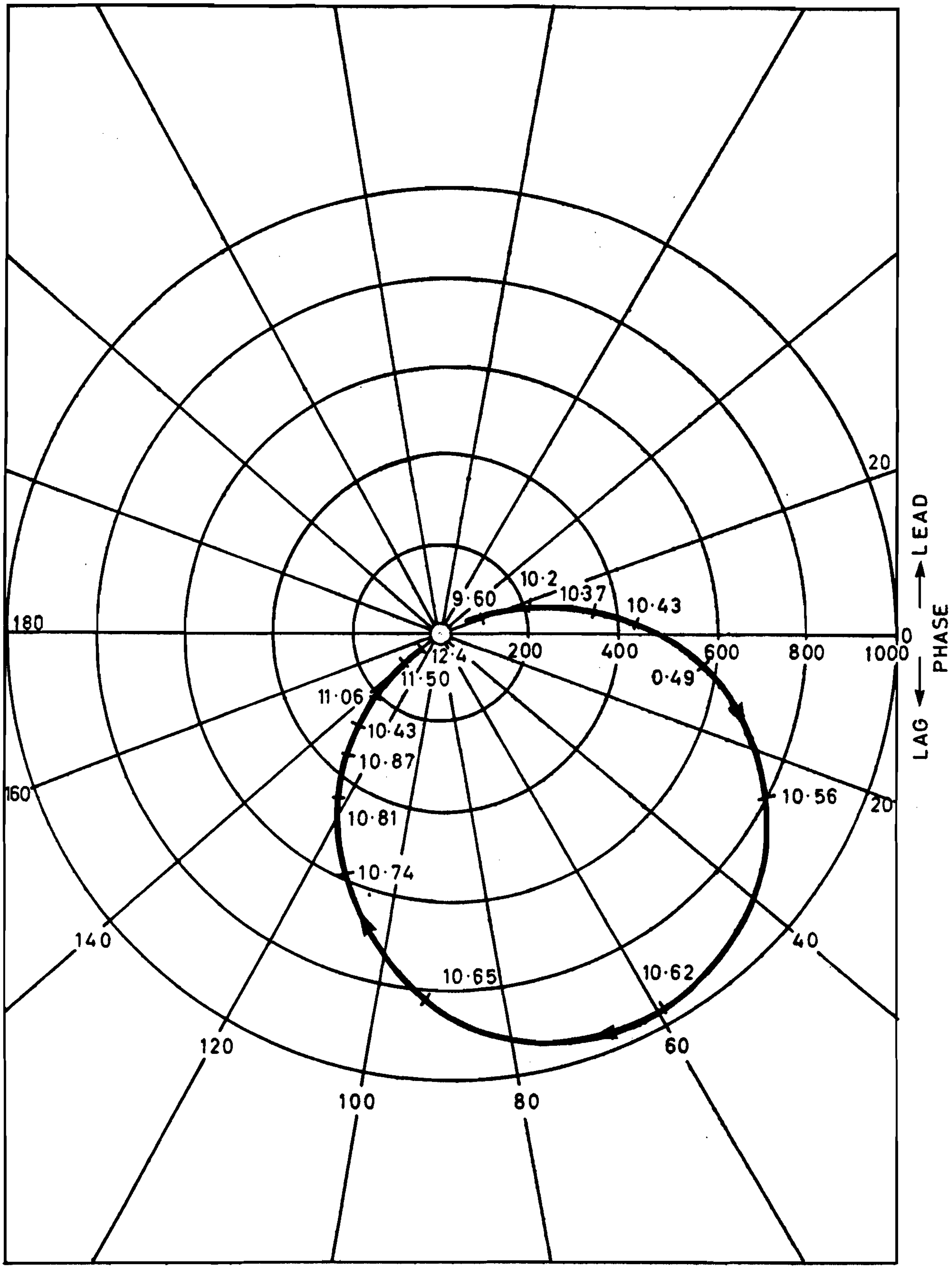

Figure 14(a) Nyquist Diagram for ω Between 9·6 and 11·5

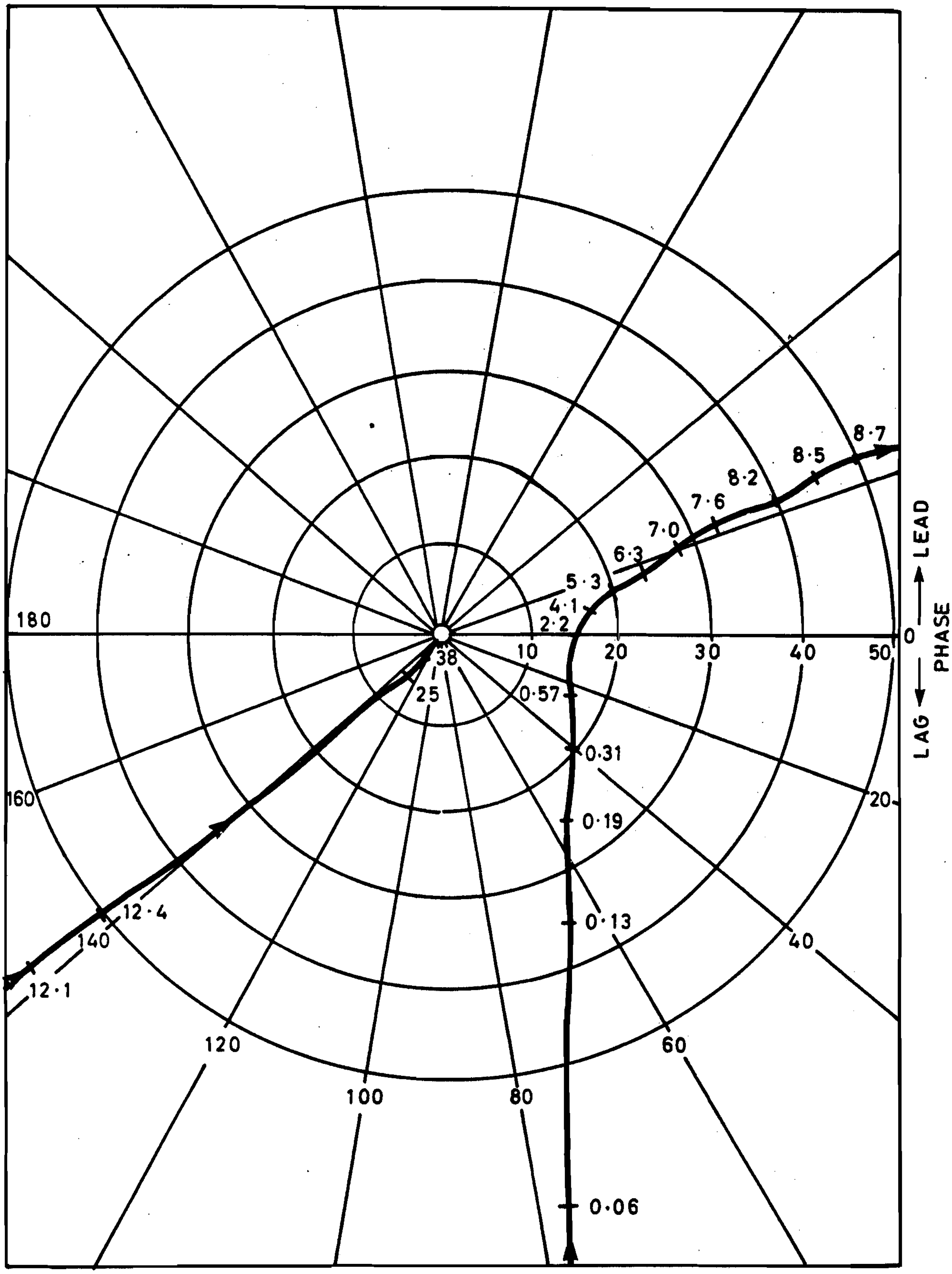

Figure 14(b). Nyquist Diagram for ω between 0·06 and 8·7 and between 12·1 and 38

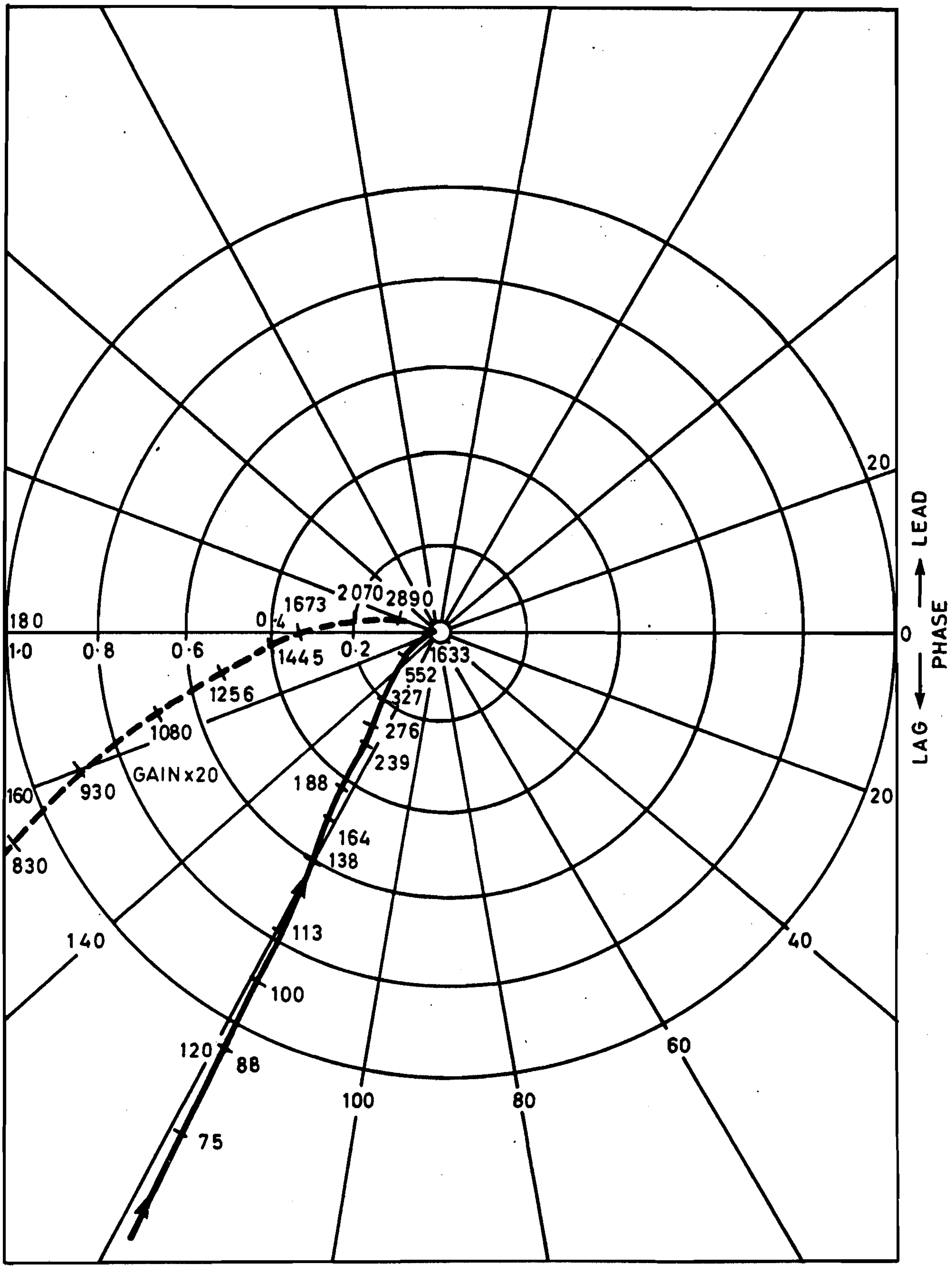

Figure 14(c). Nyquist Diagram for ω between 75 and 1633

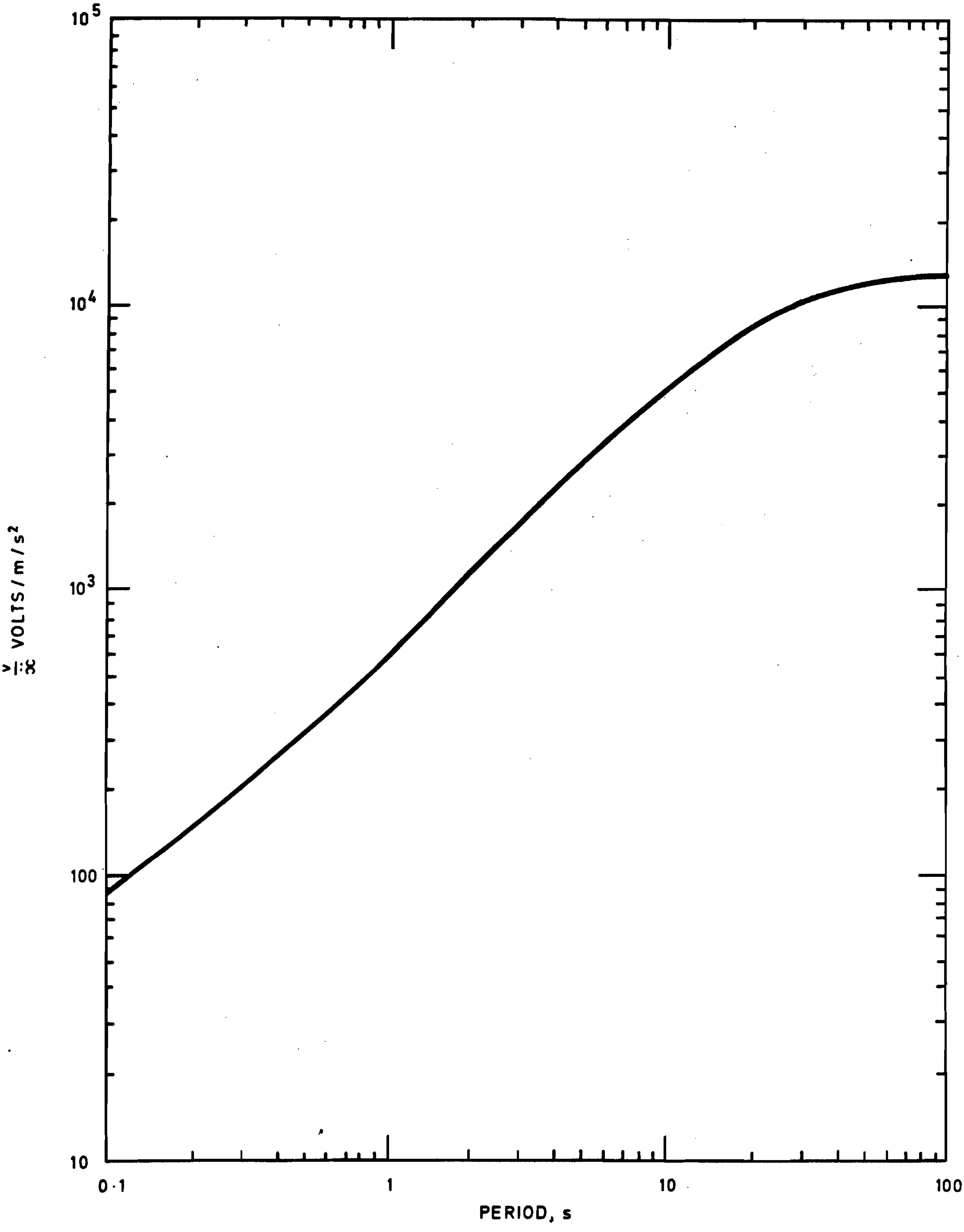

Figure 15(a). Response of Closed Loop to Ground Acceleration

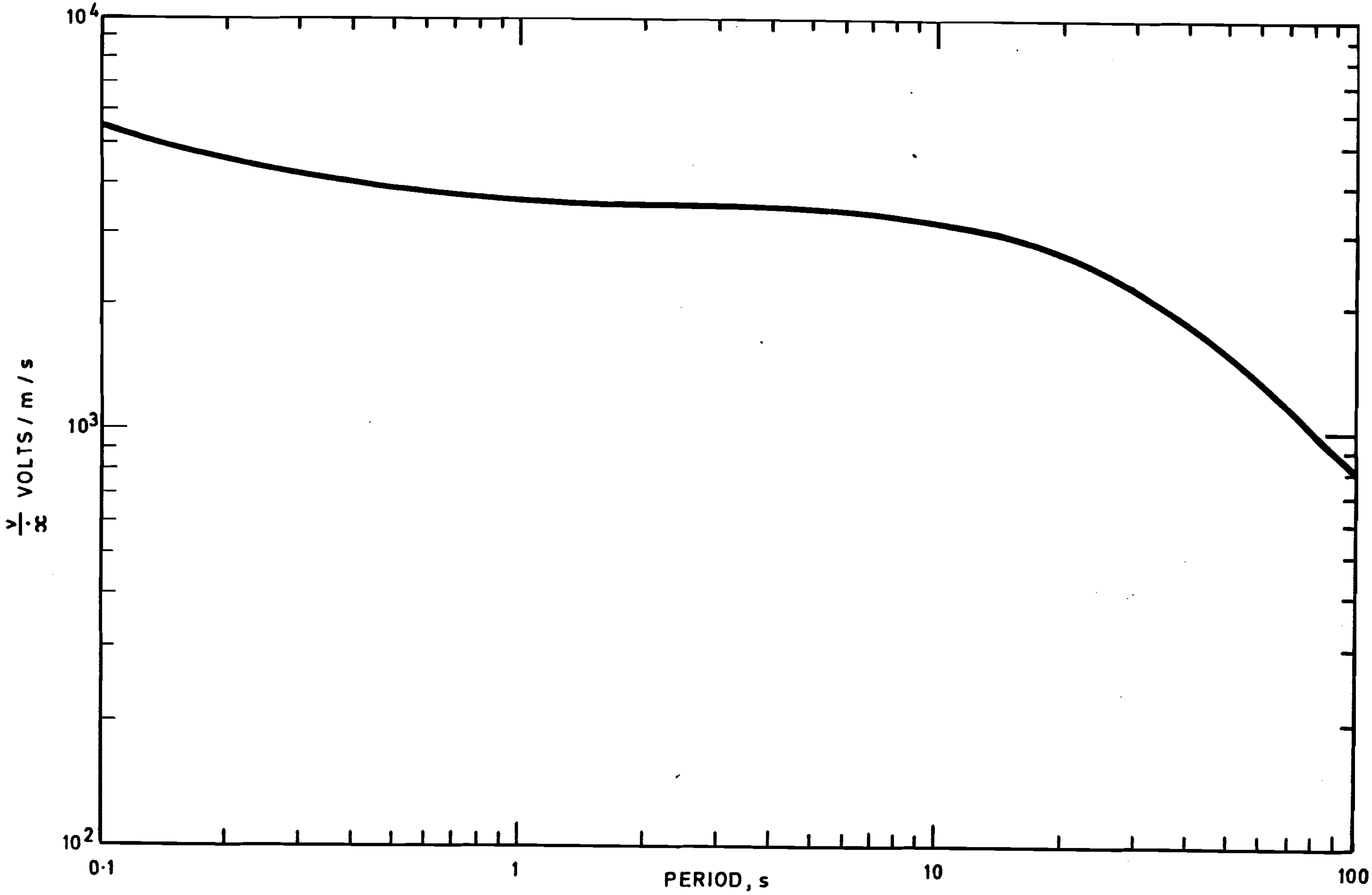

Figure 15(b) Response of Closed Loop to Ground Velocity

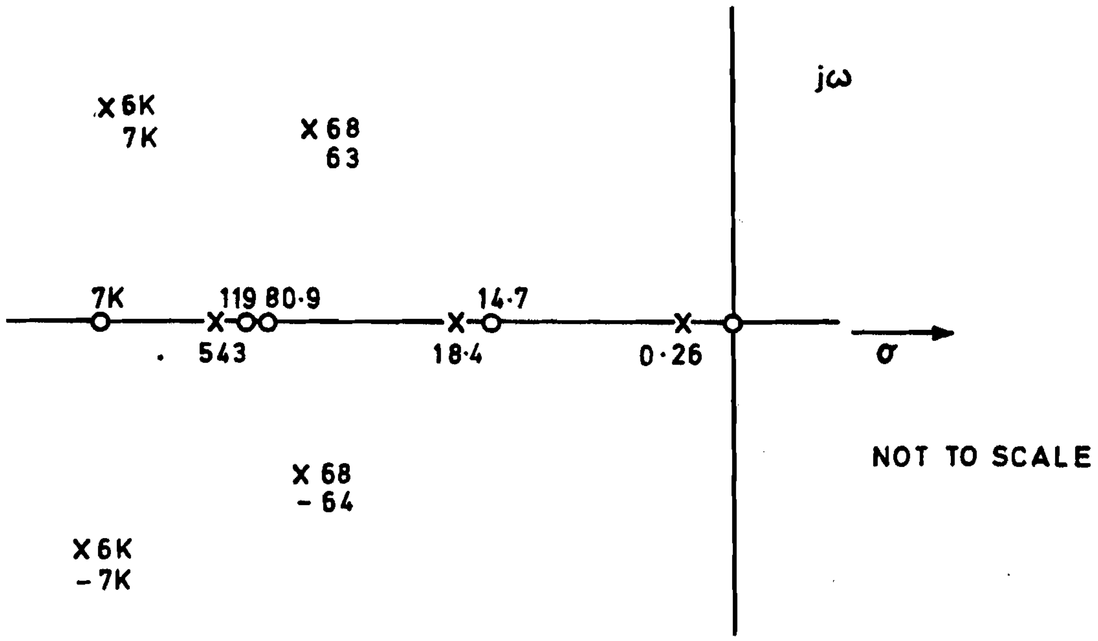

Figure 16(a). Pole Zero Constellation for Closed Loop Velocity Response

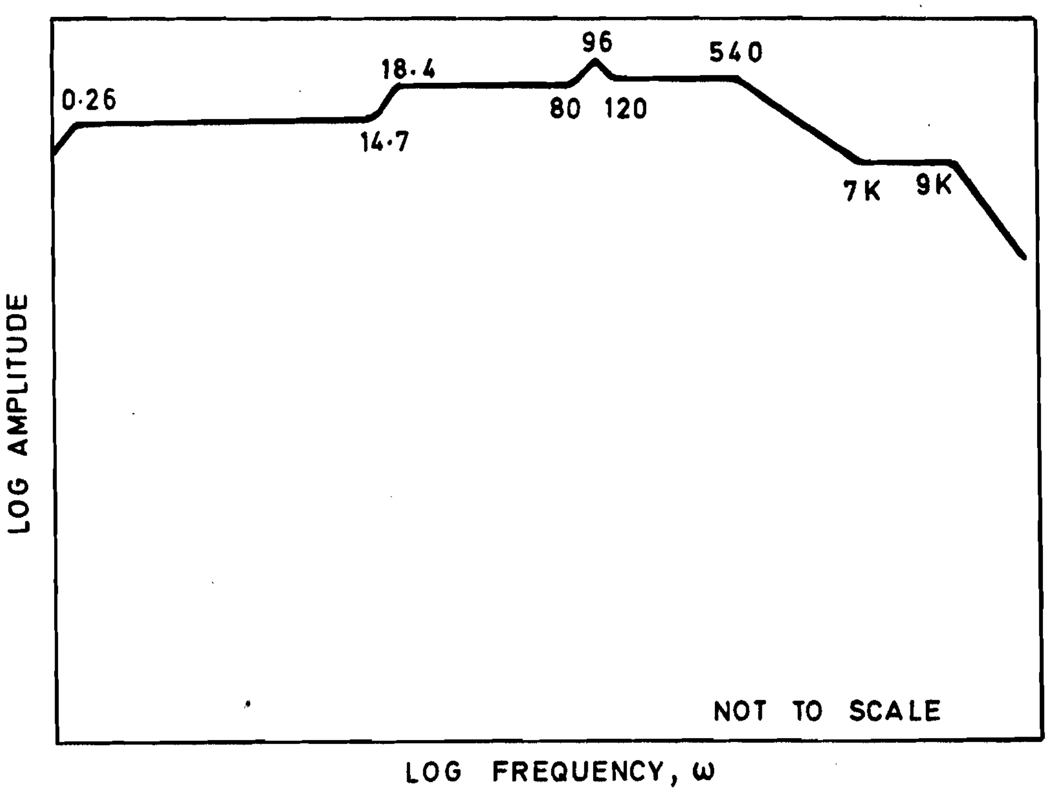

Figure 16(b) Bode Plot for Closed Loop Velocity Response

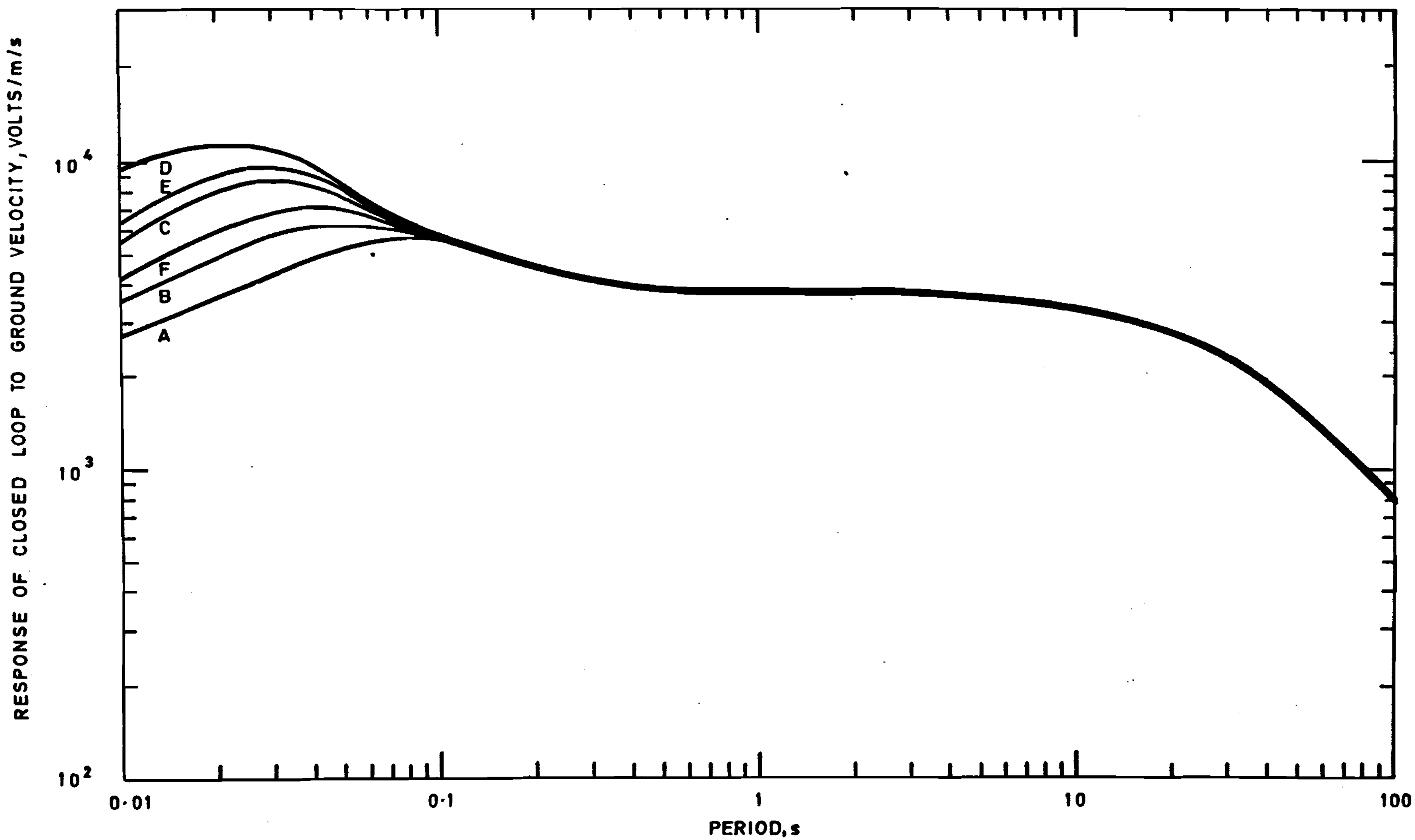

OPEN LOOP GAIN OF SEISMOMETER
A = $0 \cdot 34 \times 10^6$ V/m
B = $0 \cdot 45 \times 10^6$ V/m
C = $0 \cdot 68 \times 10^6$ V/m
D = $1 \cdot 05 \times 10^6$ V/m
E = $0 \cdot 75 \times 10^6$ V/m
F = $0 \cdot 52 \times 10^6$ V/m

Figure 17. Closed Loop Velocity Responses for Six Different Mk IIIC Seismometers

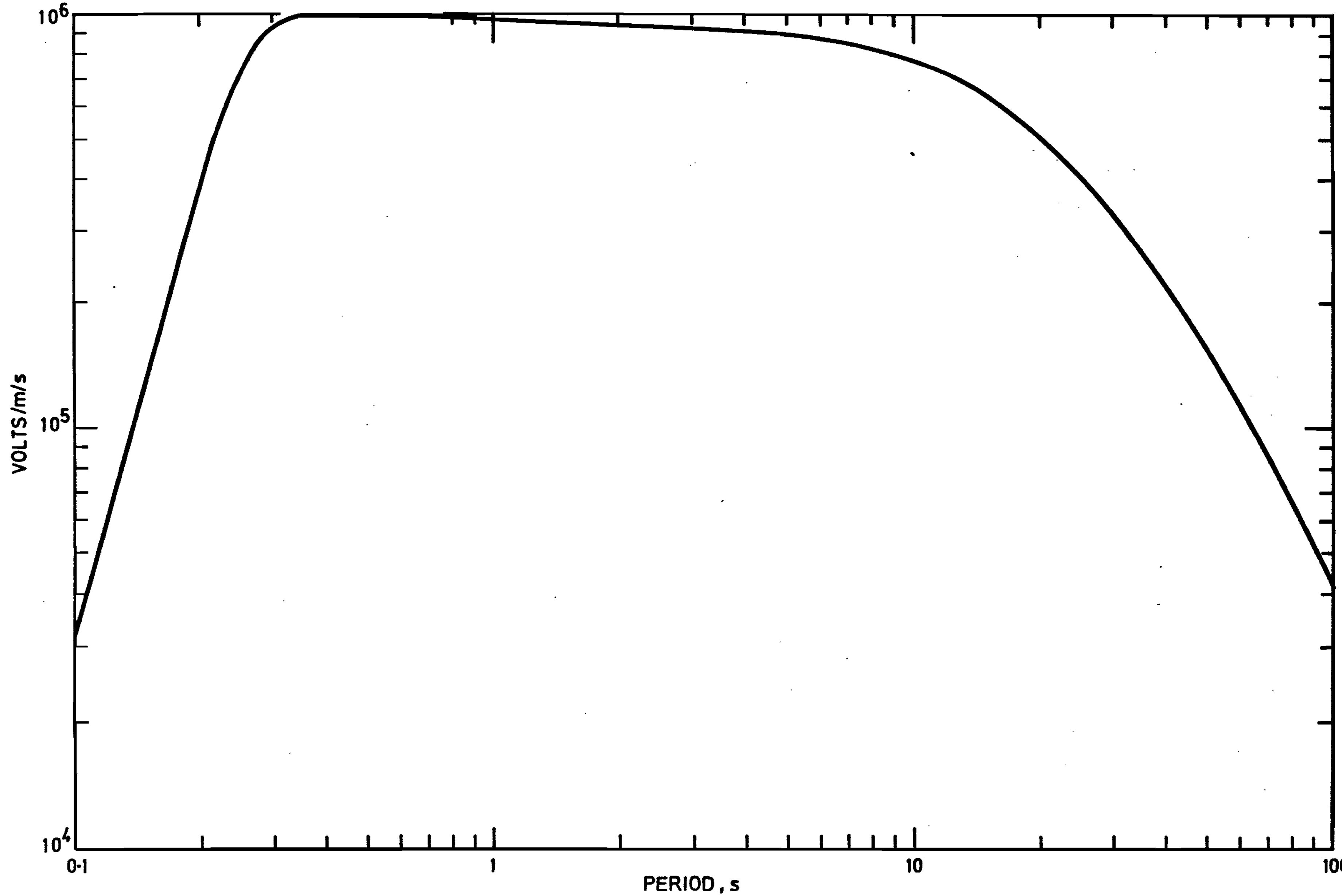

Figure 18(a). VBB Response to Ground Velocity

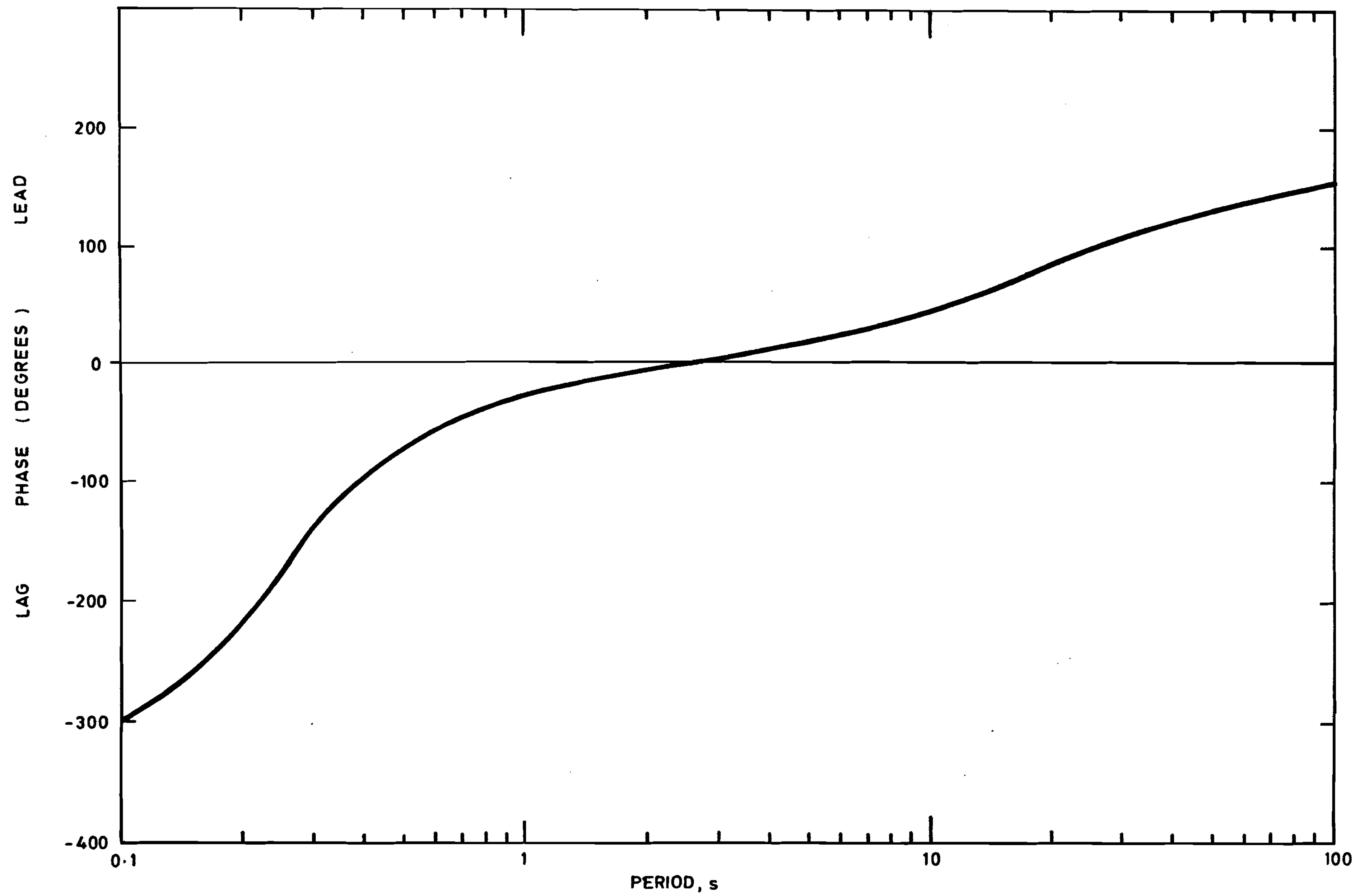

Figure 18(b) VBB Phase Response to Ground Velocity

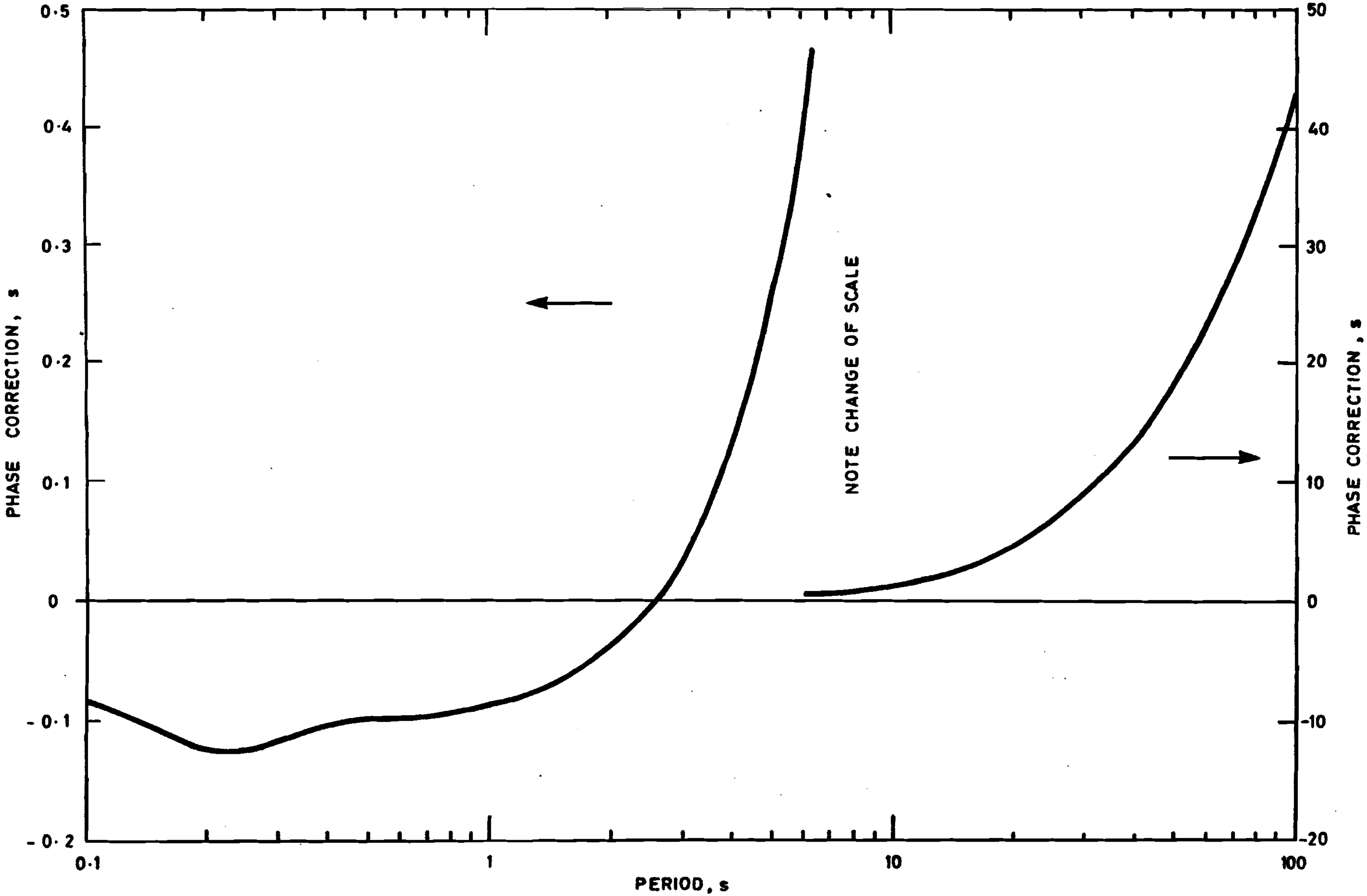

Figure 18 (c). VBB Phase Correction for Ground Velocity

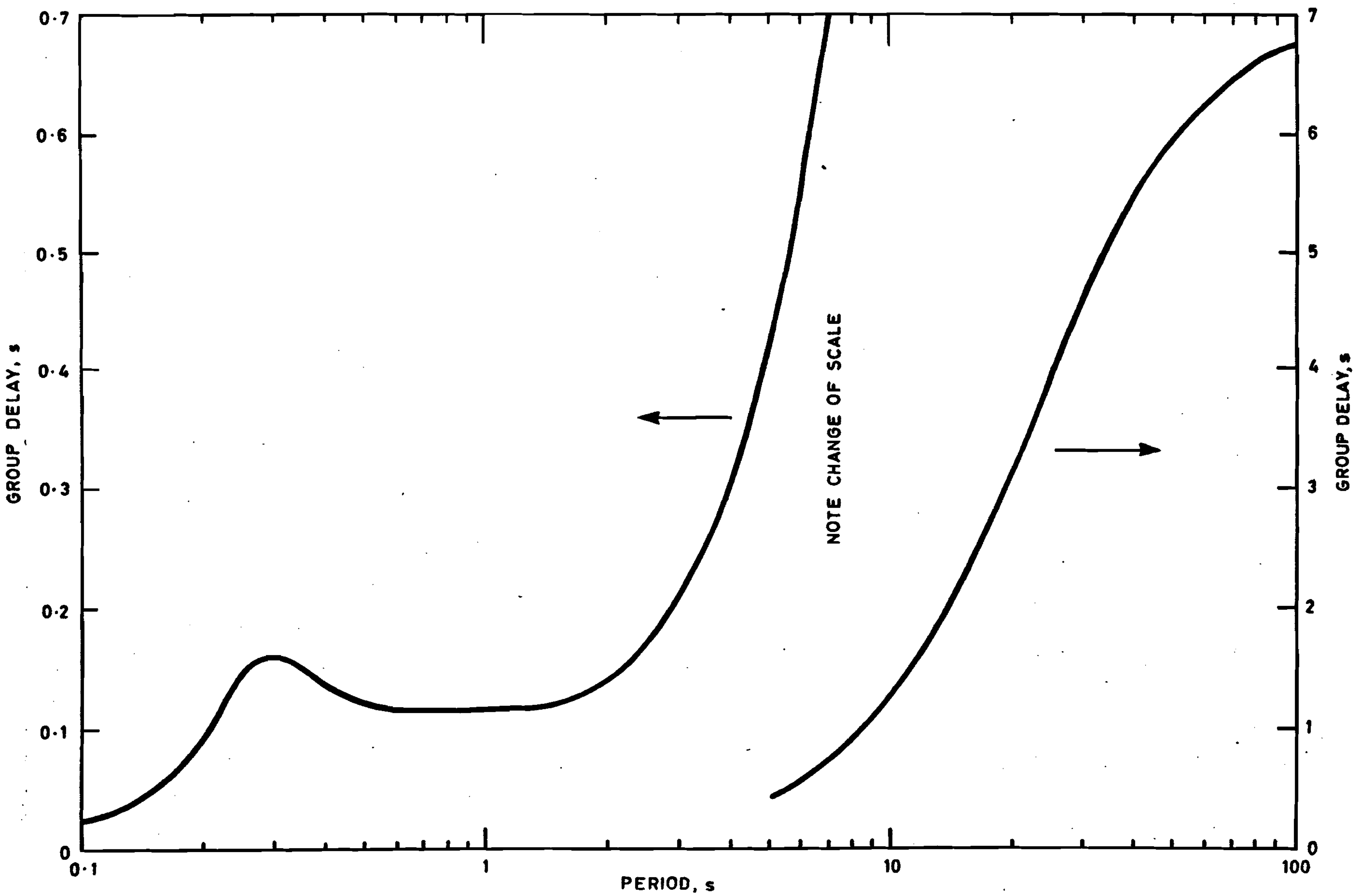

Figure 18(d). VBB Group Delay for Ground Velocity

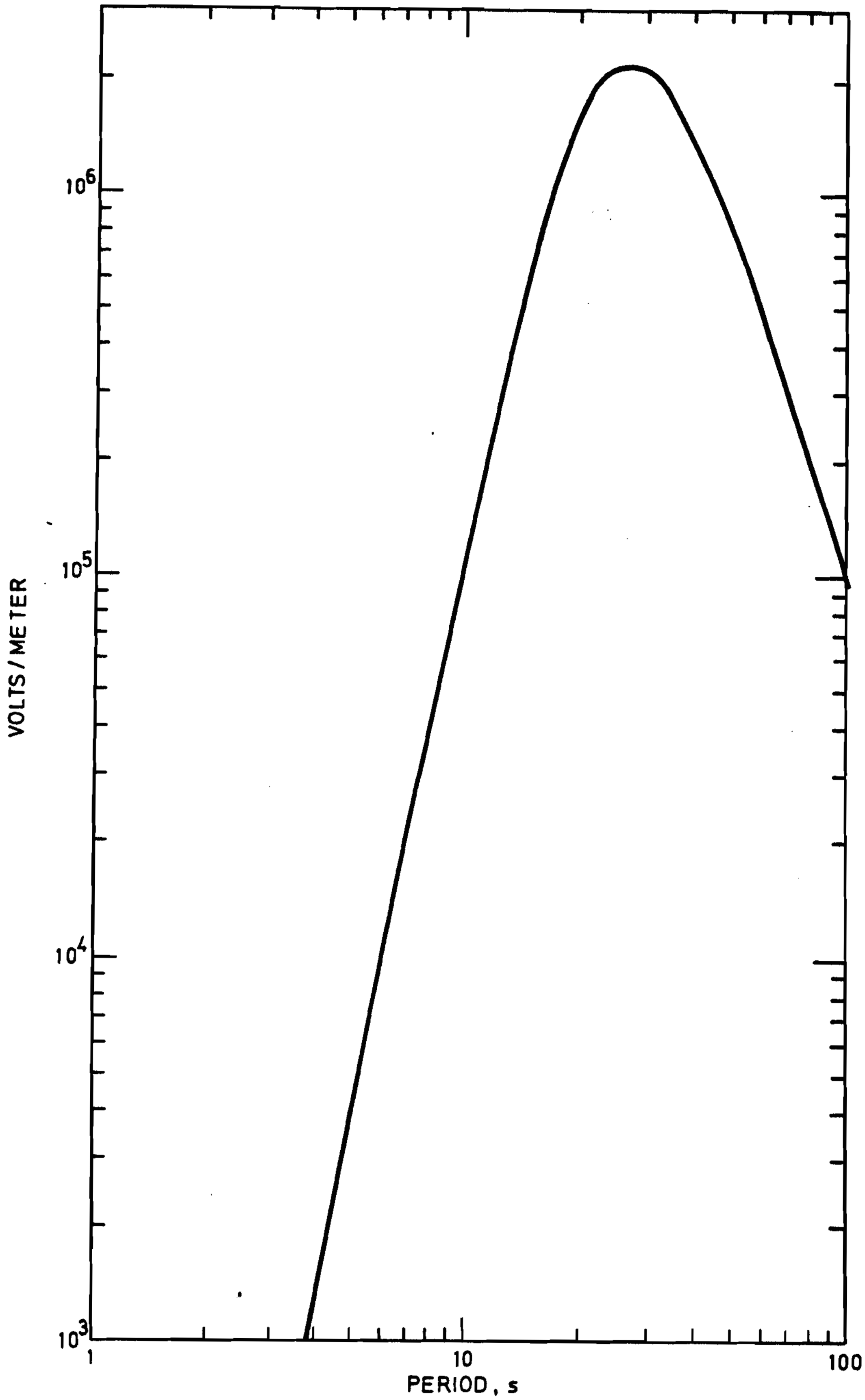

Figure 19(a) LPNB Response to Ground Displacement

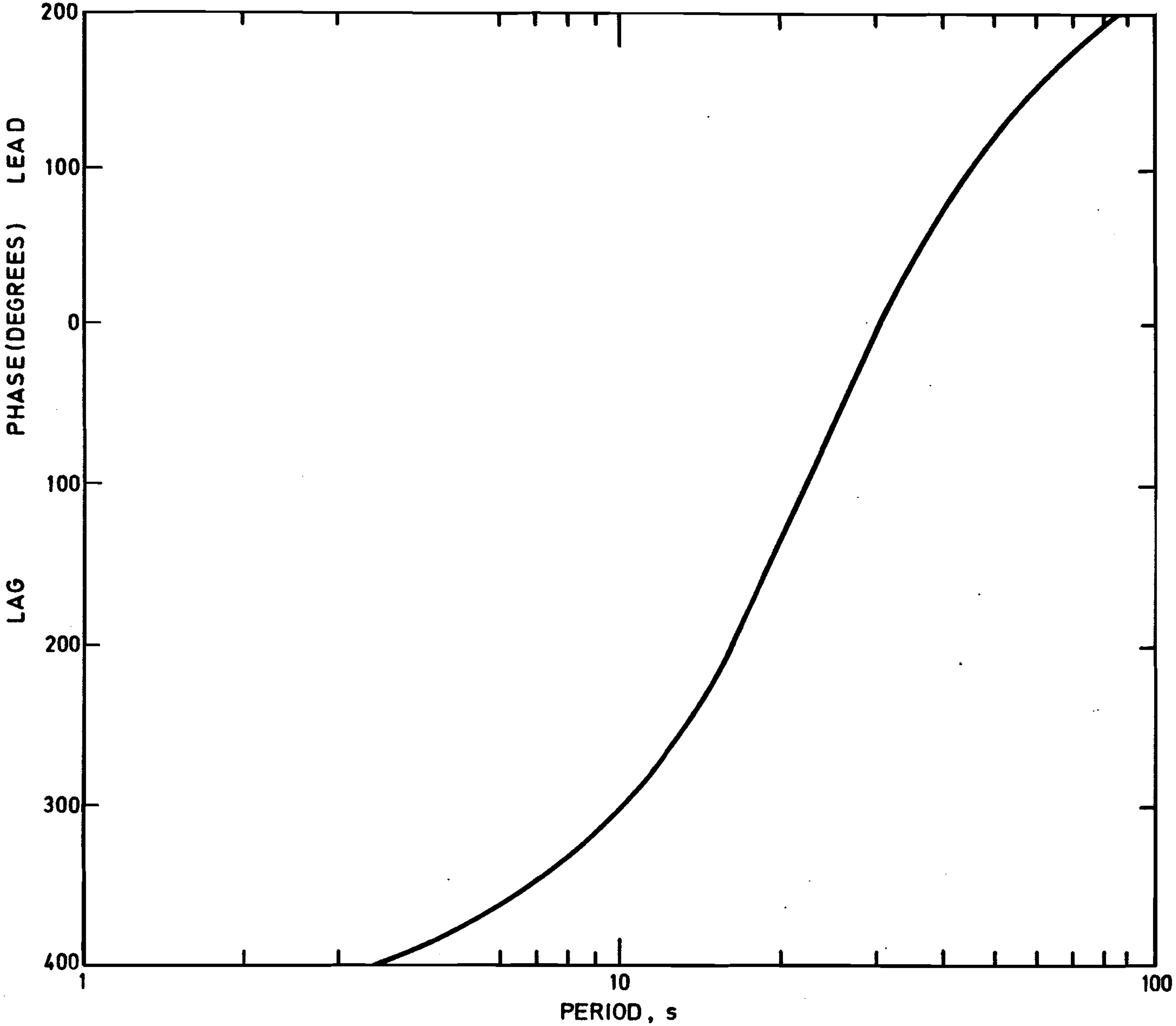

Figure 19(b). LPNB Phase Response to Ground Displacement

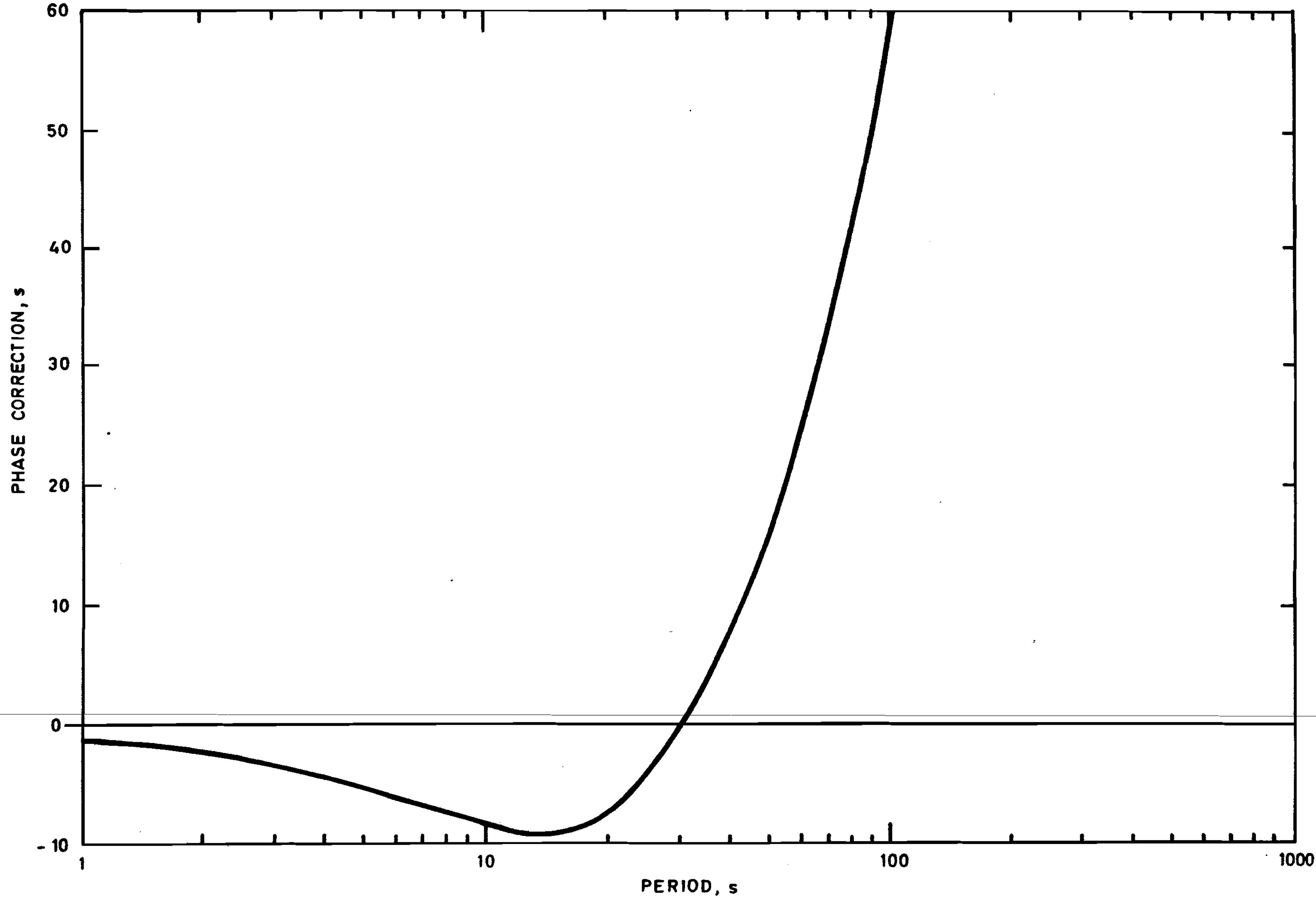

Figure 19(c). LPNB Phase Corrections for Ground Displacement

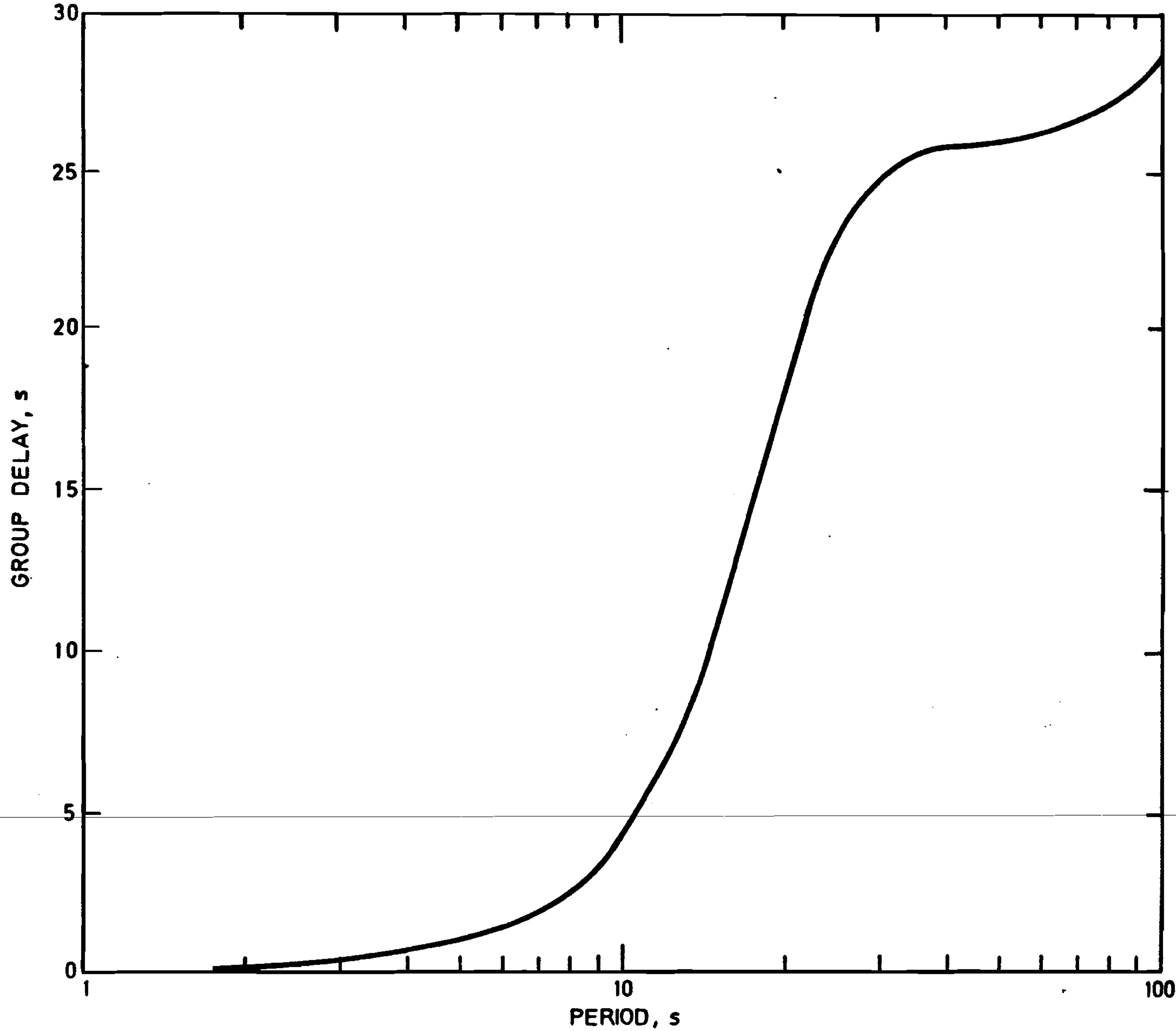

Figure 19(d) LPNB Group Delay for Ground Displacement

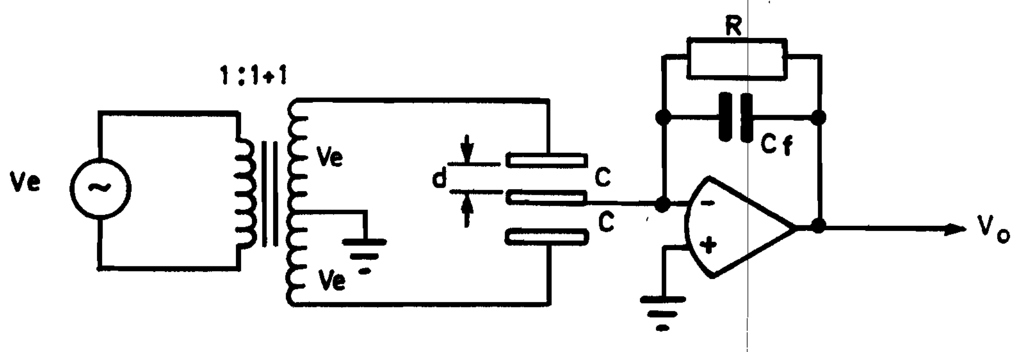

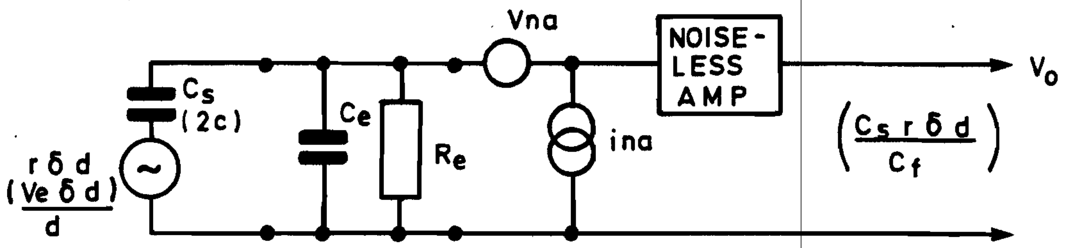

C_s	TRANSDUCER CAPACITANCE	~20pF
Ce	PARALLEL STRAY CAPACITANCE	~20pF
R_e	EFFECTIVE PARALLEL RESISTANCE (BIAS + STRAYS)	~5MΩ
Rnv	NOISE EQUIVALENT RESISTANCE OF AMPLIFIER	~1KΩ
Rni		~10MΩ
r	SENSITIVITY OF TRANSDUCER	~5x10^{3}V/m

$$R_n = R_{nv}\left[\{(C_e + C_s)/C_s\}^2 + (\omega^2 C_s^2 R_e^2)^{-1}\right] + (\omega^2 C_s^2)^{-1}(R_{ni}^{-1} + R_e^{-1})$$

Figure 20. Noise Equivalent Circuit for Displacement Transducer

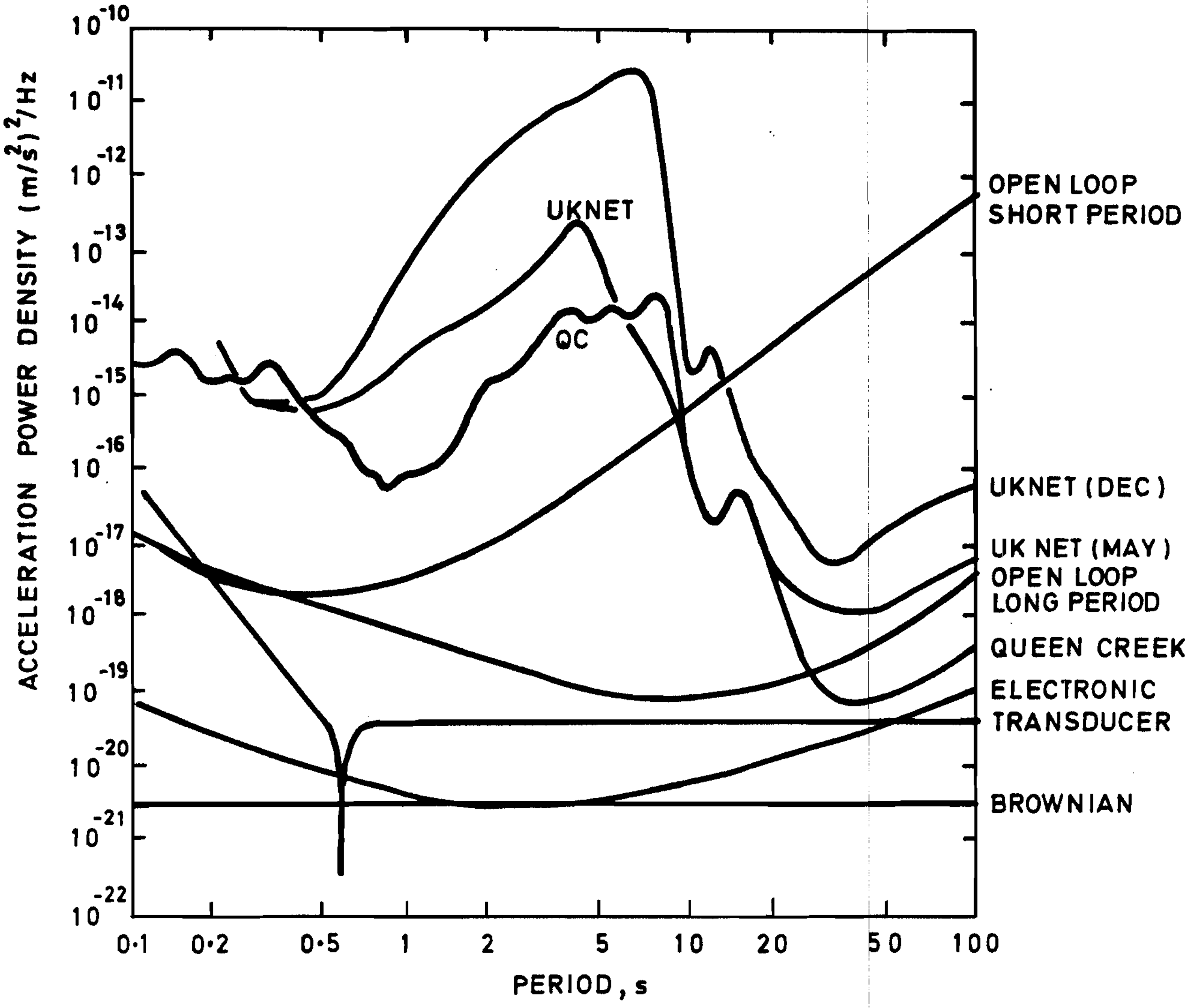

Figure 21. Instrument Noise and Seismic Noise Acceleration Power Density Spectra

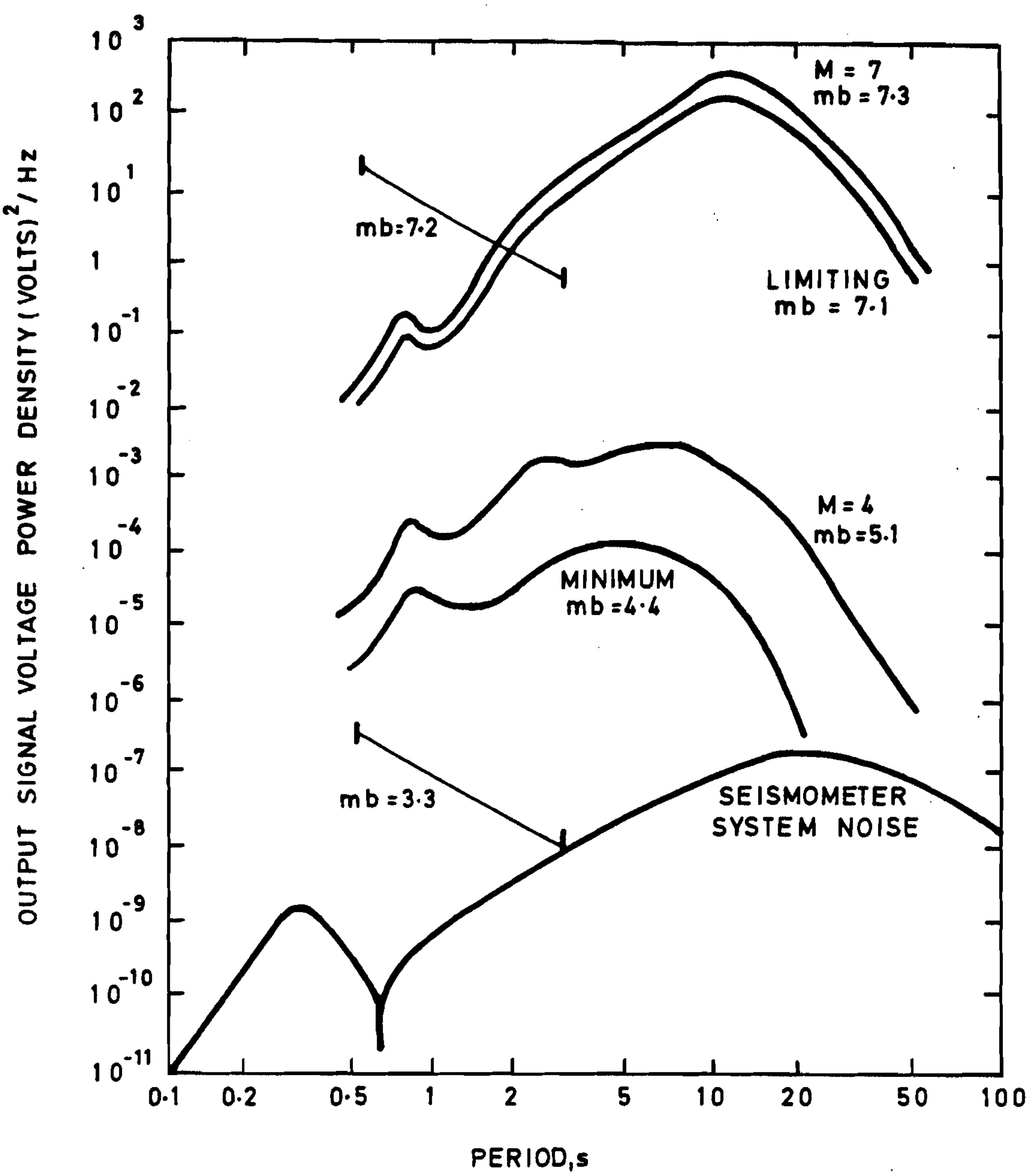

Figure 22. Spectra of VBB Output Signals for Model Events and System Noise

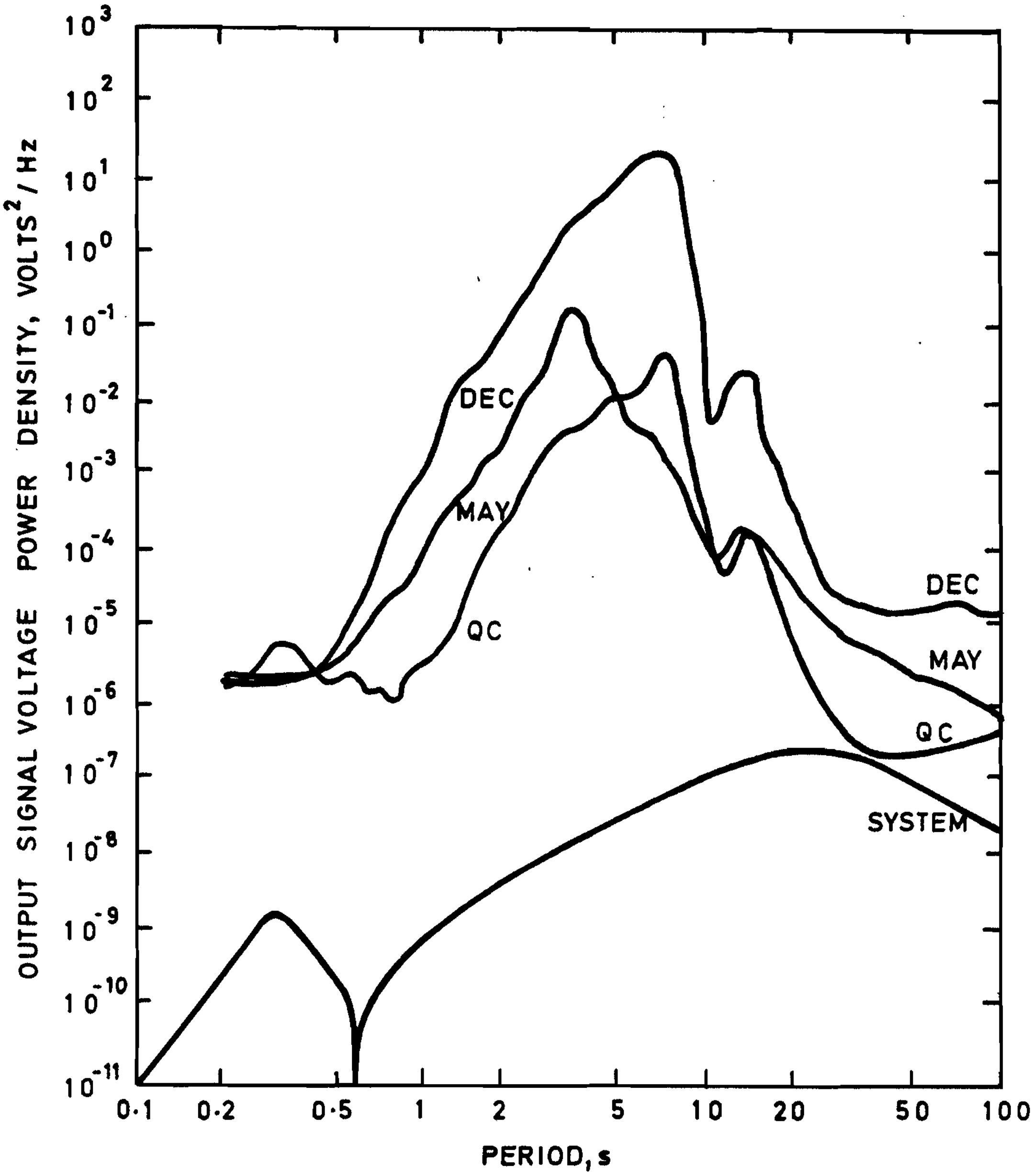

Figure 23. Spectra of VBB Output for Seismic and System Noise

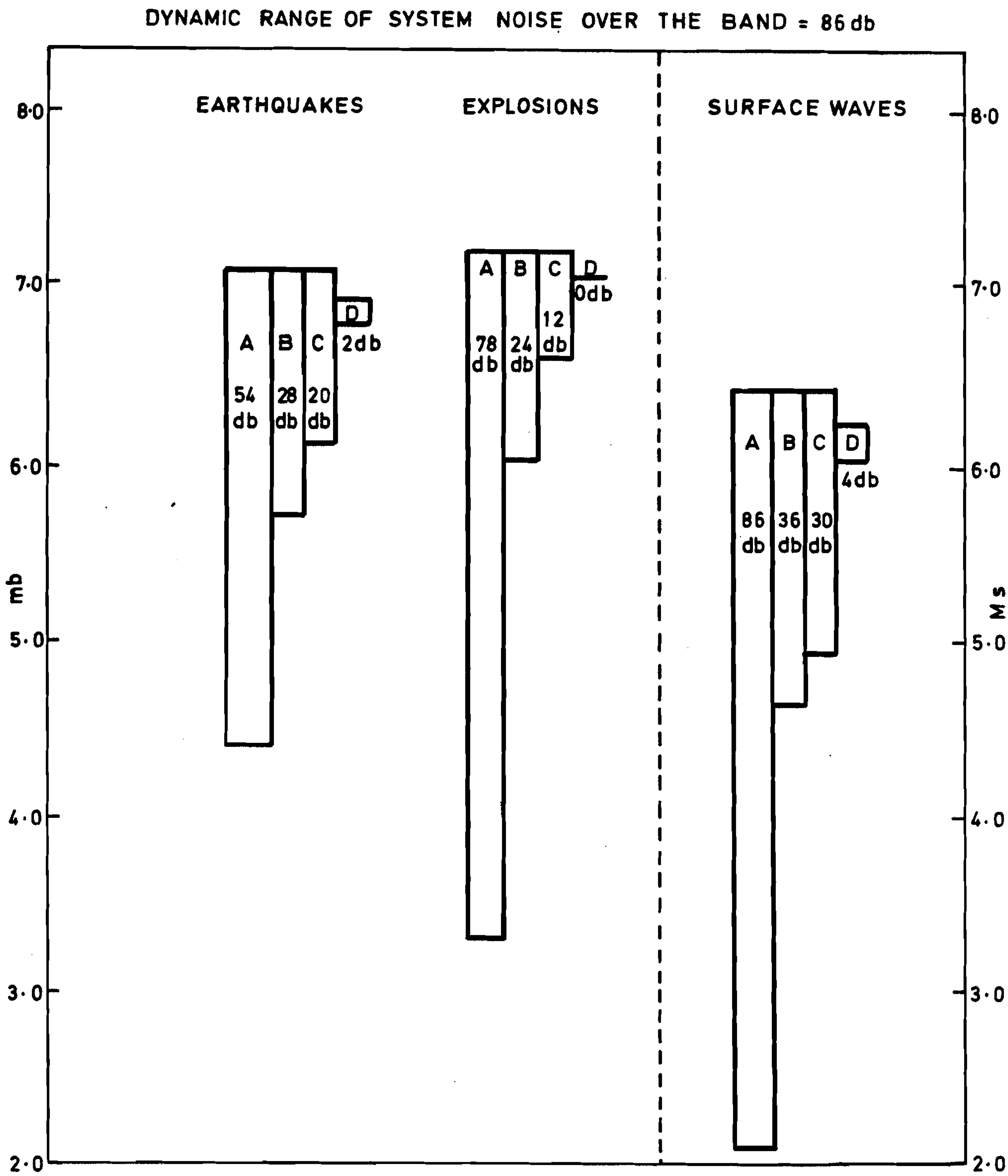

A CONSIDERING SYSTEM NOISE ONLY
B CONSIDERING SEISMIC NOISE WITH QUEEN CREEK SPECTRUM
C CONSIDERING SEISMIC NOISE WITH UKNET (MAY)
D CONSIDERING SEISMIC NOISE WITH UKNET (DECEMBER)

Figure 24. Ranges of Magnitude for VBB Output Signals

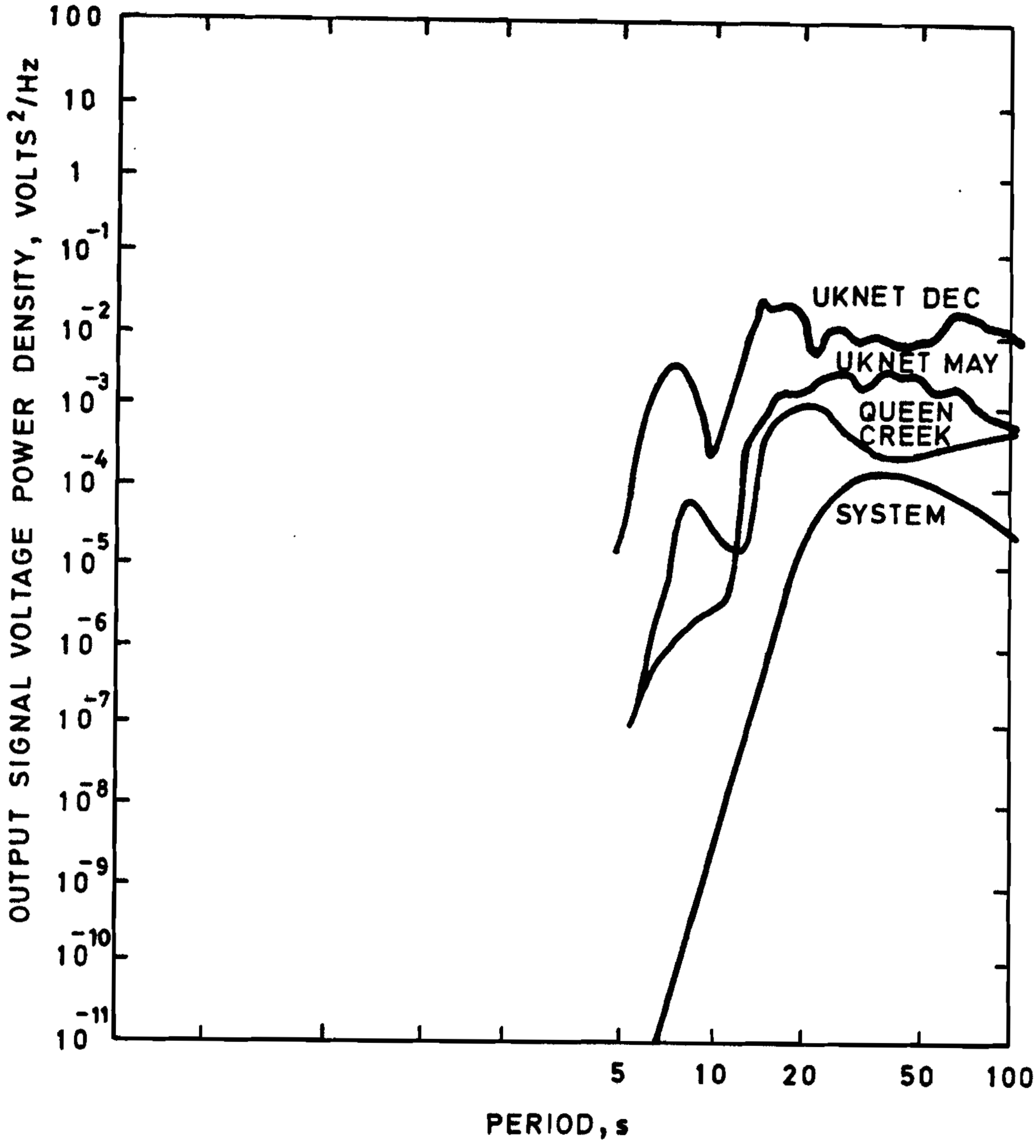

Figure 25. Spectra of LPNB Output for System and Seismic Noise

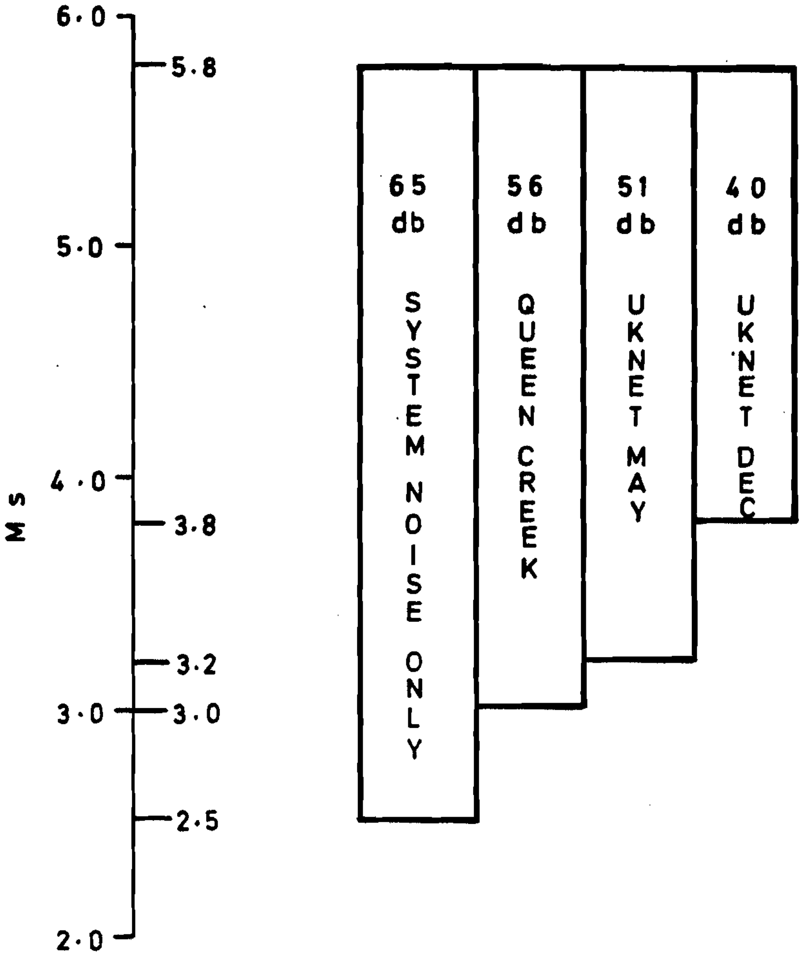

Figure 26. Ranges of Magnitude for LPNB Output Signals

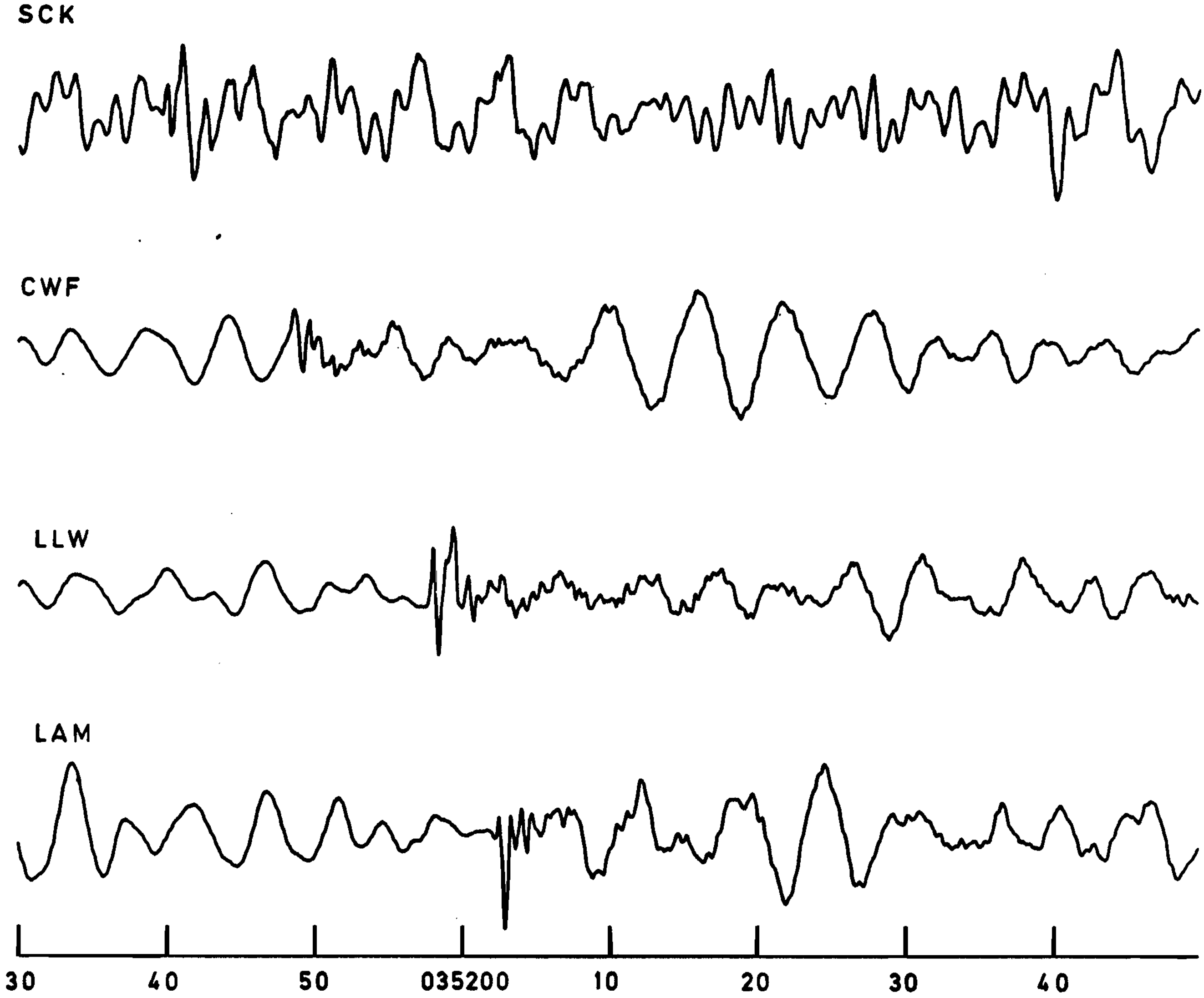

Figure 27. Velocity Broad Band (VBB) Signals from Four UKNet Stations.

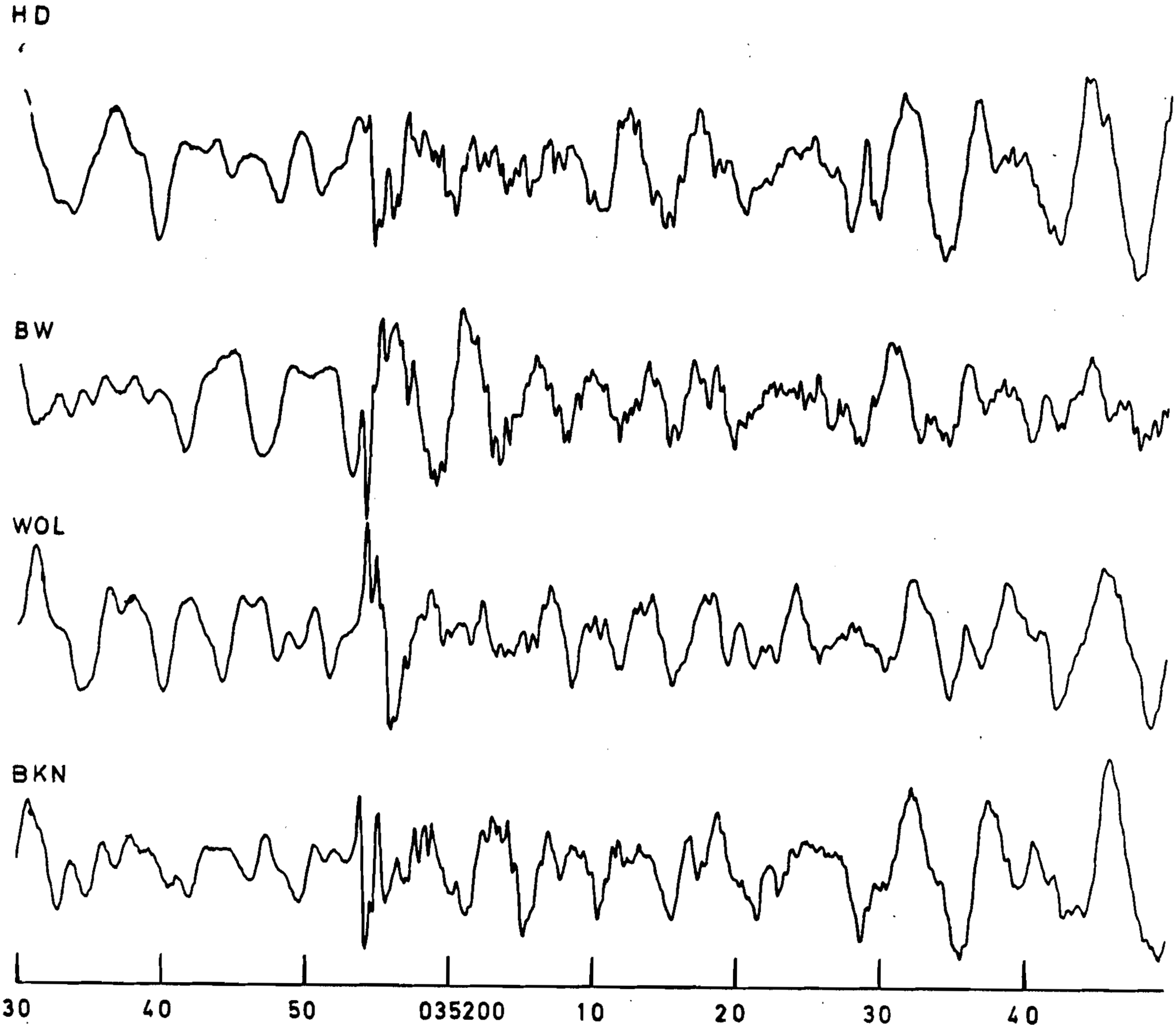

Figure 28 Velocity Broad Band (VBB) Signals from Four Local Stations

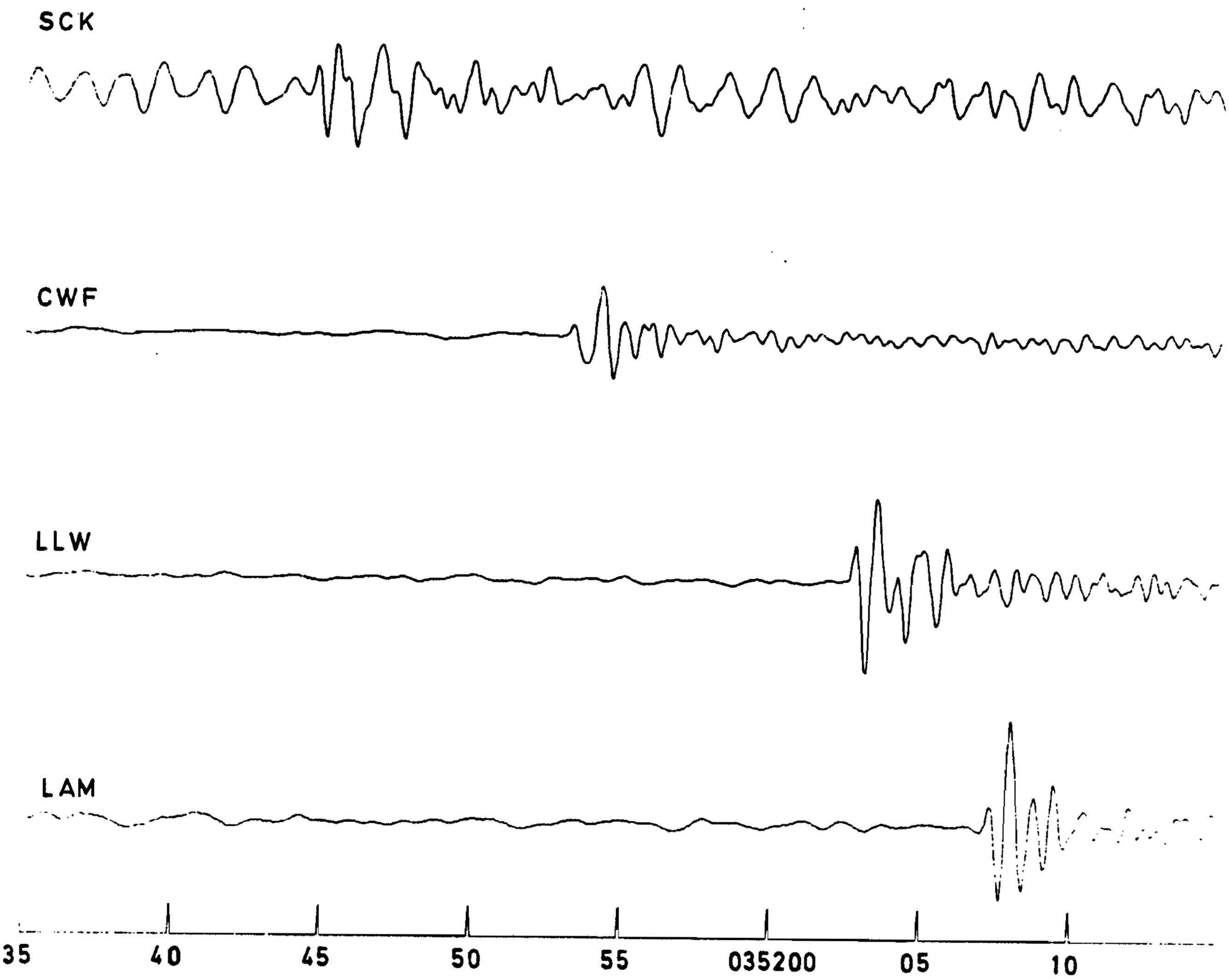

Figure 29. Short Period Signals from VBB (Four UKNet Stations)

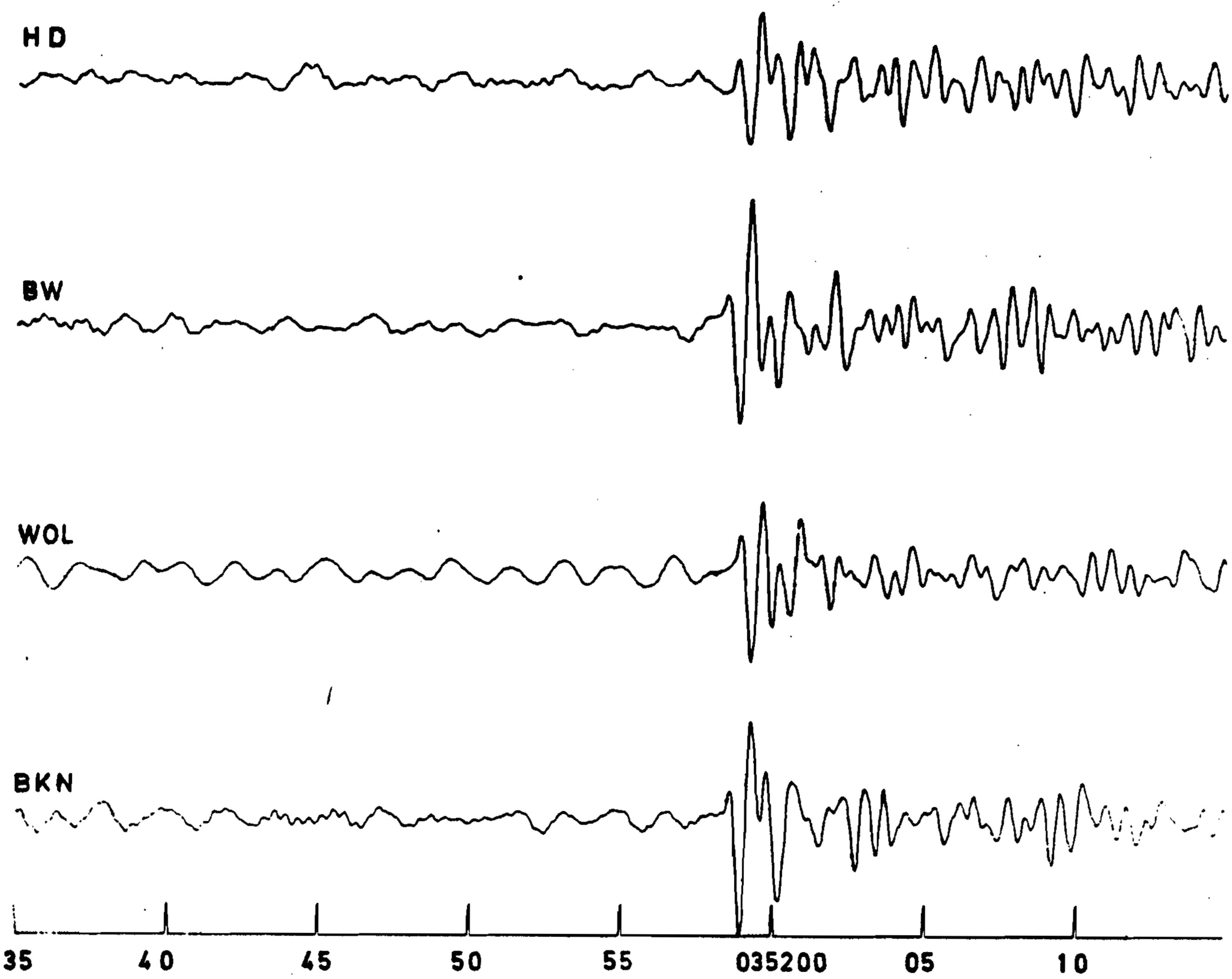

Figure 30. Short Period Signals from VBB (Four Local Stations)

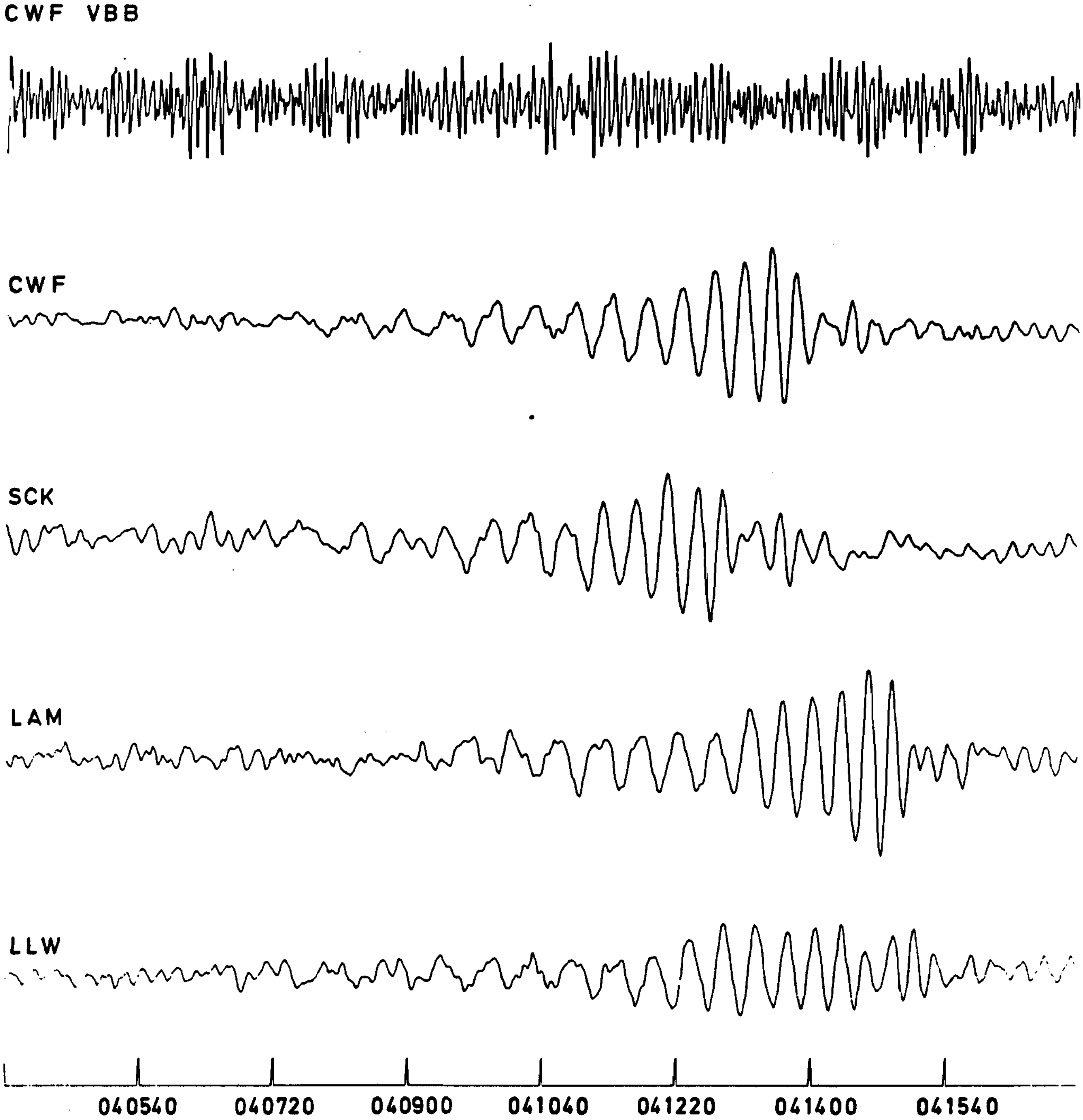

Figure 31. Surface Waves Derived from VBB (Four UKNet Stations.

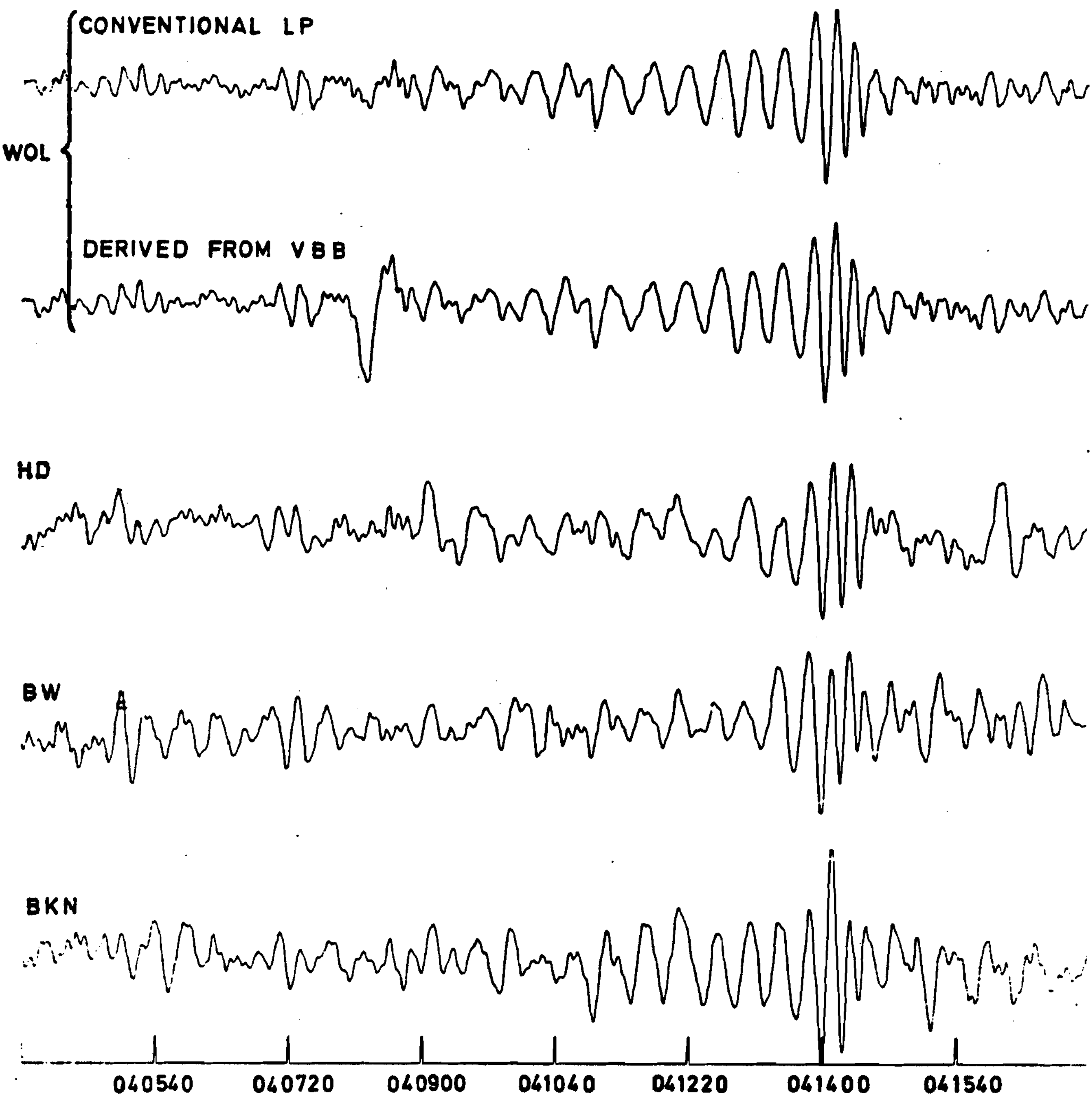

Figure 32. Surface Waves Derived from VBB (Four Local Stations.)

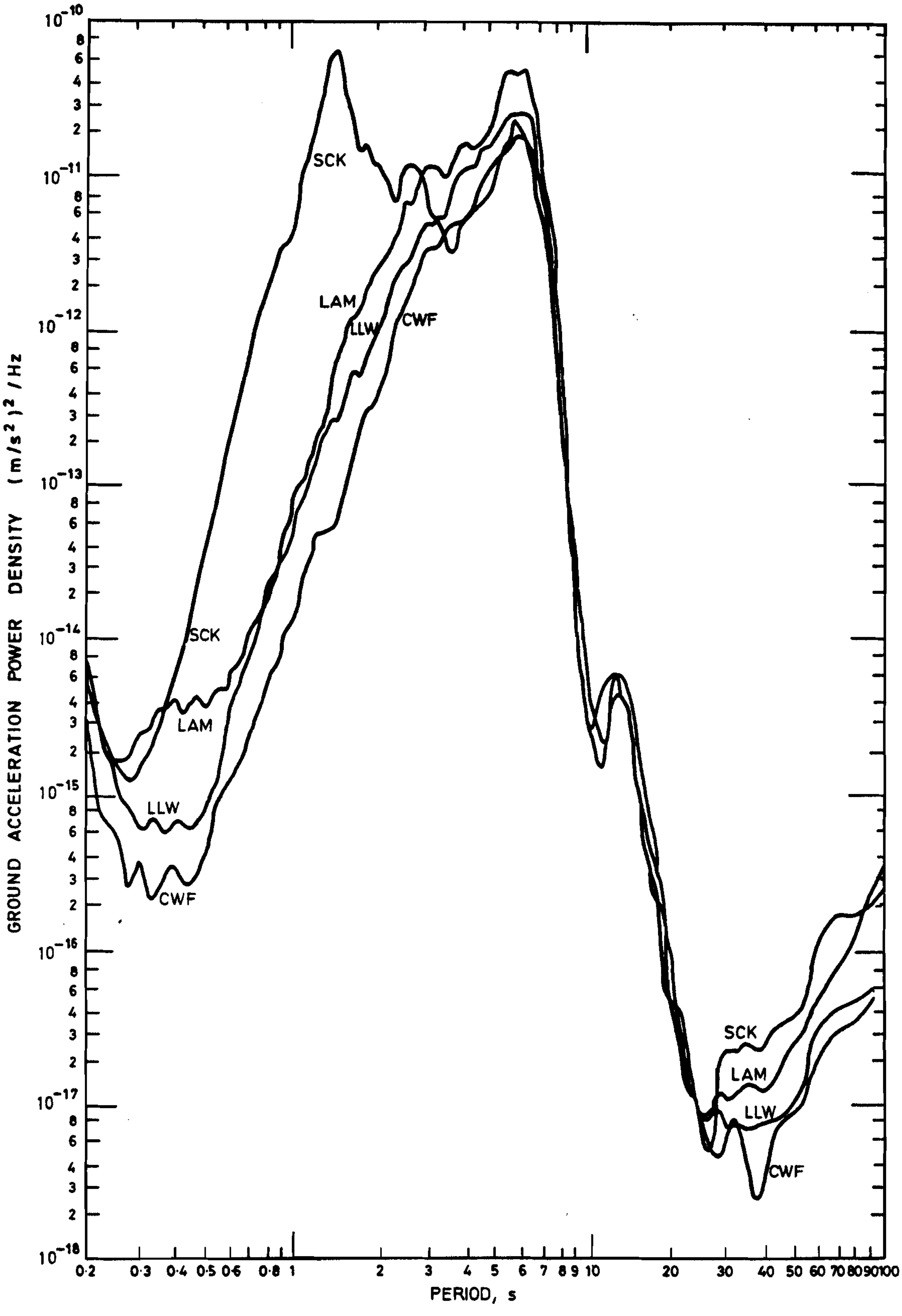

Figure 33. Smoothed Spectra of Seismic Noise at Four UKNet Sites (December)

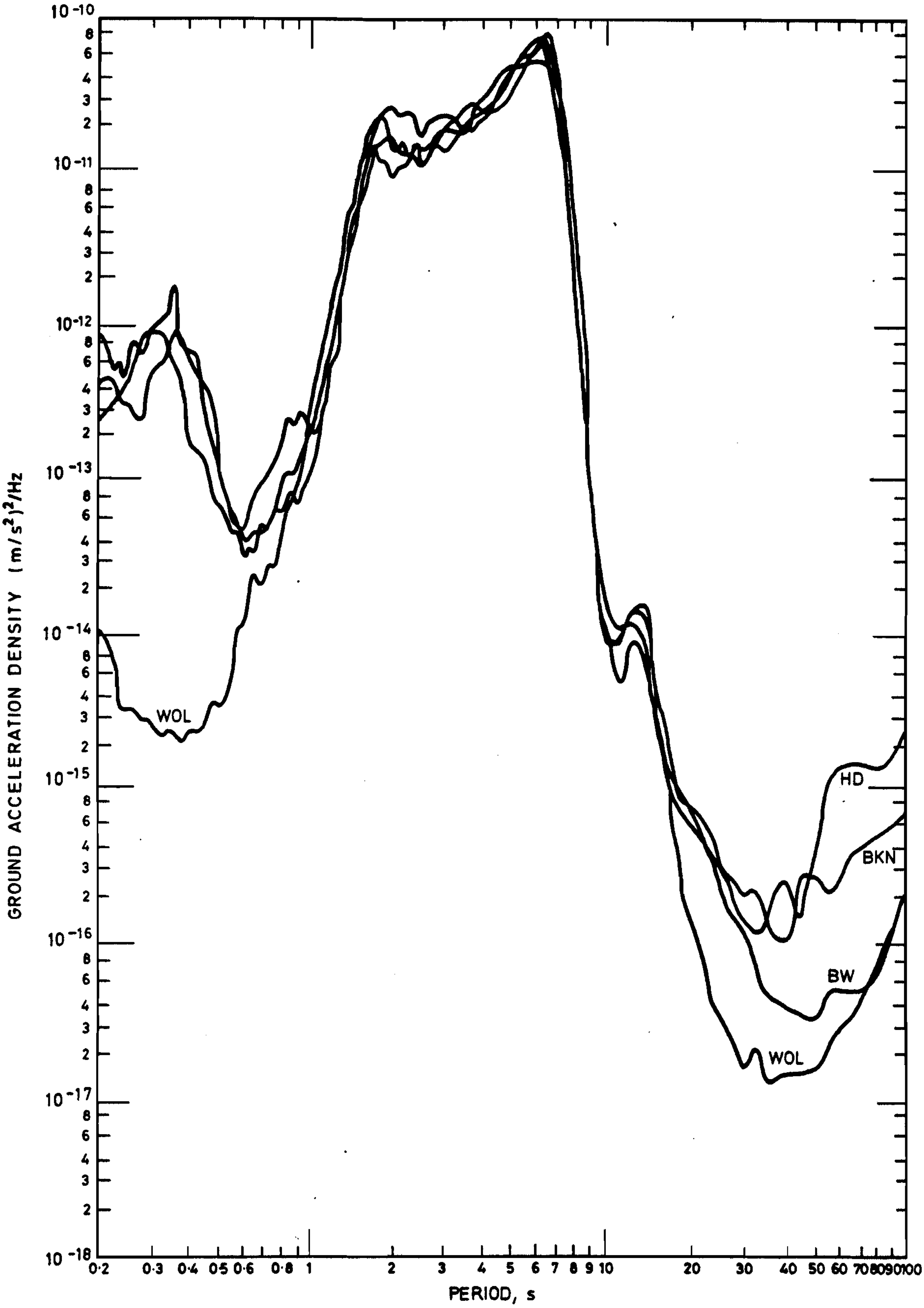

Figure 34. Smoothed Spectra of Seismic Noise at Four BNA Sites (December)

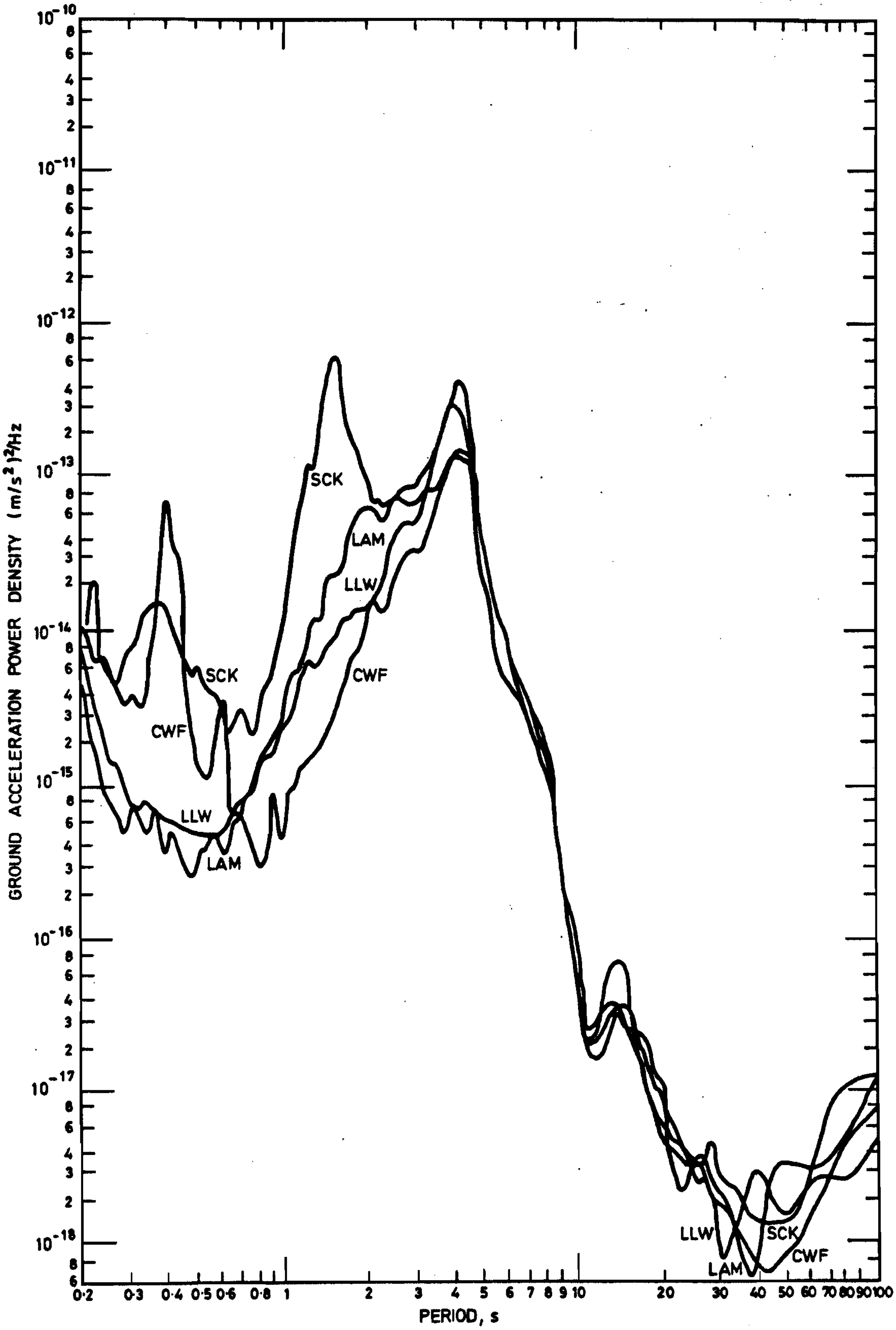

Figure 35. Smoothed Spectra of Seismic Noise at Four UKNet Sites (May)

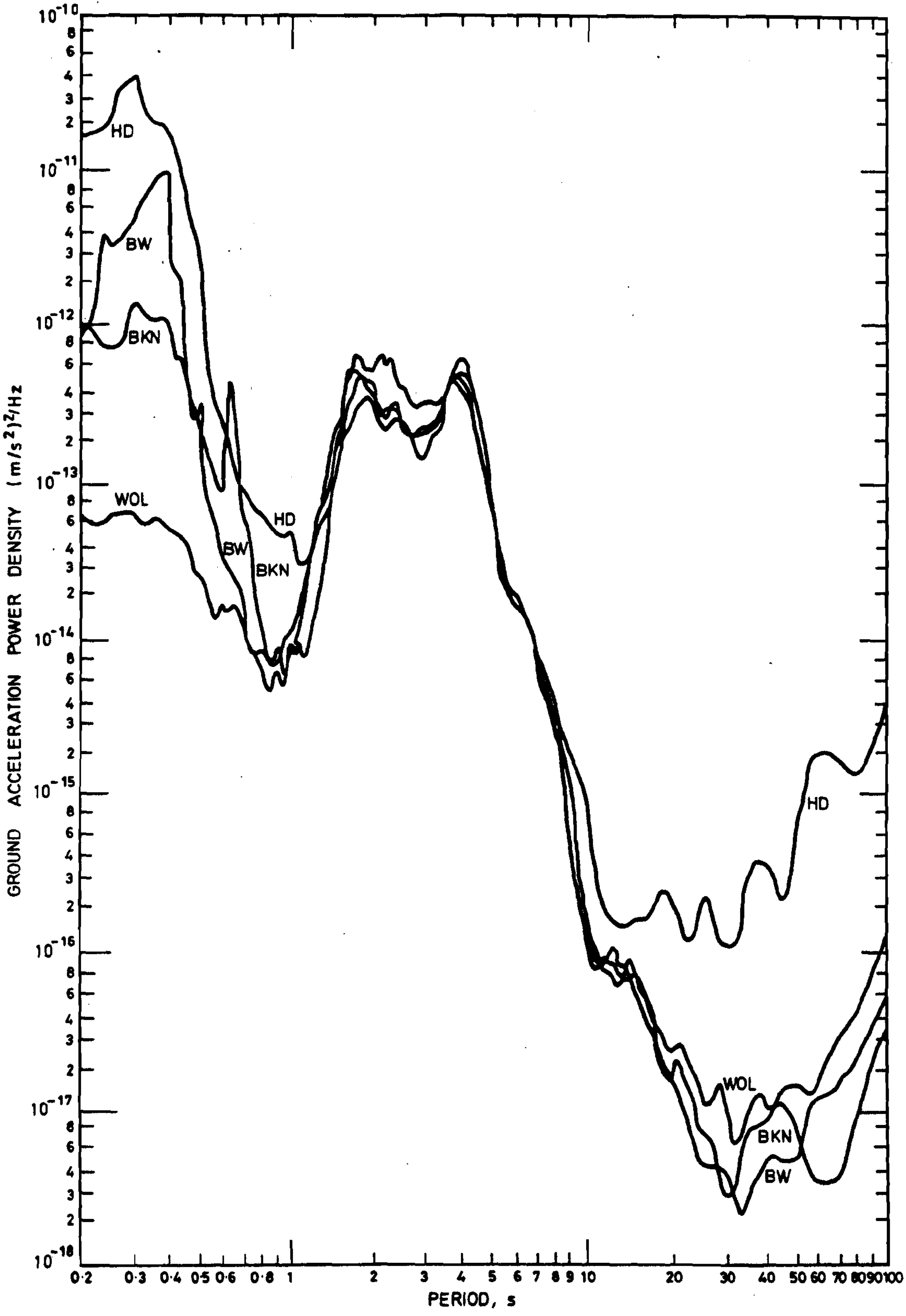

Figure 36. Smoothed Spectra of Seismic Noise at Four BNA Sites (May)

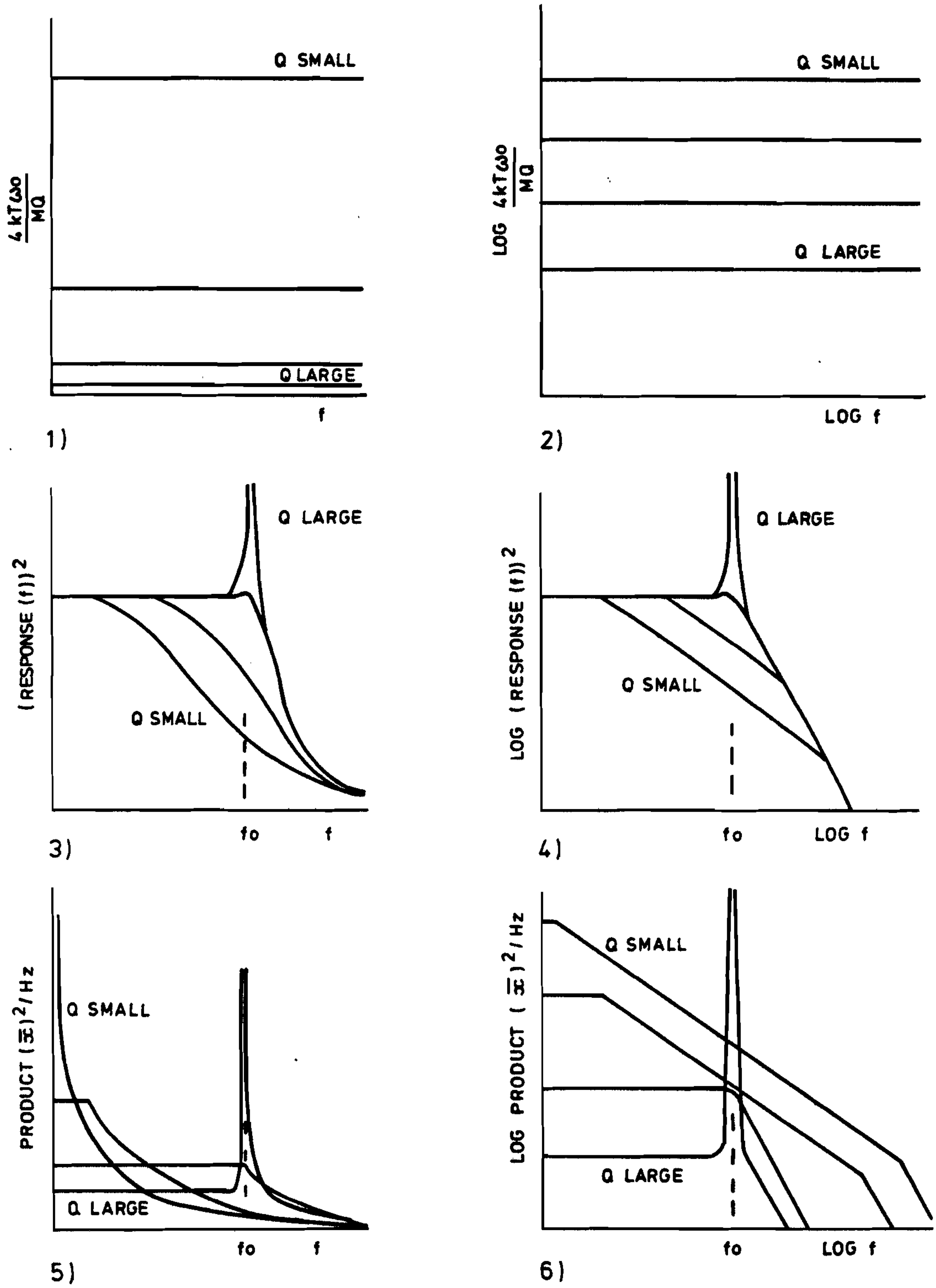

FIGURE 37. Response to Brownian Forces for Different Values of 'Q'

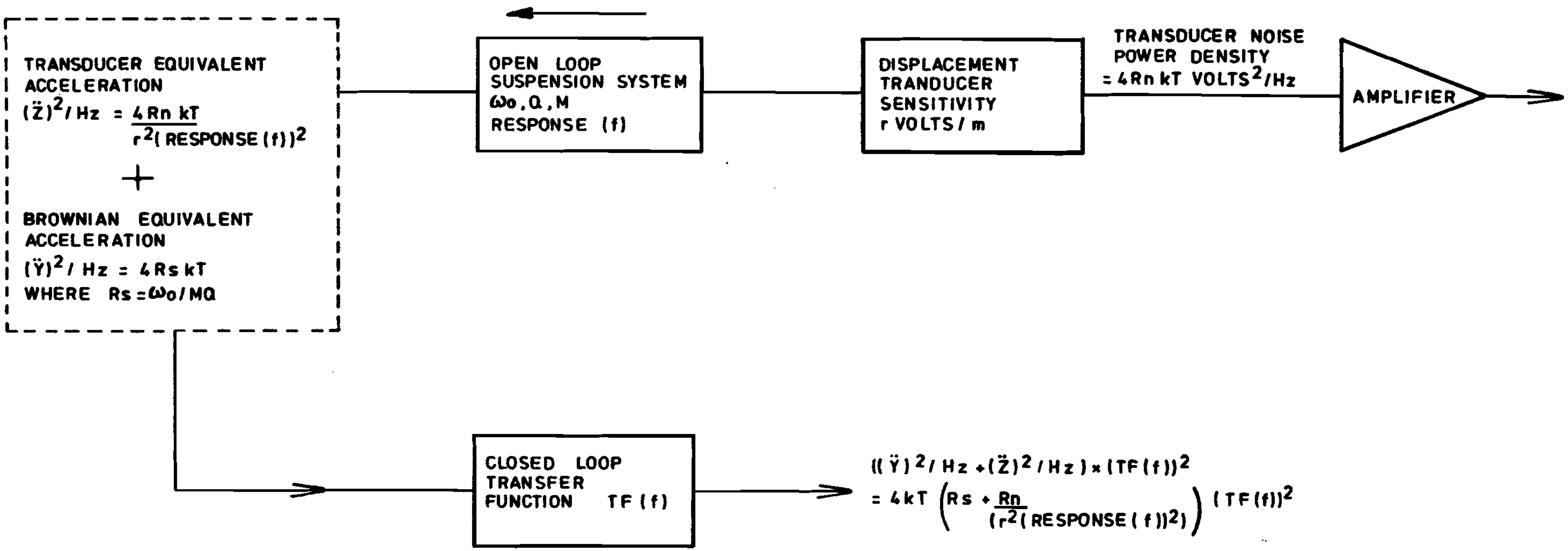

FIGURE 38. Block Diagram to Determine Transducer Noise Equivalent Acceleration

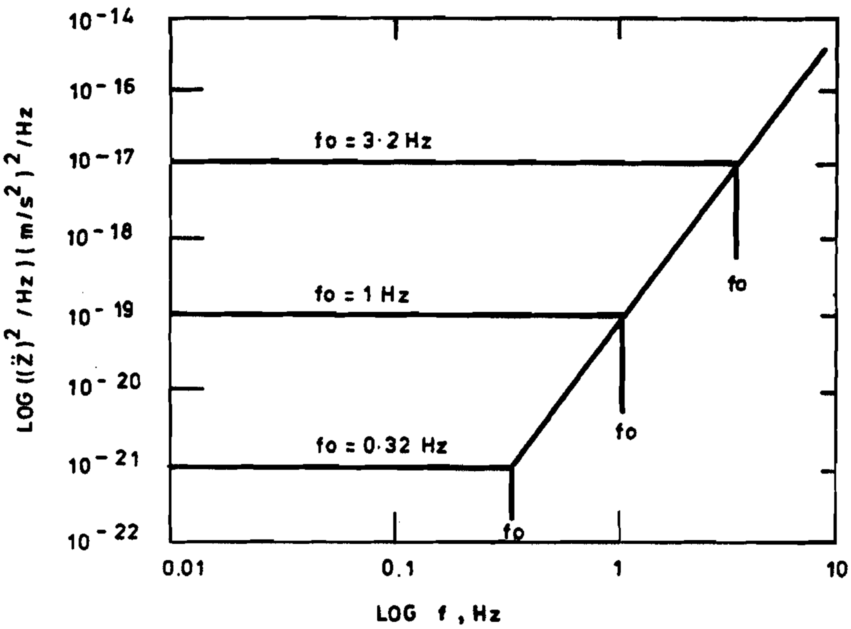

FIGURE 39 Variation of Transducer Noise Equivalent Acceleration with Natural Frequency.

DOCUMENT CONTROL SHEET

Overall security classification of sheet ......UNCLASSIFIED..

(As far as possible this sheet should contain only unclassified information. If it is necessary to enter classified information, the box concerned must be marked to indicate the classification eg (R), (C) or (S)).

1. DRIC Reference (if known)	2. Originator's Reference	3. Agency Reference	4. Report Security Classification
-	AWRE Report No. 024/83	-	UNLIMITED

5. Originator's Code (if known)	6. Originator (Corporate Author) Name and Location
-	Atomic Weapons Research Establishment, Aldermaston, Berkshire
5a. Sponsoring Agency's Code (if known)	**6a. Sponsoring Agency (Contract Authority) Name and Location**
-	-

7. Title

The Mk IIIC Vertical Component Force Balance Seismometer System.
Part 1: Design and Development

7a. Title in Foreign Language (in the case of Translation)

-

7b. Presented at (for Conference Papers). Title, Place and Date of Conference

-

8. Author 1.Surname, Initials	9a. Author 2	9b. Authors 3, 4	10. Date	pp	ref
Burch R F	-	-	February 1984	108	23

11. Contract Number	12. Period	13. Project	14. Other References
-	-	-	-

15. Distribution Statement

No restriction

16. Descriptors (or Keywords) (TEST)

Seismometers

Abstract

AWRE Blacknest have developed, in co-operation with the University of Reading, a broad band seismometer system for the measurement of the vertical component of ground motion. It consists essentially of a short period seismometer to which a capacitance displacement transducer has been added. By the use of electronic feedback, a force balance system is operated which enables the instrument to provide adequate signals over the frequency band of seismological interest (typically 0.01 to 10 Hz) and eliminates the requirement for separate short period and long period instruments.